Introduction to high-energy plasma astrophysics

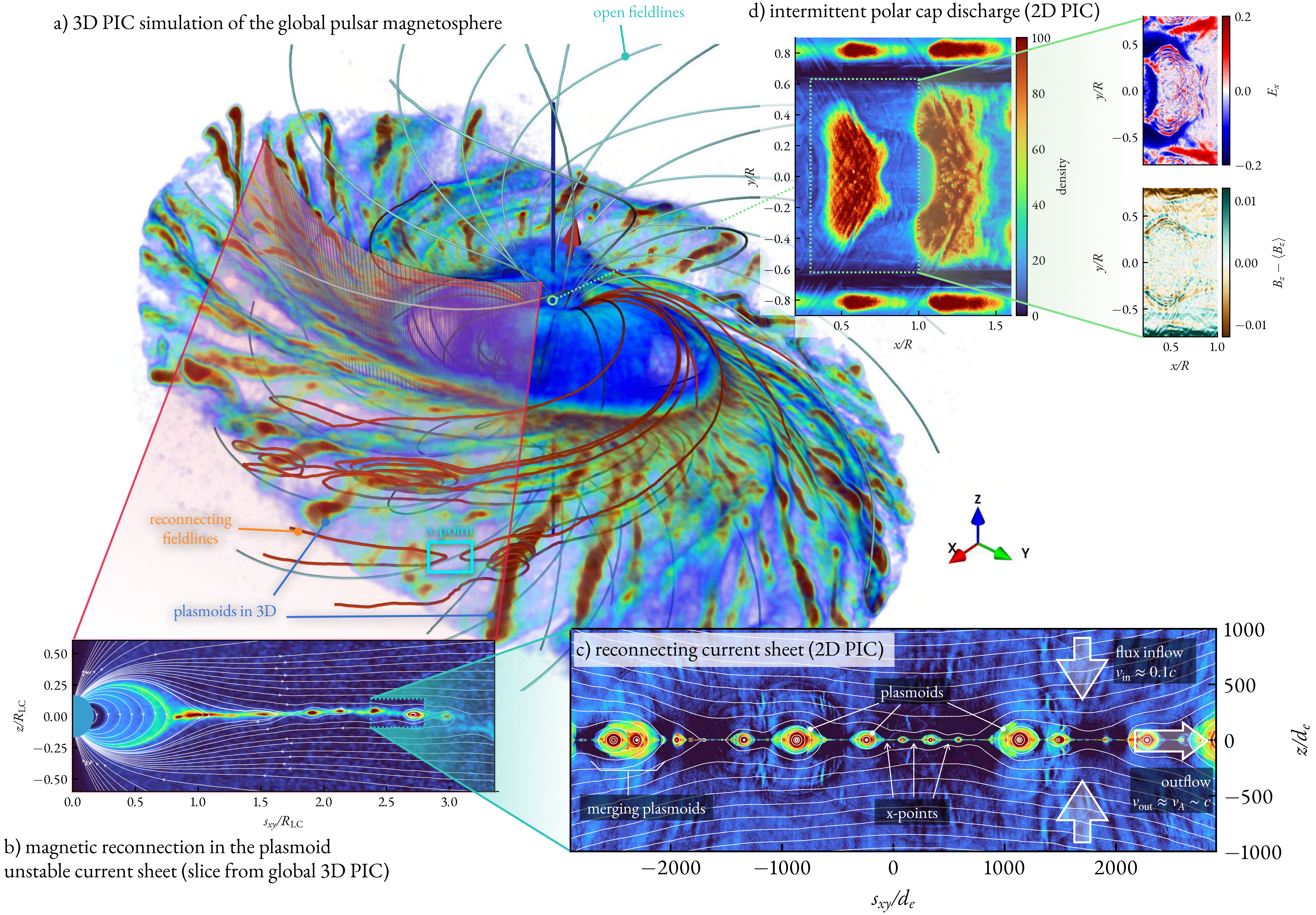

Sasha Philippov (University of Maryland, College Park), June 2, 2023

Lecture Plan

- Introduction to radiative processes and radiative relativistic reconnection.
- Examples of astrophysical systems.
    - Neutron stars: pulsars (mainly), a bit on magnetars
    - Black holes

Introduction

What are the interesting physical effects to look out for?

- Inverse Compton & synchrotron cooling

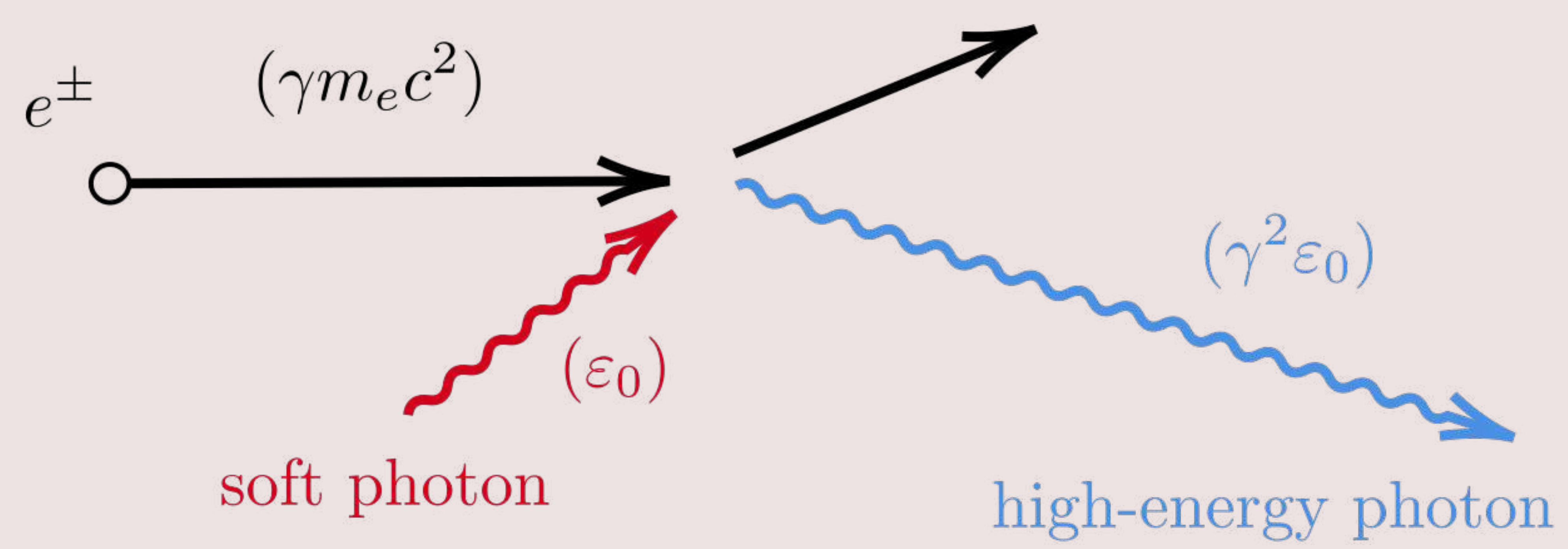

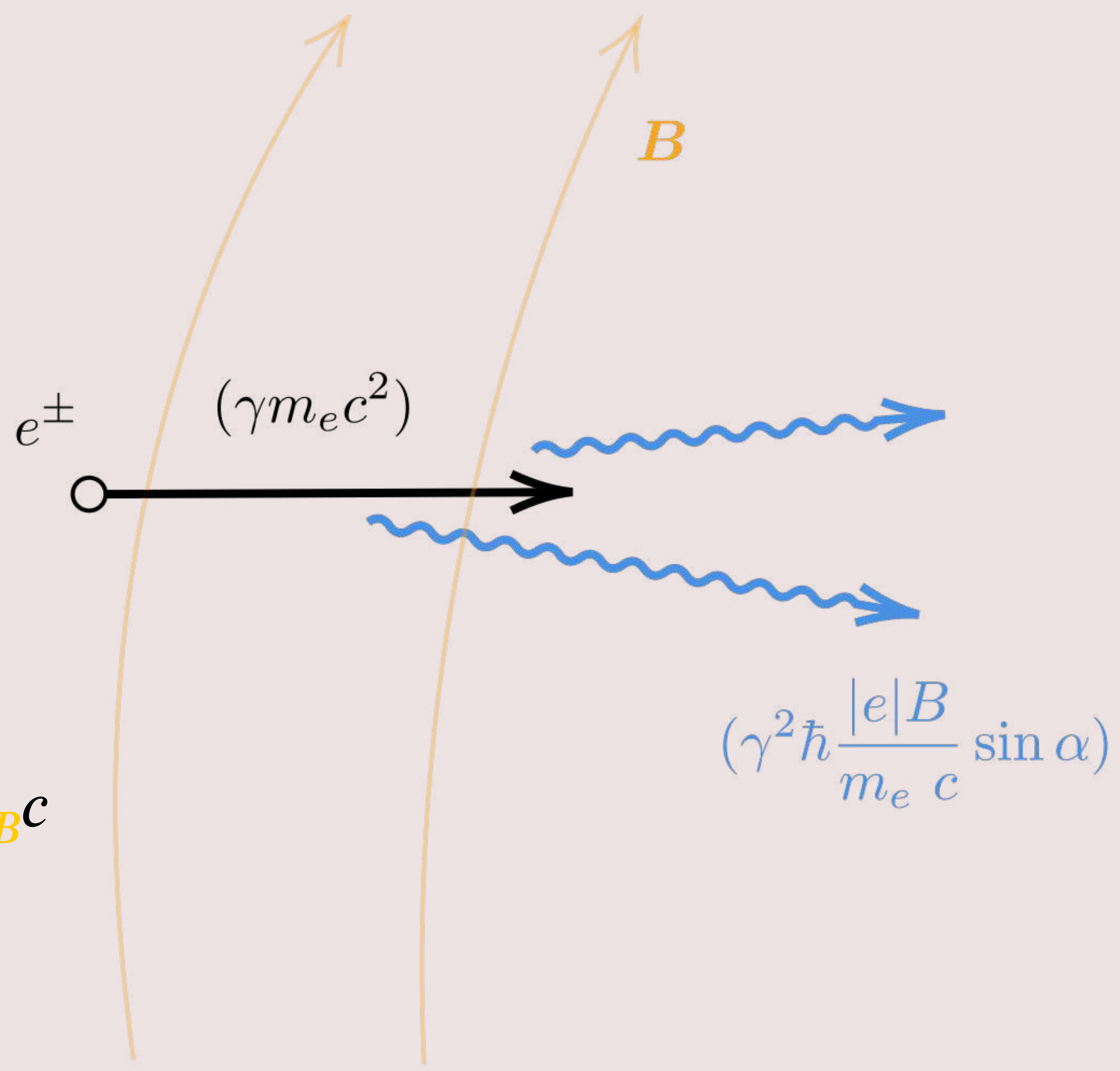

$$\frac{d(\gamma m_e c^2)}{dt} = 2\sigma_T \gamma^2 U_s c$$

$$\frac{d(\gamma m_e c^2)}{dt} = 2\sigma_T \gamma^2 \sin\alpha U_B c$$

Introduction

What are the interesting physical effects to look out for?

- Inverse Compton & synchrotron cooling
- Compton scattering (incl. down-scattering)

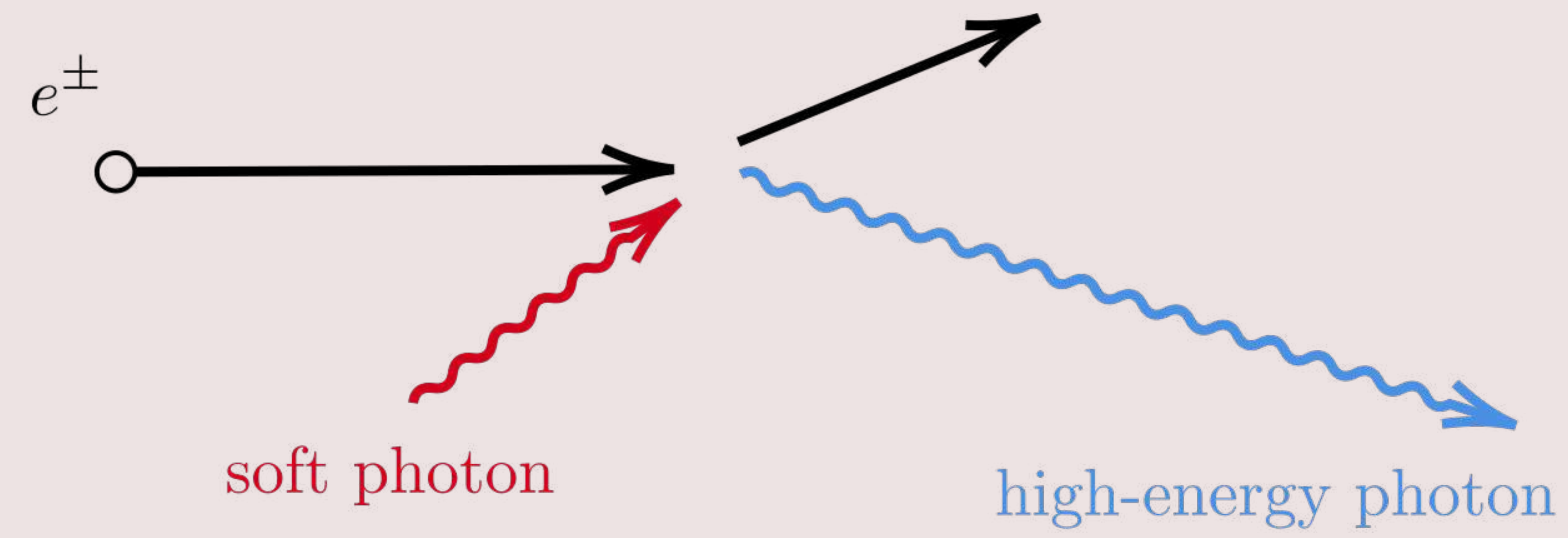

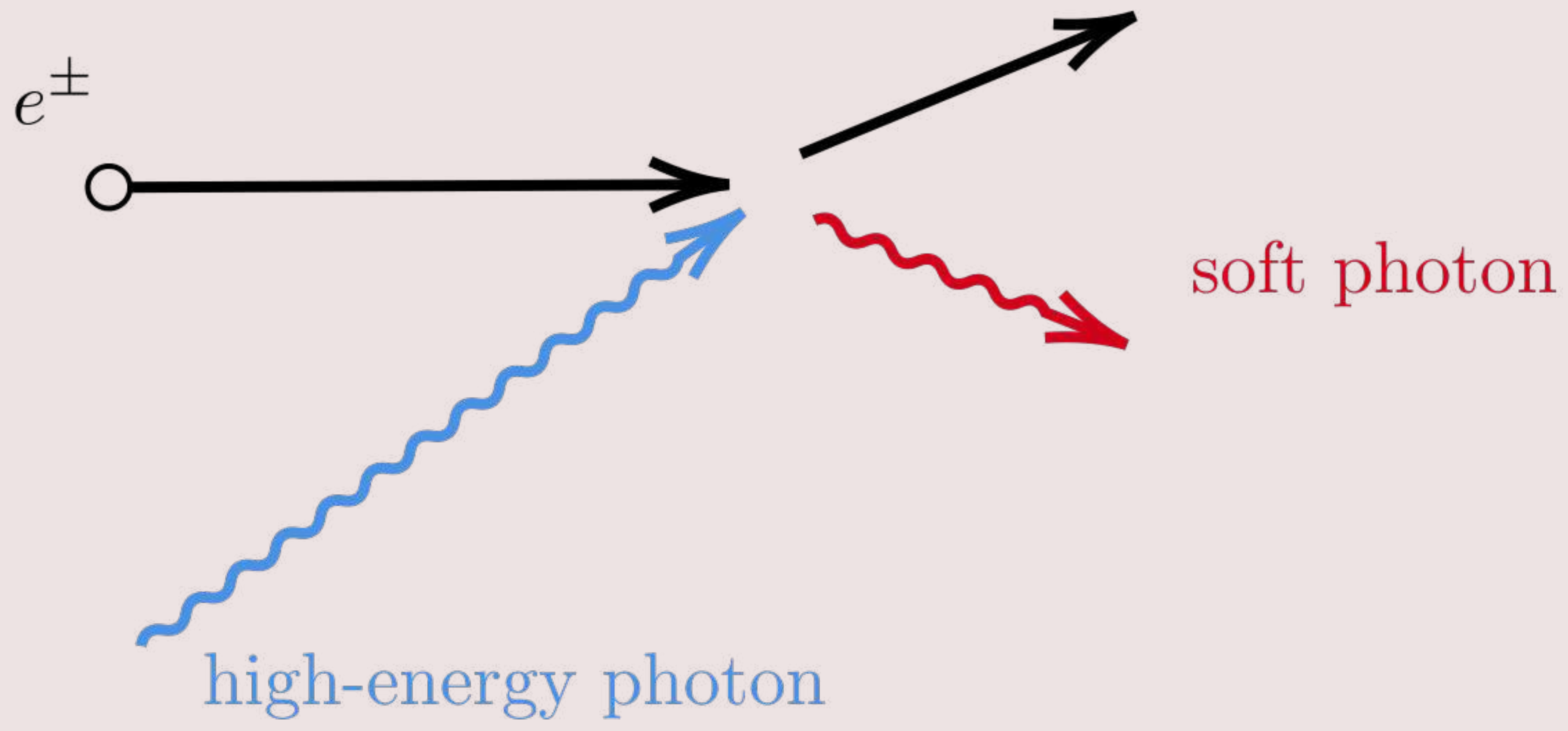

when scatterings are too frequent: $T_{\text{ph}} \leftrightarrow T_{e^{\pm}}$

Introduction

What are the interesting physical effects to look out for?

- Inverse Compton & synchrotron cooling
- Compton scattering (incl. down-scattering)
- Two-photon pair-production/-annihilation

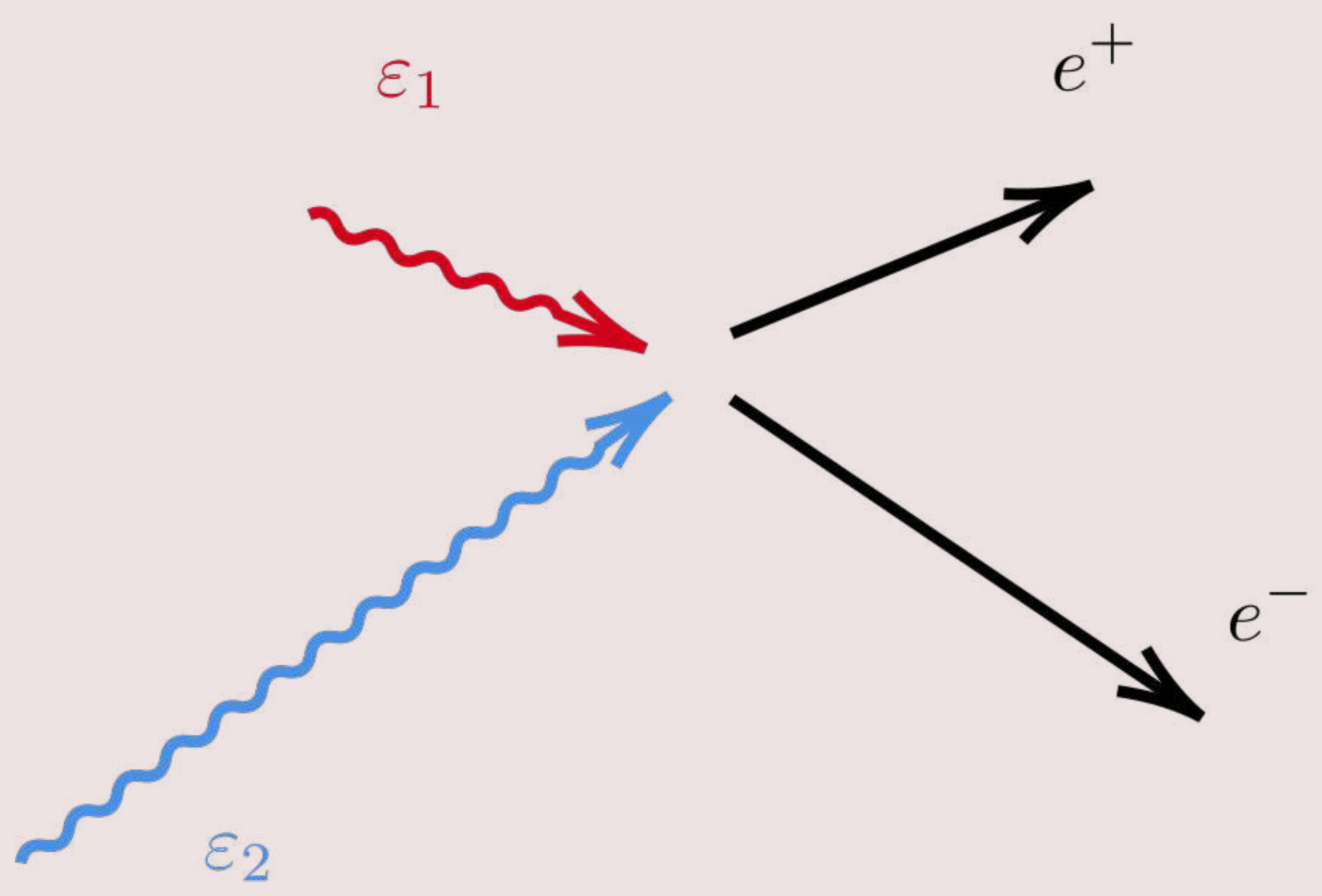

allowed when $\varepsilon_1\varepsilon_2(1-\cos\theta) \geq \left(2m_e c^2\right)^2$

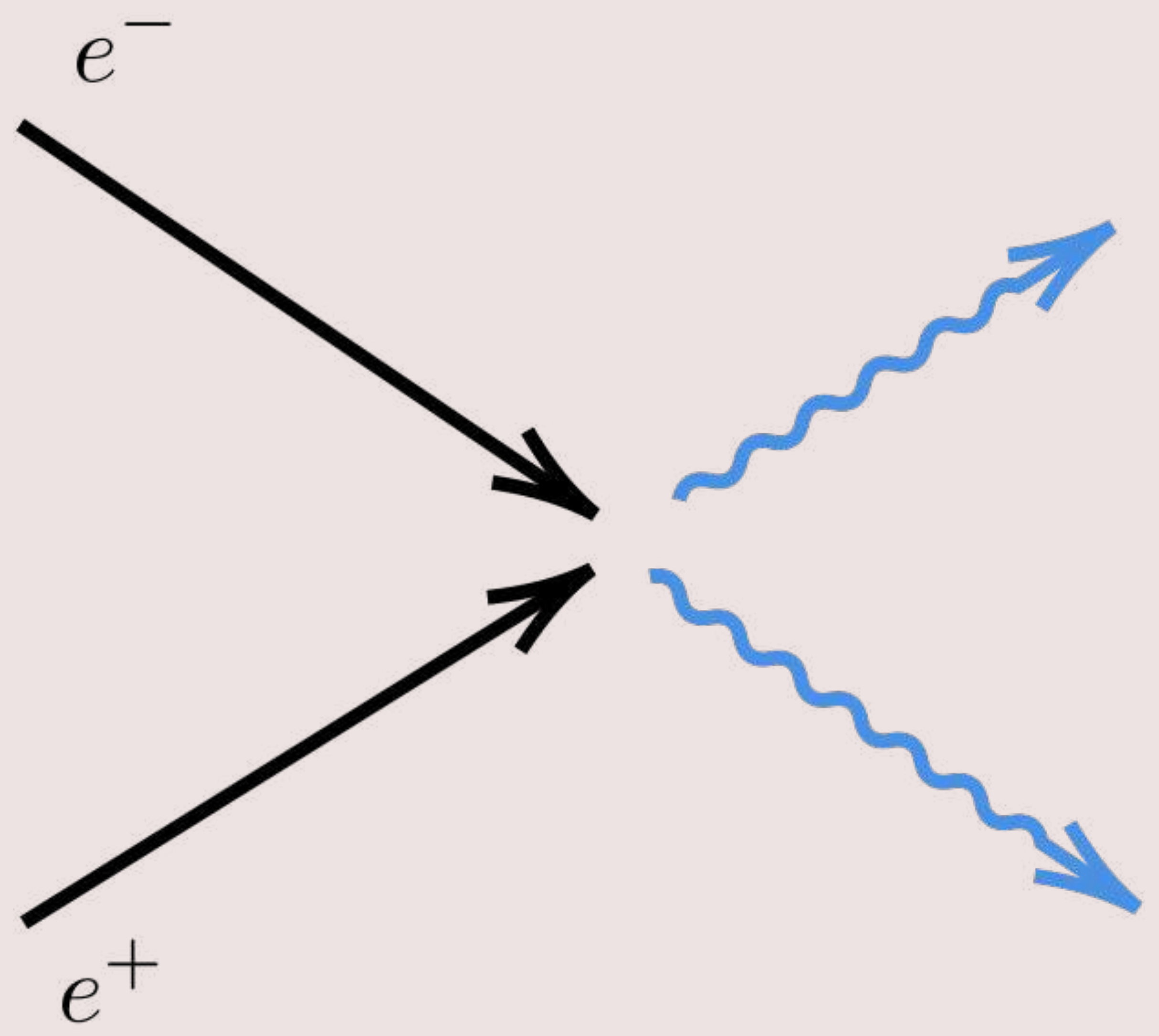

when important, can be an abundant source of ~MeV photons

Introduction

What are the interesting physical effects to look out for?

- Inverse Compton & synchrotron cooling
- Compton scattering (incl. down-scattering)
- Two-photon pair-production/-annihilation
- Synchrotron absorption

becomes important at (typically) low frequencies:

$$\sigma(\omega) \approx 467 \frac{1}{137\,\alpha_F} \cdot \sigma_T \frac{m_e c^2}{\hbar \omega_B} \left(\frac{\gamma \omega}{\omega_B} \right)^{-5/3}$$

when important, may introduce effective electron/positron collisionality
(for the low-energy particles)

Introduction

What are the interesting physical effects to look out for?

- Inverse Compton & synchrotron cooling
- Compton scattering (incl. down-scattering)
- Two-photon pair-production/-annihilation
- Synchrotron absorption
- Near-Schwinger field effects ($B_S \approx 10^{13}$G)
  - $\gamma + B \rightarrow e^- + e^+$ (pair-production)
  - $\gamma + B \rightarrow \gamma + \gamma + B$ (photon splitting)
  - Modified pair-production/-annihilation channels
  - Higher-order effects + resonances

For a detailed overview see *Thompson, & Kostenko (2018-2020)*

Introduction

What are the interesting physical effects to look out for?

- Inverse Compton & synchrotron cooling
- Compton scattering (incl. down-scattering)
- Two-photon pair-production/-annihilation
- Synchrotron absorption
- Near-Schwinger field effects ($B_S \approx 10^{13}$G)
  - $\gamma + B \rightarrow e^- + e^+$ (pair-production)
  - $\gamma + B \rightarrow \gamma + \gamma + B$ (photon splitting)
  - Modified pair-production/-annihilation channels
  - Higher-order effects + resonances
- Multi-body channels (typically less important, since $\sigma \propto \alpha_F, \alpha_F^2, \alpha_F^4$)
  - $\gamma + e^\pm \rightarrow \gamma + e^\pm + \gamma$ (double Compton scattering)
  - $e^- + e^+ \rightarrow \gamma + \gamma + \gamma$ (three photon annihilation)
  - $\gamma + e^\pm \rightarrow e^\pm + e^+ + e^-$
  - $e^\pm + e^\pm \rightarrow e^\pm + e^\pm + e^+ + e^-$

For a detailed overview see *Svensson (1984, 1987)*

- For neutrinos from AGN, need hadronic processes
  - p-p, produces protons and pions
  - photo-meson

$$p + p \rightarrow p + p + \pi^+ + \pi^- + \dots$$

$$p + \gamma \rightarrow p + a\pi^0 + b(\pi^+ + \pi^-)$$

$$\pi^+ \rightarrow \mu^+ + \nu_\mu$$

$$\pi^0 \rightarrow \gamma + \gamma$$

$$\mu^+ \rightarrow e^+ + \bar{\nu}_\mu + \nu_e$$

In proton rest frame,
$E'_\gamma \approx 2\gamma_p E_\gamma \approx 150\text{MeV}$

Introduction

Dimensionless parametrization

Introduction

Dimensionless parametrization

- magnetization parameter $\sigma = \dfrac{B^2/4\pi}{n_e m_e c^2}$ ← determines how relativistic the plasma becomes when energized by the ***B***-field dissipation

Introduction

Dimensionless parametrization

- magnetization parameter $\sigma = \dfrac{B^2/4\pi}{n_e m_e c^2}$
- compactness parameter $l = \dfrac{2U\sigma_T s}{m_e c^2}$
  - cooling timescale: $t_{\rm cool} \approx \dfrac{s/c}{\gamma l}$

determines how fast the energy is radiated away (compared to the system light crossing time s/c)

radiated power: $P = \frac{4}{3}\sigma_T \langle \gamma^2 \rangle n_e U c$

can be U_s if cooling is dominated by IC scattering, or U_B if synchrotron

Introduction

Dimensionless parametrization

- magnetization parameter $\sigma = \dfrac{B^2/4\pi}{n_e m_e c^2}$
- compactness parameter $l = \dfrac{2U\sigma_T s}{m_e c^2}$ (cooling timescale: $t_{\rm cool} \approx \dfrac{s/c}{\gamma l}$)
- burn-off limit / critical energy
  - acceleration timescale, $t_{\rm acc} \approx \dfrac{\gamma}{\beta_{\rm rec}}\omega_B^{-1}$, comparable to $t_{\rm cool}$

for inverse Compton cooling ($t_c^{-1} = \sigma_T n_e c$ – collision frequency, n_s, ε_s – number density and energy of the soft photons)

$$\gamma_{\rm rad} = \left(\frac{4\pi\beta_{\rm rec} e}{\sigma_T B}\right)^{1/2}$$

for synchrotron cooling: $\gamma_{\rm rad} \approx 10^5 \left(\dfrac{B}{10^5\ {\rm G}}\right)^{-1/2}$

  - light-crossing timescale, s/c, comparable to $t_{\rm cool} \Longrightarrow \gamma_{\rm cr} \approx 1/l$

Introduction

Dimensionless parametrization

- magnetization parameter $\sigma = \dfrac{B^2/4\pi}{n_e m_e c^2}$
- compactness parameter $l = \dfrac{2U\sigma_T s}{m_e c^2}$ (cooling timescale: $t_{\rm cool} \approx \dfrac{s/c}{\gamma l}$)
- QED optical depth + “pair-production potential”
  - Thompson optical depth, $\tau_T = \sigma_T s n_e$ (collision frequency: $t_c^{-1} = \sigma_T n_e c$): number of collisions for a photon $\approx \max(\tau_T, \tau_T^2/2)$
  - two-photon pair-production optical depth, $\tau_{\gamma\gamma} = \sigma_T s n_{\varepsilon > {\rm MeV}}$
  - Lorentz factor of the MeV-photon-producing pairs: $\gamma_Q = \begin{cases} \left(m_e c^2/\hbar\omega_B\right)^{1/2} \\ \left(m_e c^2/\varepsilon_s\right)^{1/2} \end{cases}$

for synchrotron: $\gamma_Q \approx 2 \cdot 10^4 \left(\dfrac{B}{10^5\ {\rm G}}\right)^{-1/2}$

for IC: $\gamma_Q \approx 23 \left(\dfrac{\varepsilon_s}{\rm keV}\right)^{-1/2}$

Relativistic reconnection (high-σ, $e^{\pm}$ plasma)

Sironi (PRL, 2022)

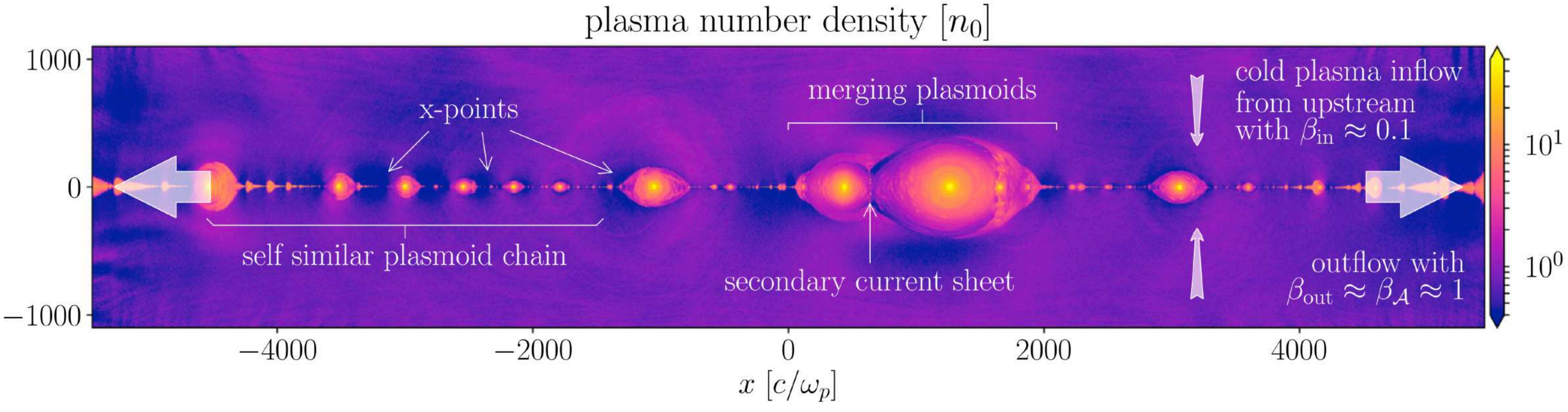

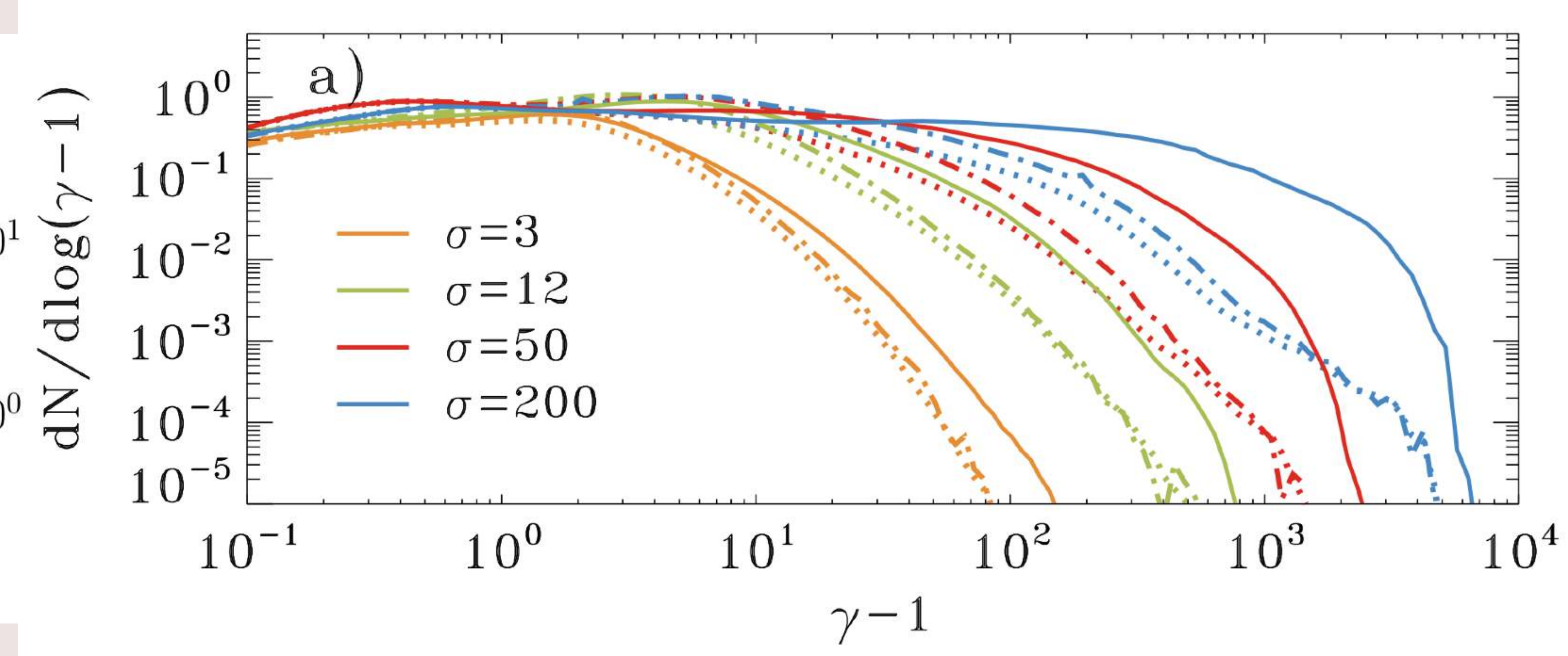

Zhang+ (2023)

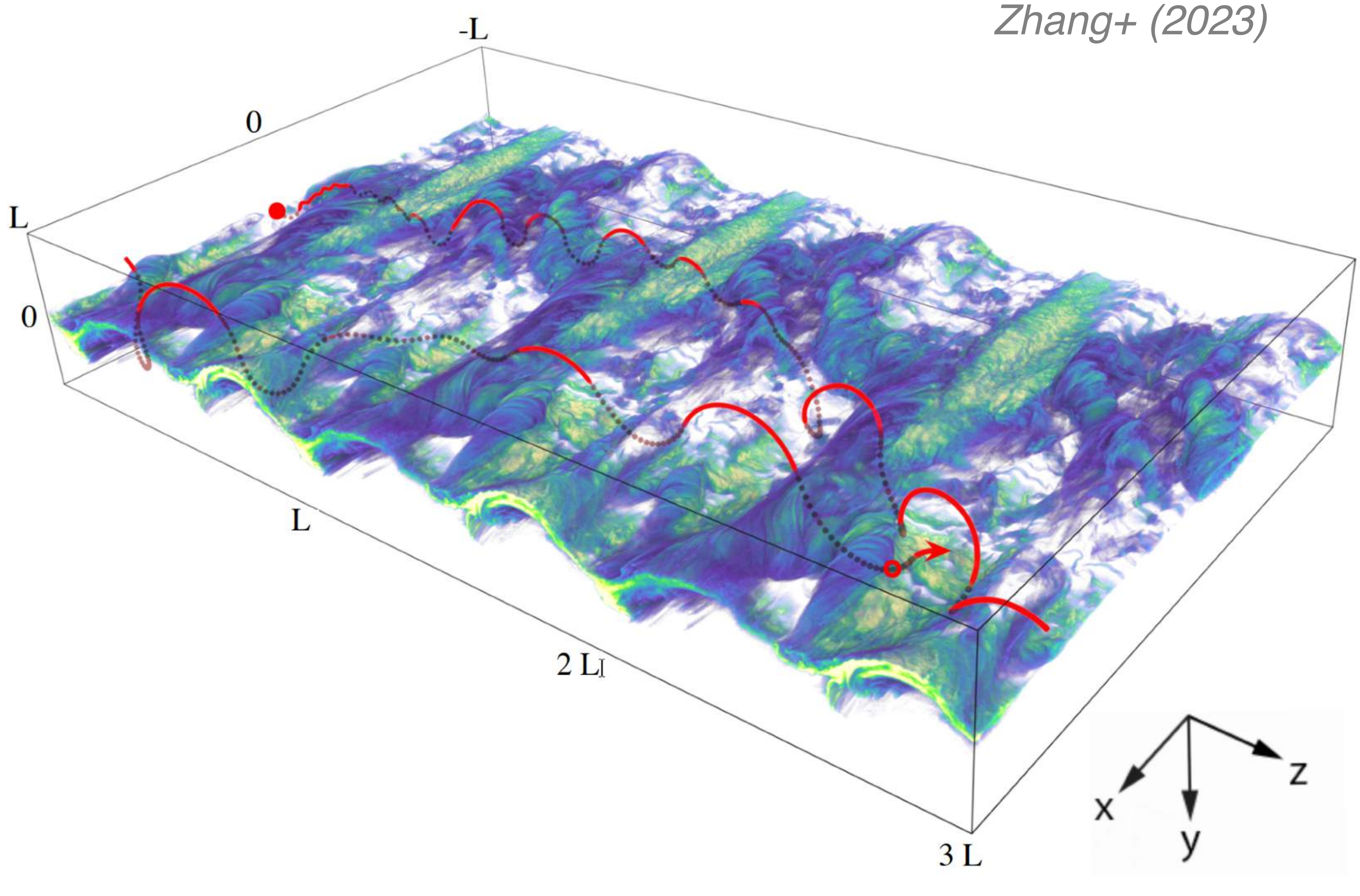

- hard power-law is formed with $p \approx 1\ldots2$ (for $\sigma \gtrsim 1$, and $B_g \lesssim 0.25\ B_{\rm up}$)
- reconnection rate: $v_{\rm in}/v_{\rm out} \sim 0.1\ldots0.3$
- pre-acceleration (up to $\sigma m_e c^2$) is dominated by $E_{\parallel}$ in x-points
  - additional pre-acceleration possible via slingshot & ideal $E_{\perp}$
- long-term acceleration (potentially to $\gg \sigma m_e c^2$) is dominated by upstream helical acceleration (3D) or plasmoid contraction (2D)
  - steeper power-law $p \approx 2\ldots3$

Radiative effects

Inverse-Compton cooling

- Postulate a (unmodeled) low-energy soft photon background with energy density, U_s
- Particles “feel” a drag force: $F_{\rm IC} \propto \left(\gamma/\gamma_{\rm rad}\right)^2$
- Varying $\gamma_{\rm rad}/\sigma$ (cooling strength)

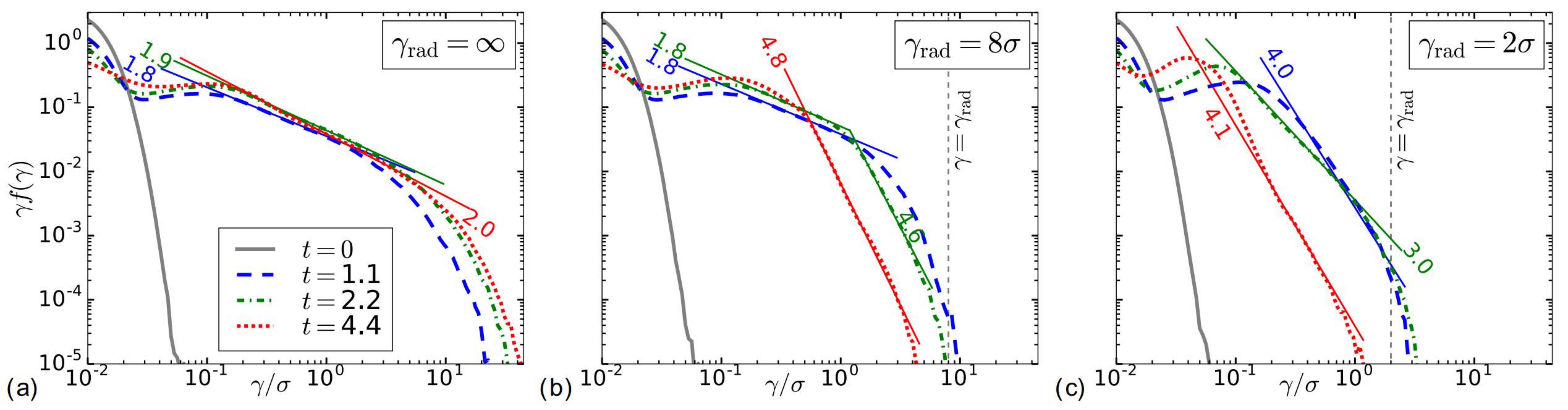

Werner+ (2019)

Results:
- particles are unable to accelerate past $\gamma_{\rm rad}$
- power-law steepens at $\gamma_{\rm br} \sim \sigma$ for slow cooling ($\gamma_{\rm rad} \geq 8\sigma$)

Radiative effects

Inverse-Compton cooling

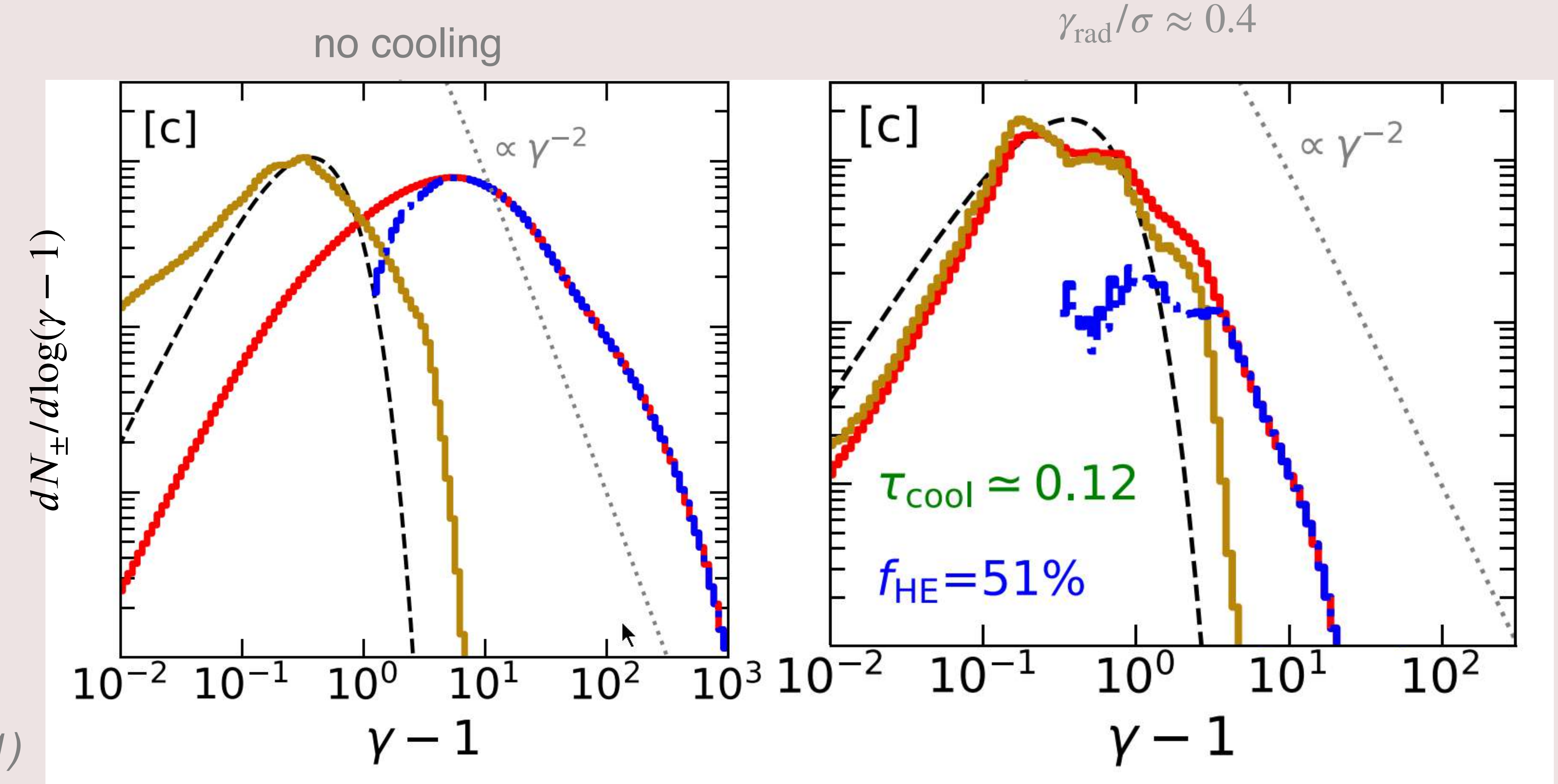

Sridhar+ (2021)

Sironi, & Beloborodov (2020)

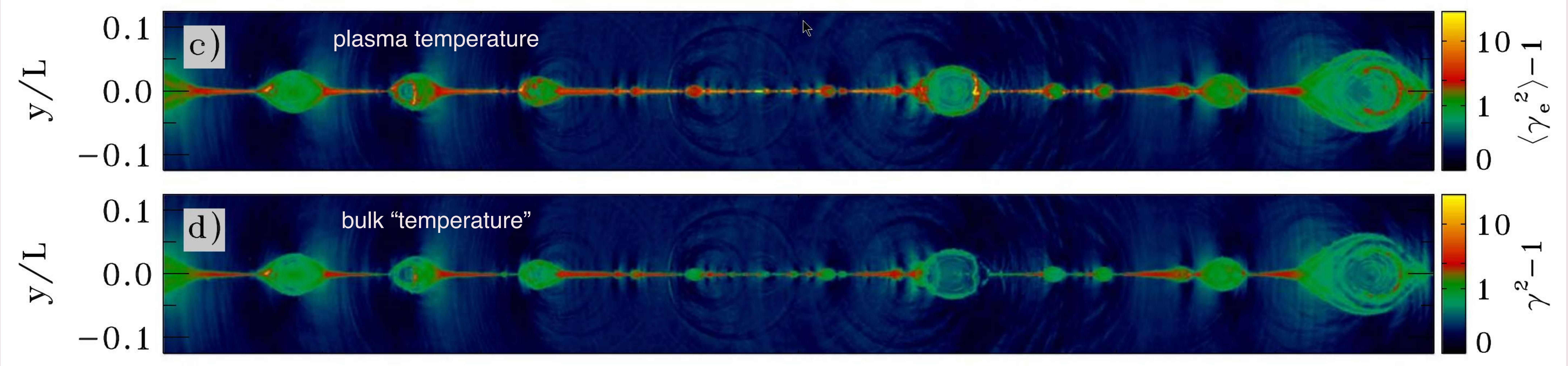

Results:

- for strong cooling bulk motions constitute most of the plasma kinetic energy
- $\Theta_{e^\pm} \leq \Gamma_{\rm bulk} \Longrightarrow$ has a direct imprint on the comptonized emission

Radiative effects

Synchrotron cooling

- Particles "feel" a drag force:

$$F_{\rm sync} \propto \widetilde{B}_\perp (\gamma/\gamma_{\rm rad})^2$$

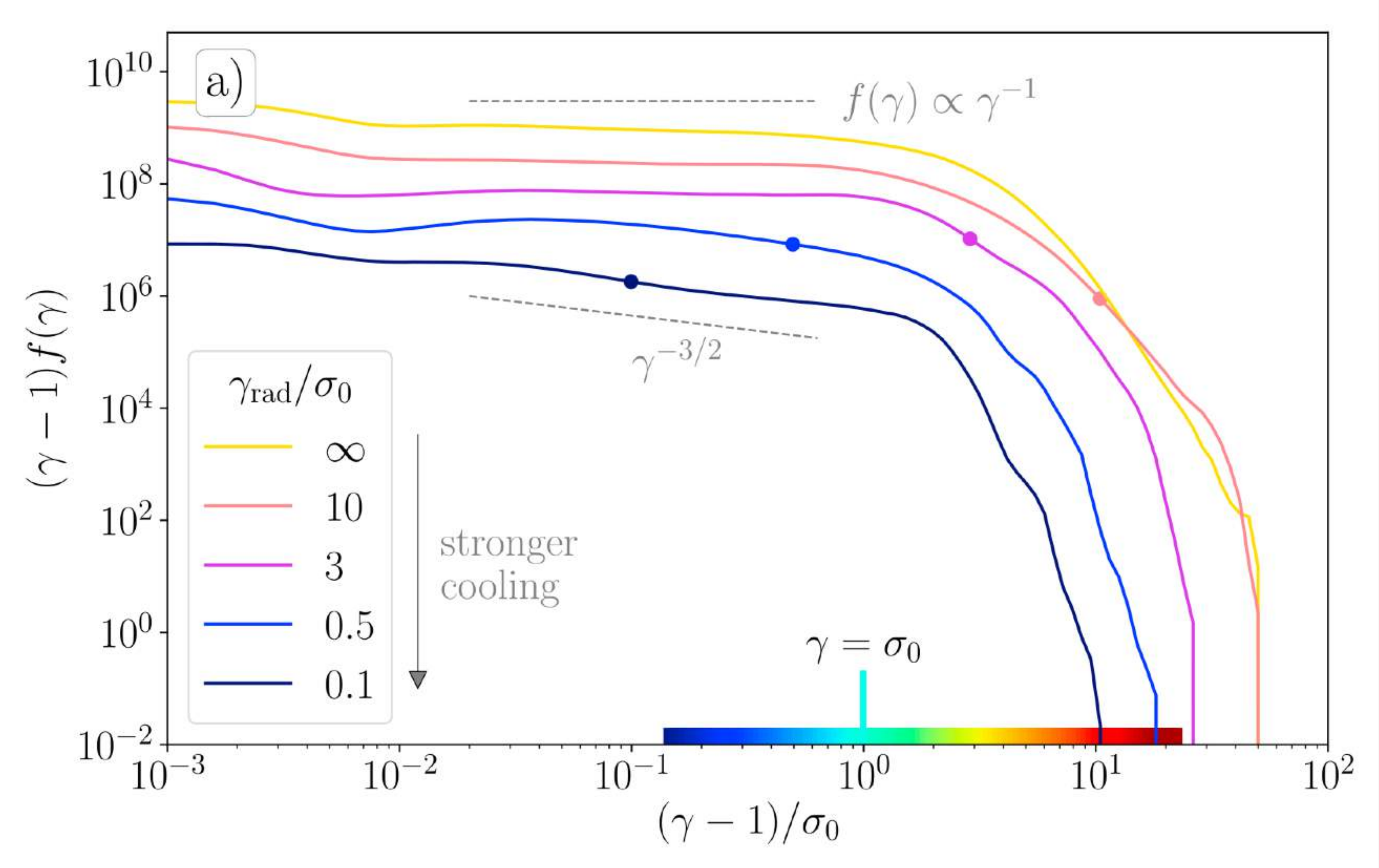

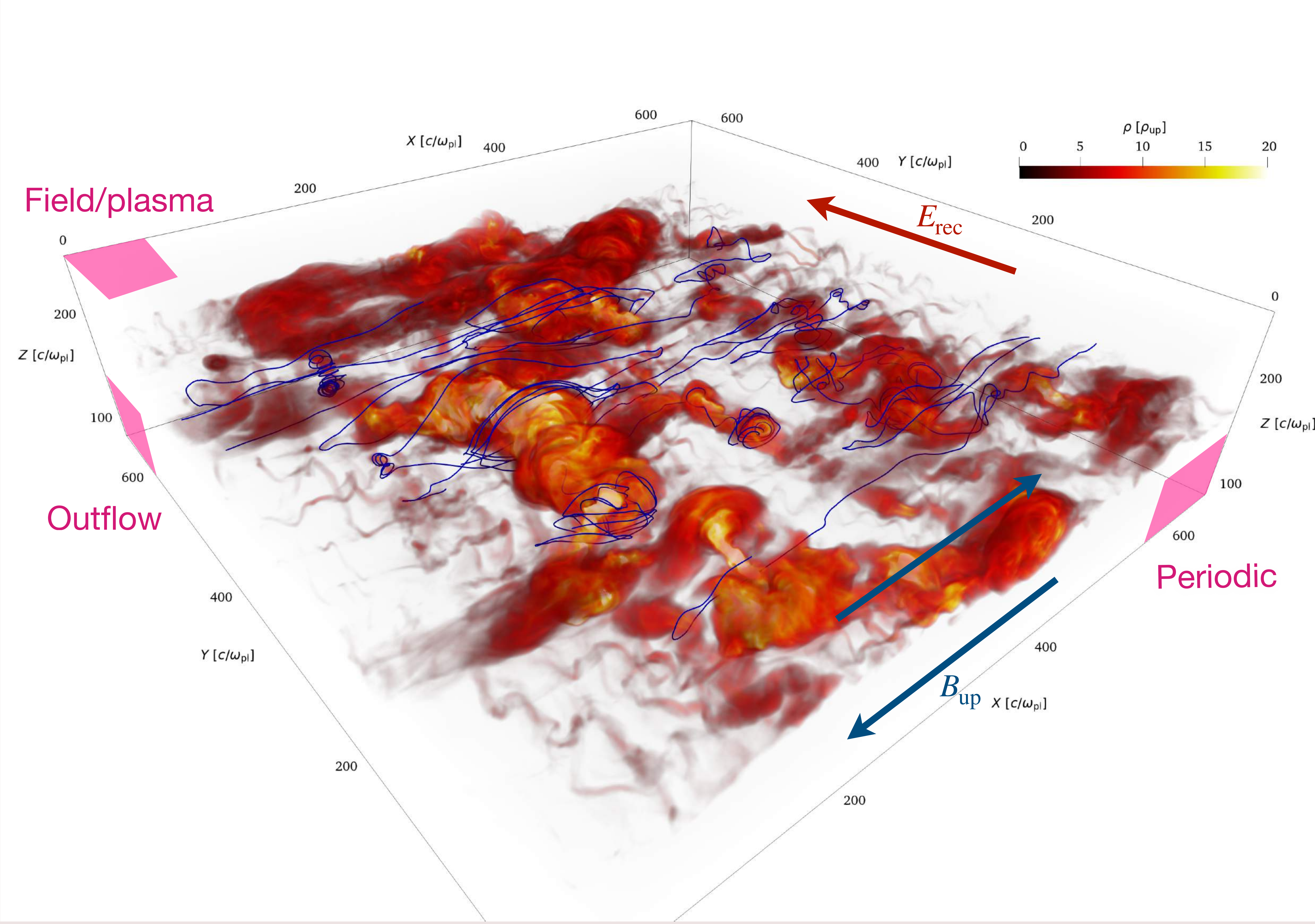

Results:

- even for strong cooling ($\gamma_{\rm rad} \leq \sigma$) particle distribution is (almost) unchanged ($p \sim 1\ldots2$) and extends to $\gamma_{\rm cut} \sim \sigma$
- acceleration & cooling happens at different locations in space
- for $\gamma_{\rm rad} \leq \sigma$ emission peaks at $\varepsilon_p \sim \hbar\omega_B \gamma_{\rm rad}^2$ (≈ 16 MeV!) with a cutoff near $\varepsilon_c \sim \varepsilon_p(\sigma/\gamma_{\rm rad})$
- internal temperatures of plasmoids is dropped to $\approx \gamma_{\rm rad}$ (hence the emission peak) $\Longrightarrow$ thinner current sheets for stronger cooling

Chernoglazov+ (arxiv, 2023)

Radiative effects

Synchrotron cooling

- Particles "feel" a drag force: $F_{\rm sync} \propto \widetilde{B}_\perp (\gamma/\gamma_{\rm rad})^2$

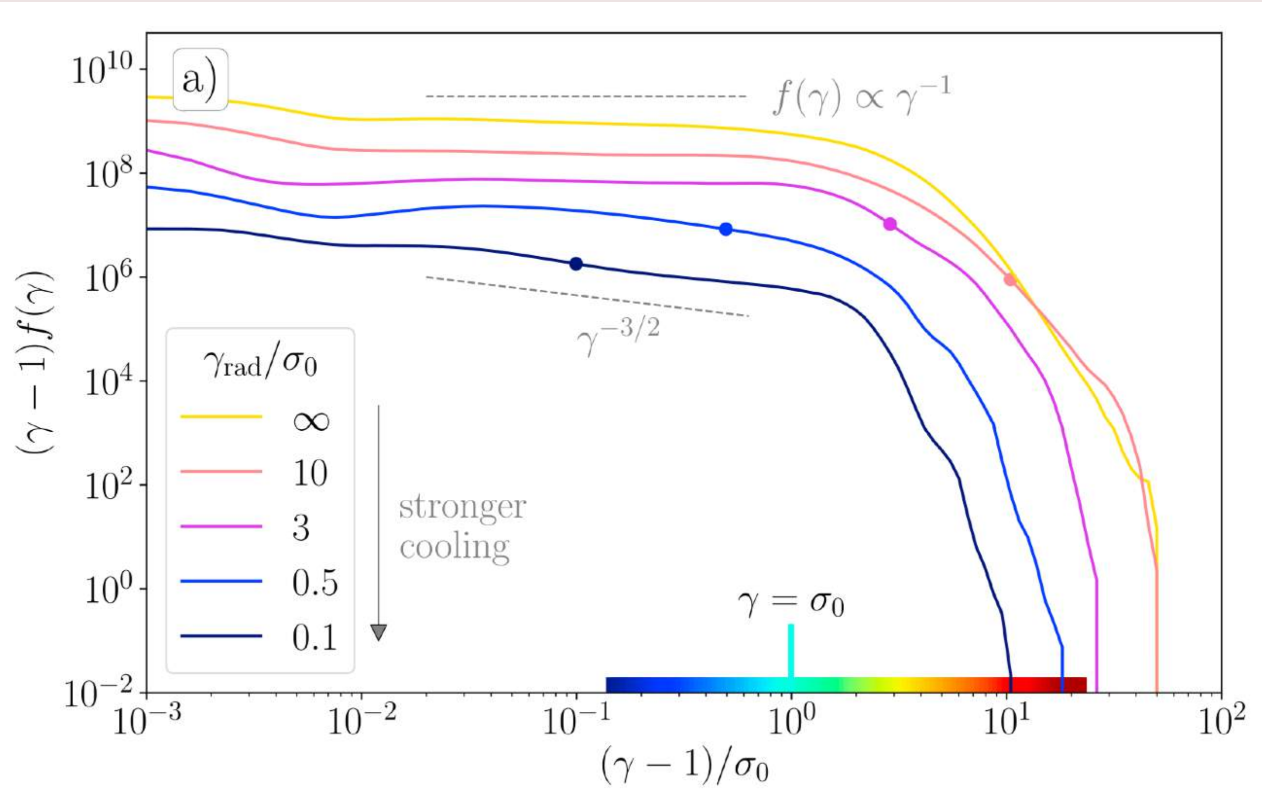

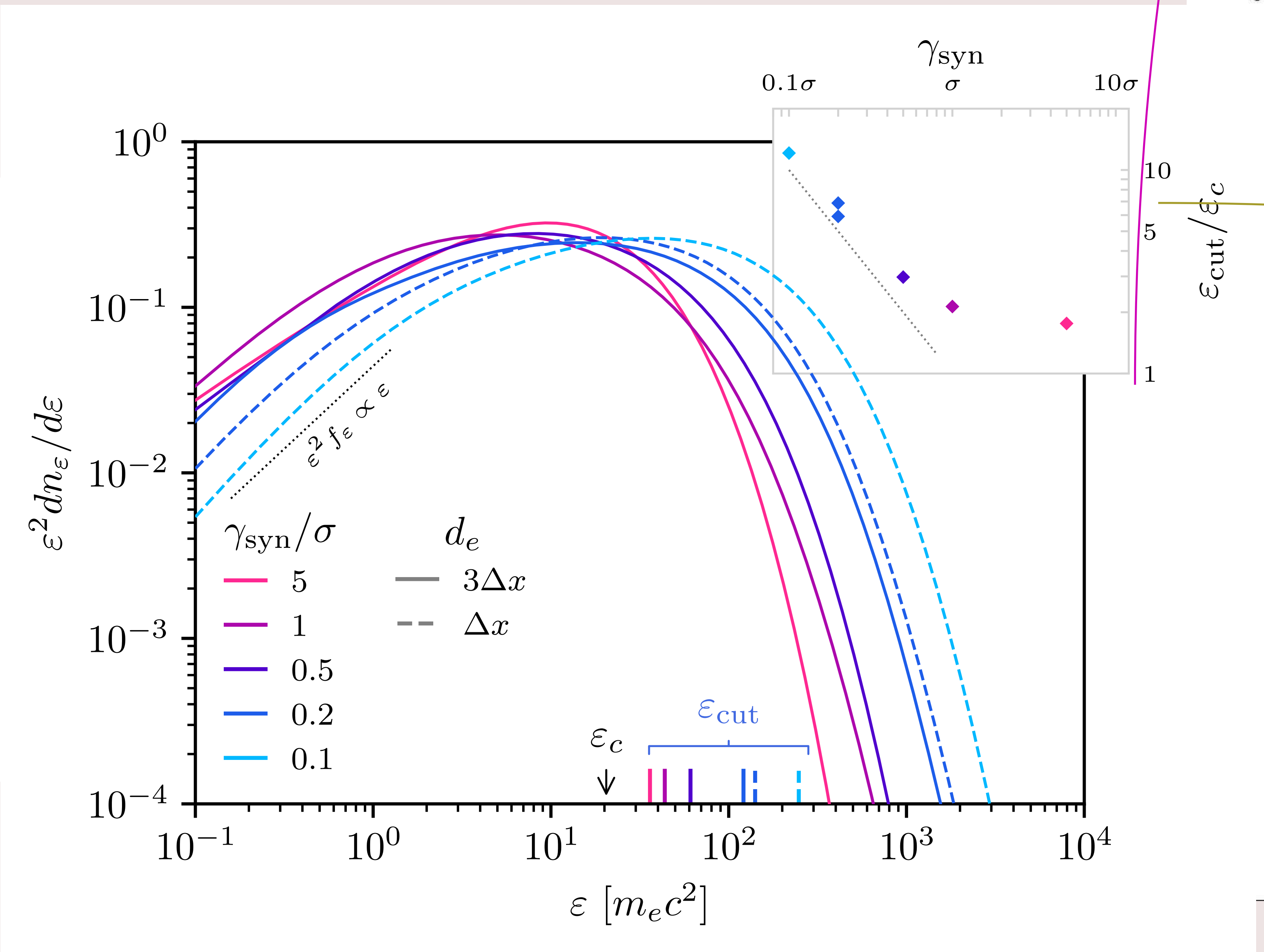

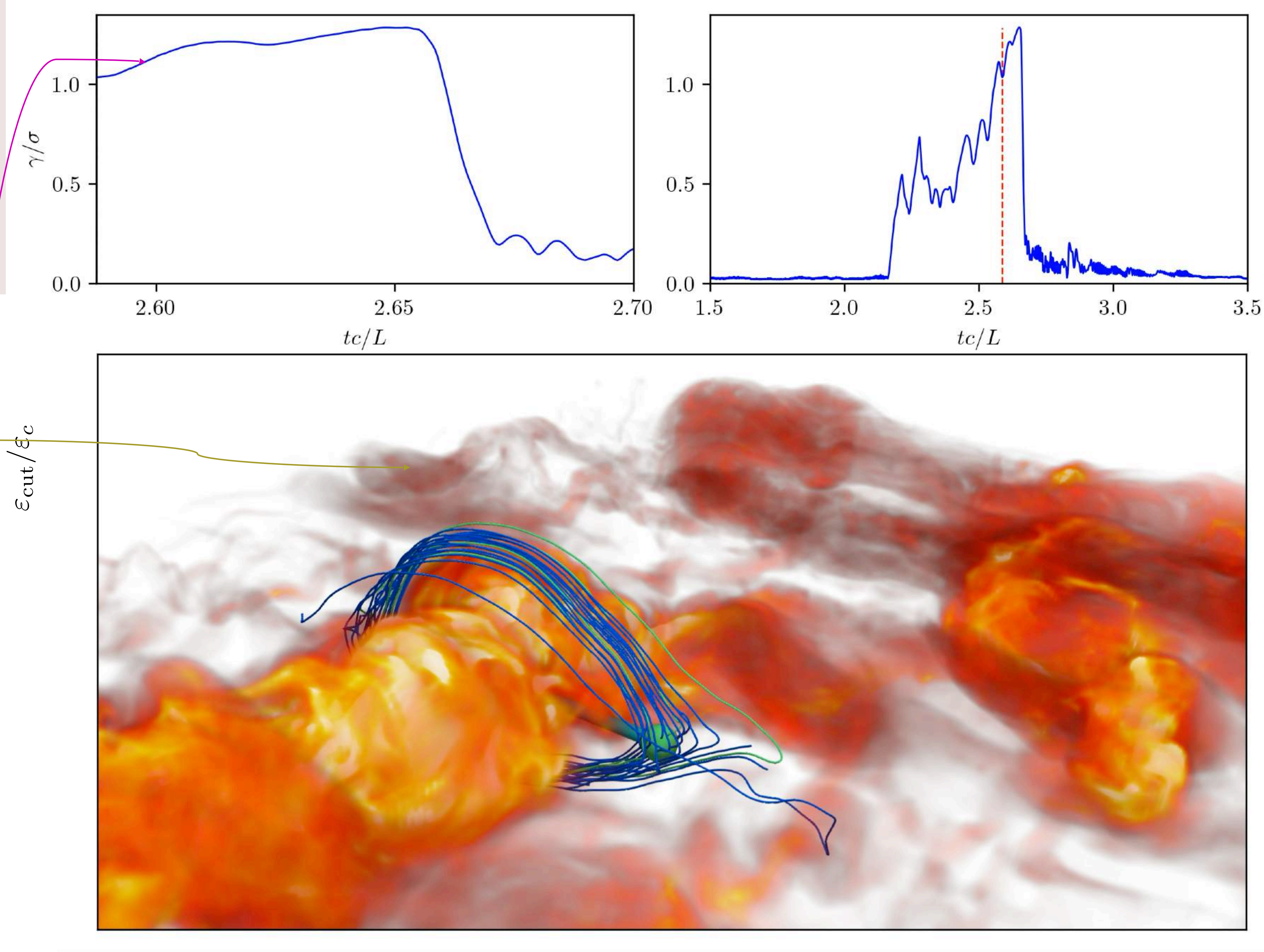

Chernoglazov+ (arxiv, 2023)

Results:

- even for strong cooling ($\gamma_{\rm rad} \leq \sigma$) particle distribution is (almost) unchanged ($p \sim 1\dots2$) and extends to $\gamma_{\rm cut} \sim \sigma$
- acceleration & cooling happens at different locations in space
- for $\gamma_{\rm rad} \leq \sigma$ emission peaks at $\varepsilon_p \sim \hbar\omega_B \gamma_{\rm rad}^2$ (≈ 16 MeV!) with a cutoff near $\varepsilon_c \sim \varepsilon_p(\sigma/\gamma_{\rm rad})$
- internal temperatures of plasmoids is dropped to $\approx \gamma_{\rm rad}$ (hence the emission peak) $\Longrightarrow$ thinner current sheets for stronger cooling

Hakobyan+ (2019)

QED effects

Two-photon pair-production

- strong sync. cooling & $\gamma\gamma \rightarrow e^{\pm}$ pair production (Breit-Wheeler)
- photons are emitted, and their interaction is modeled as two-body collisions
- $\tau_{\gamma\gamma} \ll 1$ (most of the photons escape)

self-consistent modeling is crucial!

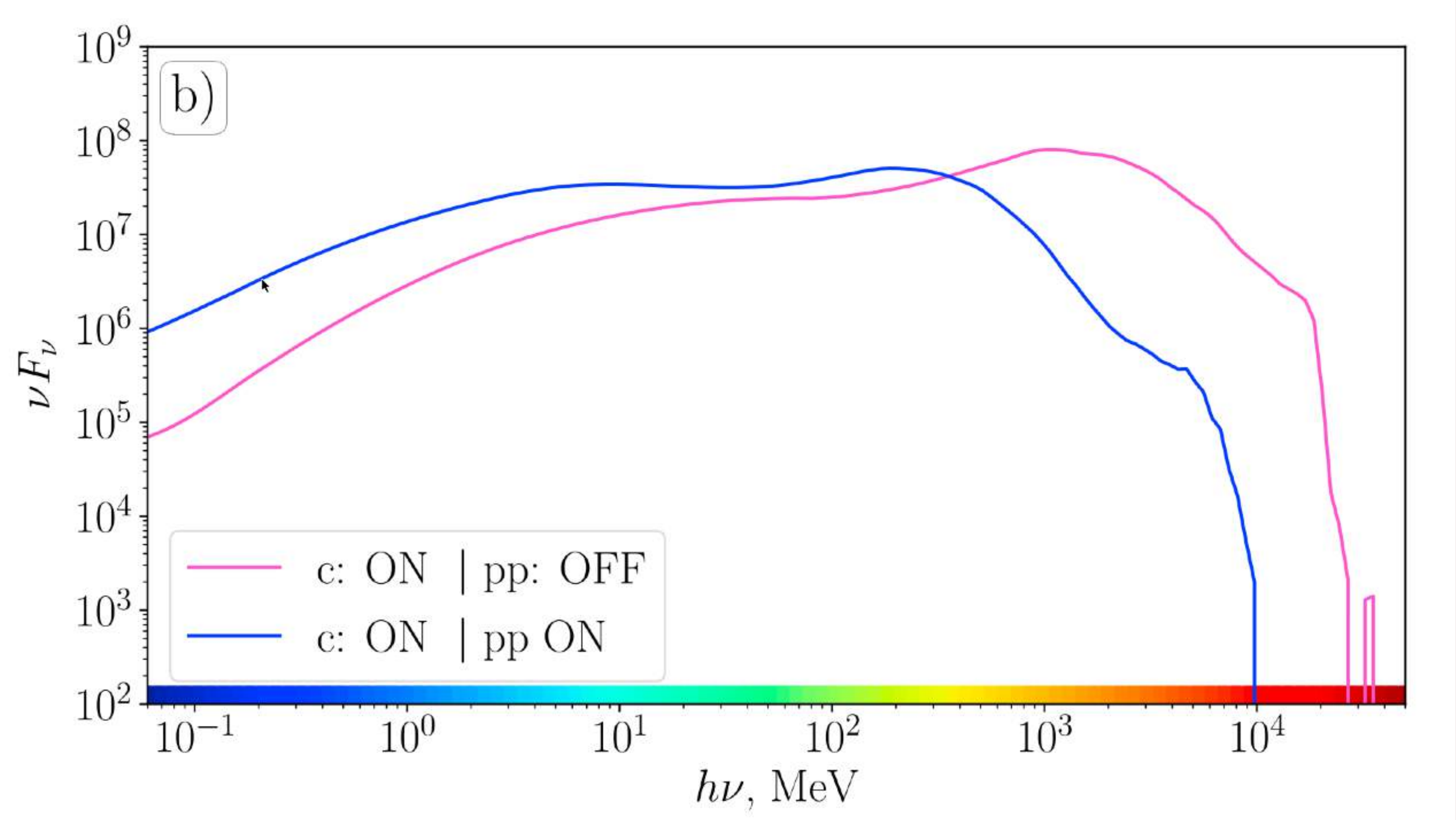

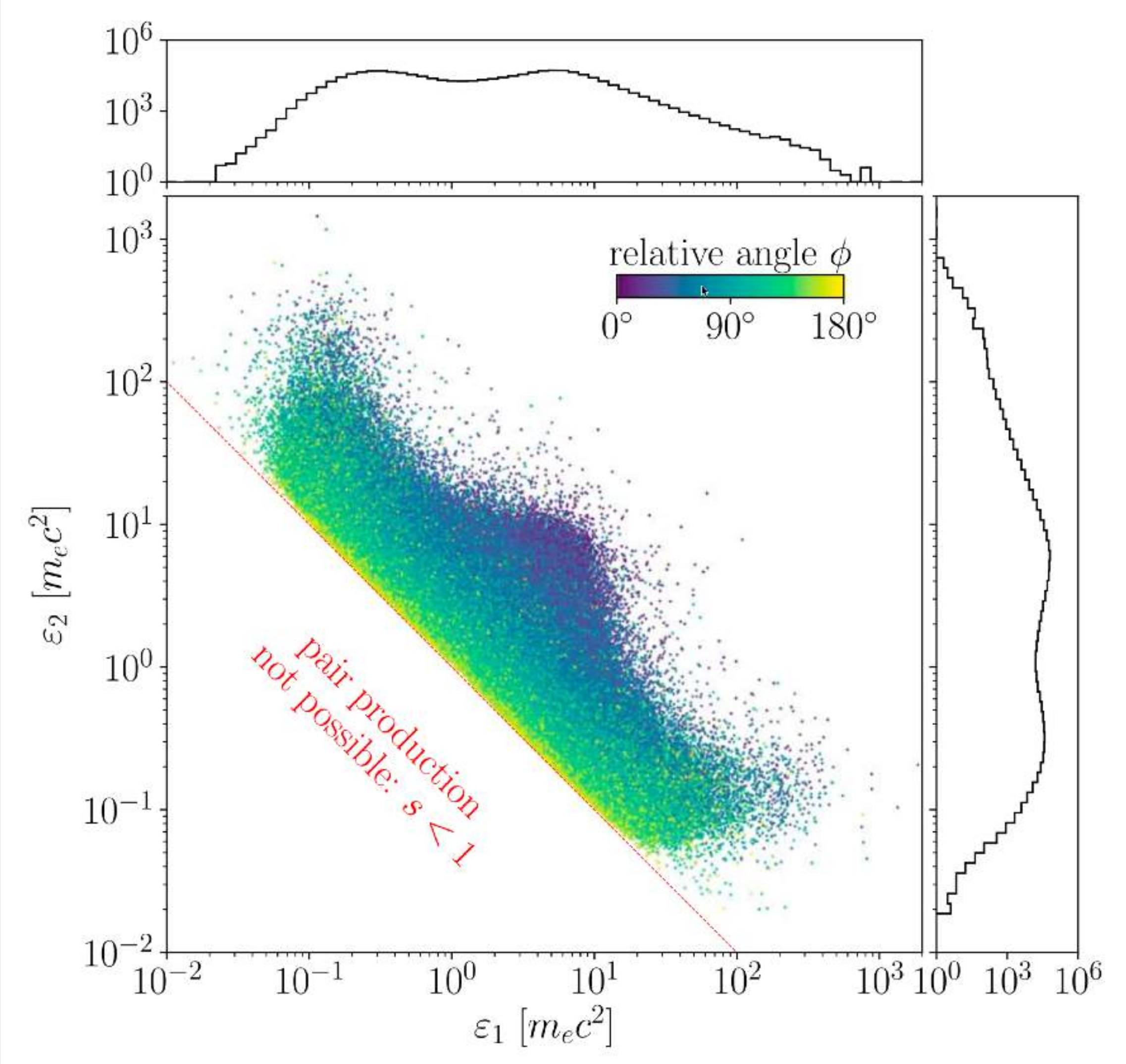

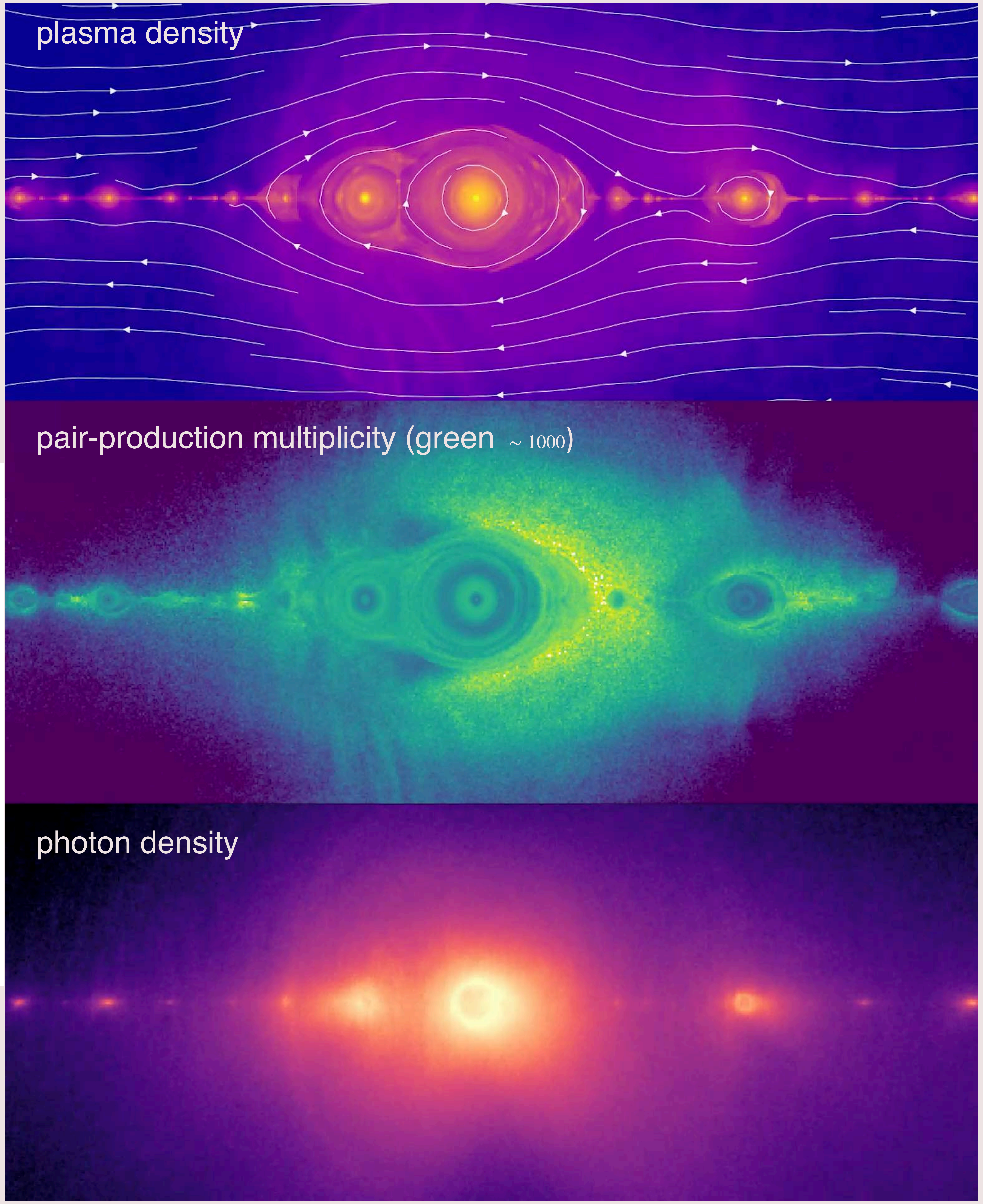

Results:

- magnetization σ is self-consistently regulated by pair-production feedback
- produced pairs constitute a separate emission peak (at low energies)

Astrophysical relevance

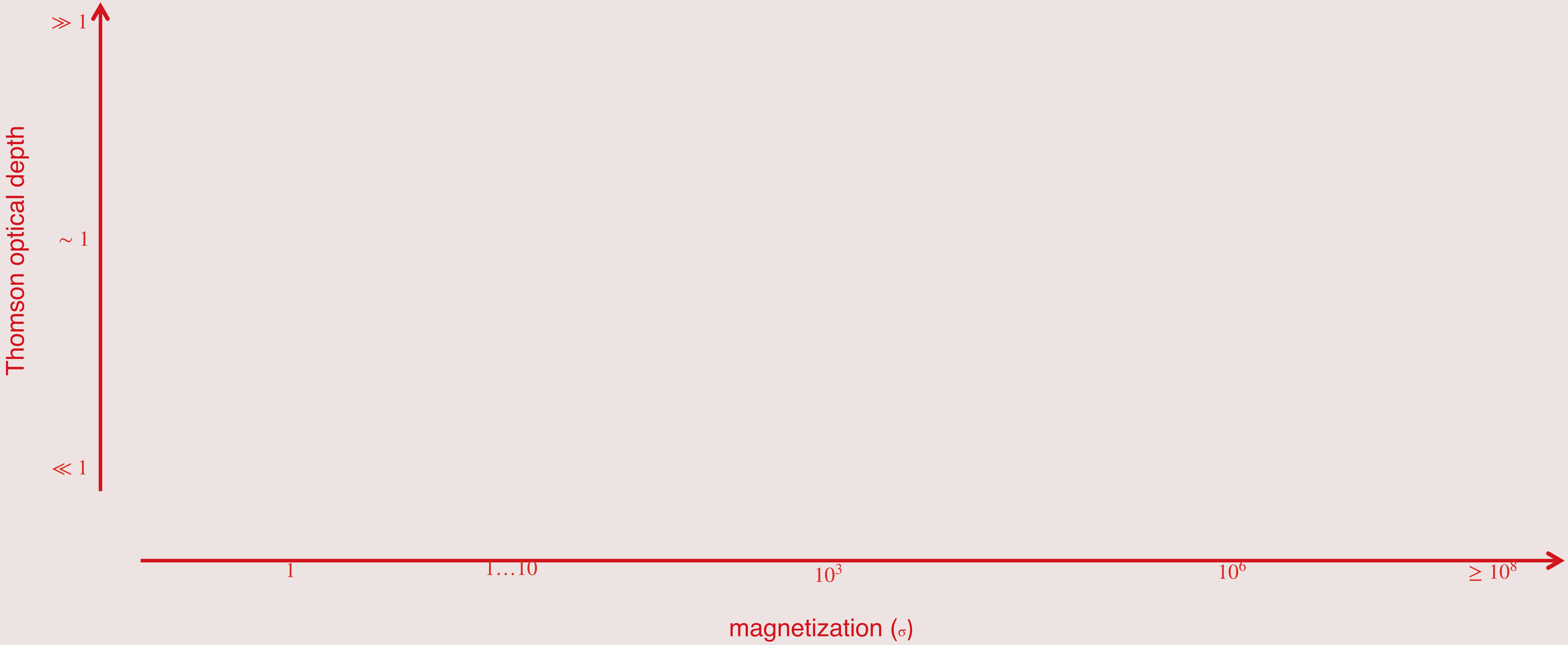

see *Uzdensky, & Goodman (2008)*, *Belobrodov (2017)*, *Sironi, & Beloborodov (2020)*, *Sridhar+ (2021, 2023)*, *Groselj+ (2023)*

Astrophysical relevance

Cyg X-1, *Gierlinski+ (1999)*

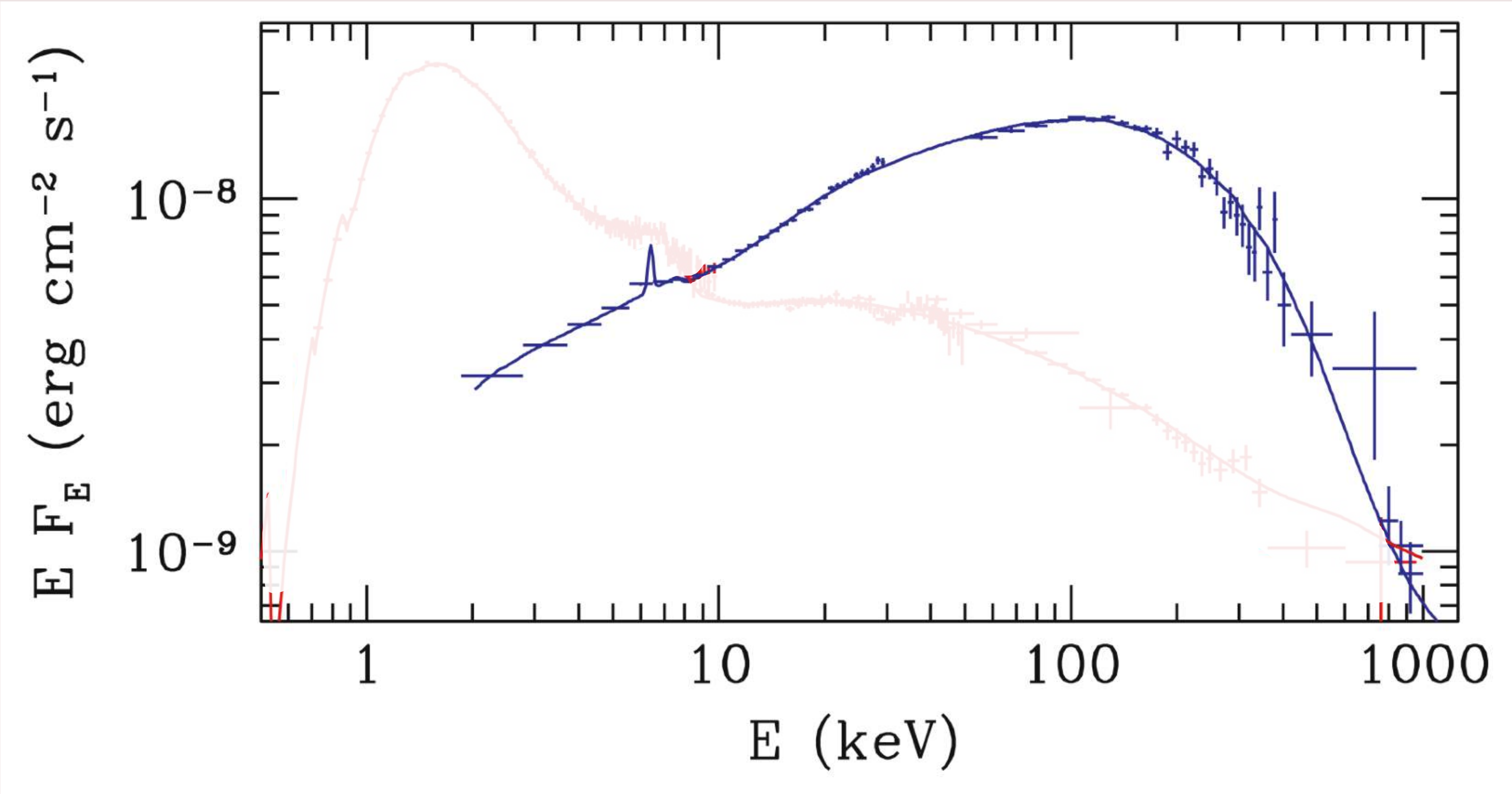

+ polarization measurements by IXPE

- $\tau_T = n_e \sigma_T s \sim 1, \sigma \sim 1\ldots10$
- $\gamma_{\rm rad} \gg \sigma$ (weak cooling), but $l_B \gg 1$ (large compactness)
- $T_e \sim T_{\rm ph} \sim 100$ keV
- $e^{\pm}$-production/-annihilation balance

Thomson optical depth

$\gg 1$

~ 1

$\ll 1$

XRB coronae

1 | $1\ldots10$ | 10^3 | 10^6 | $\geq 10^8$

magnetization (σ)

see *Giannios, & Uzdensky (2019), Petropoulou+ (2019), Christie+ (2019), Davelaar+ (2020), Sironi+ (2020), Davelaar+ (in prep.)*

Astrophysical relevance

Cen A jet, *EHT (2021)*

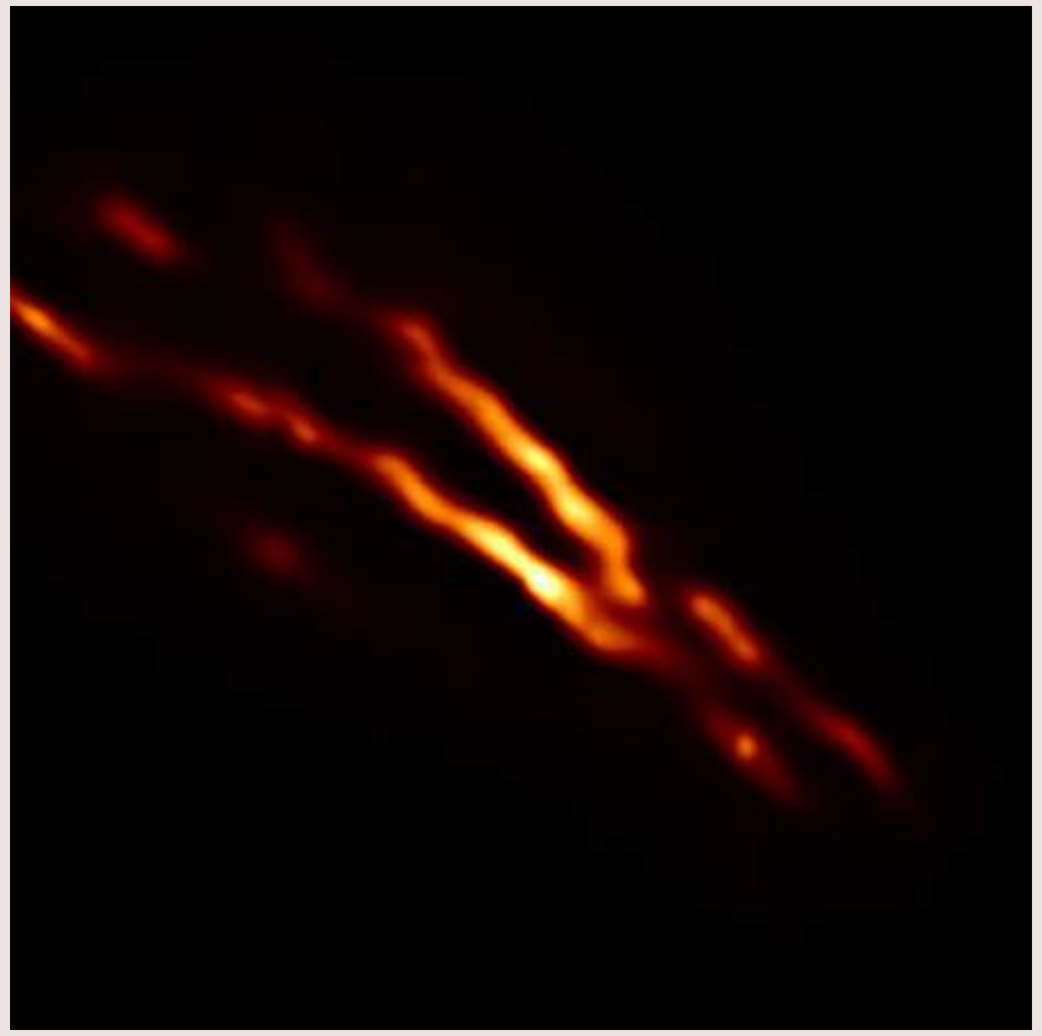

M87* polarized jet, *ALMA (2021)*

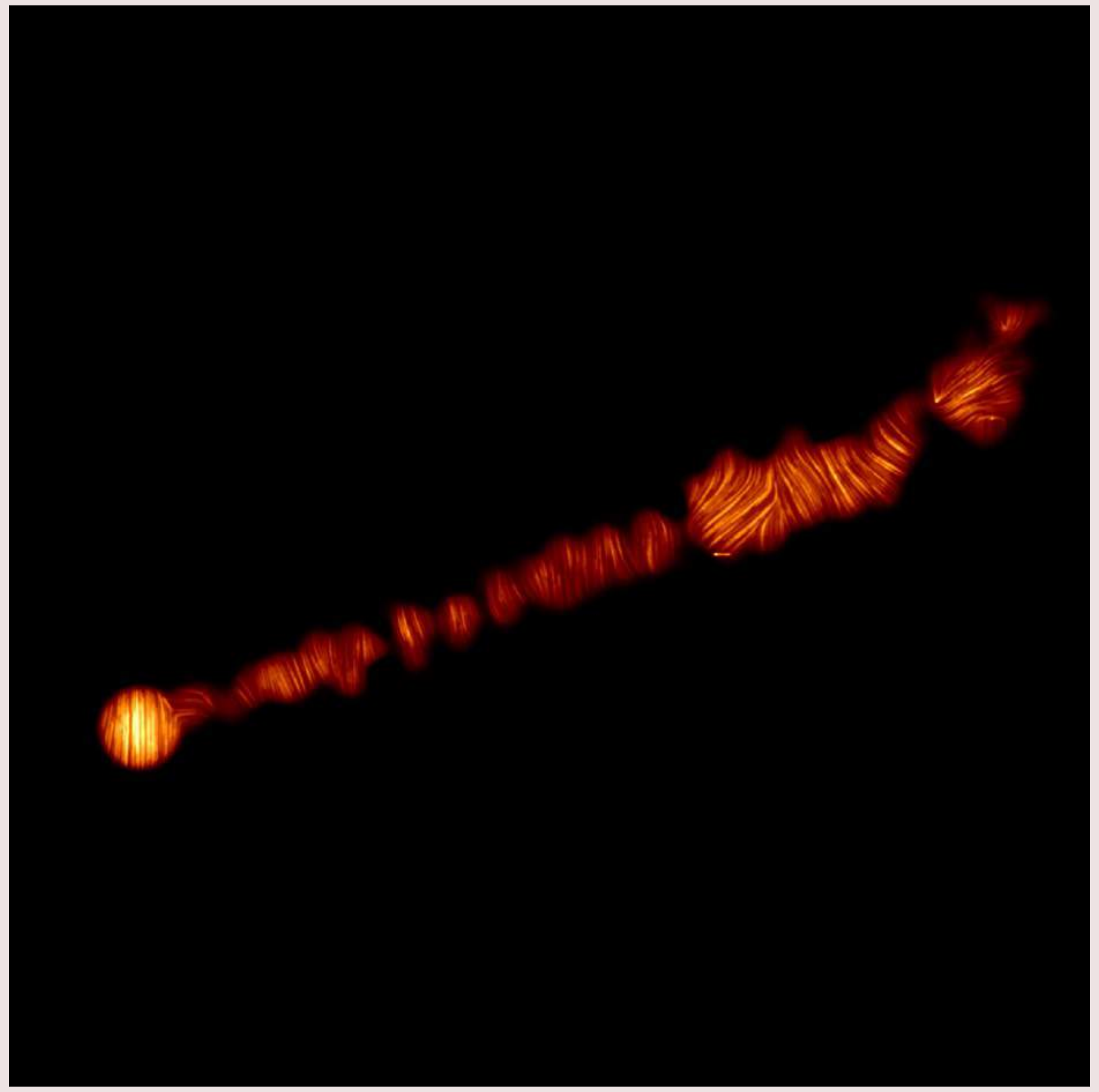

- stripes *or* reconnection-mediated KHI
- reconnection-mediated kink-instability

Thomson optical depth: $\gg 1$, ~ 1, $\ll 1$

XRB coronae

AGN jets

1 $1\ldots10$ 10^3 10^6 $\geq 10^8$

magnetization (σ)

see *Porth+ (2021), Uzdensky (DPP talk), Aimar+ (2023), Zhdankin+ (2023), Ripperda+ (in prep.)*

Astrophysical relevance

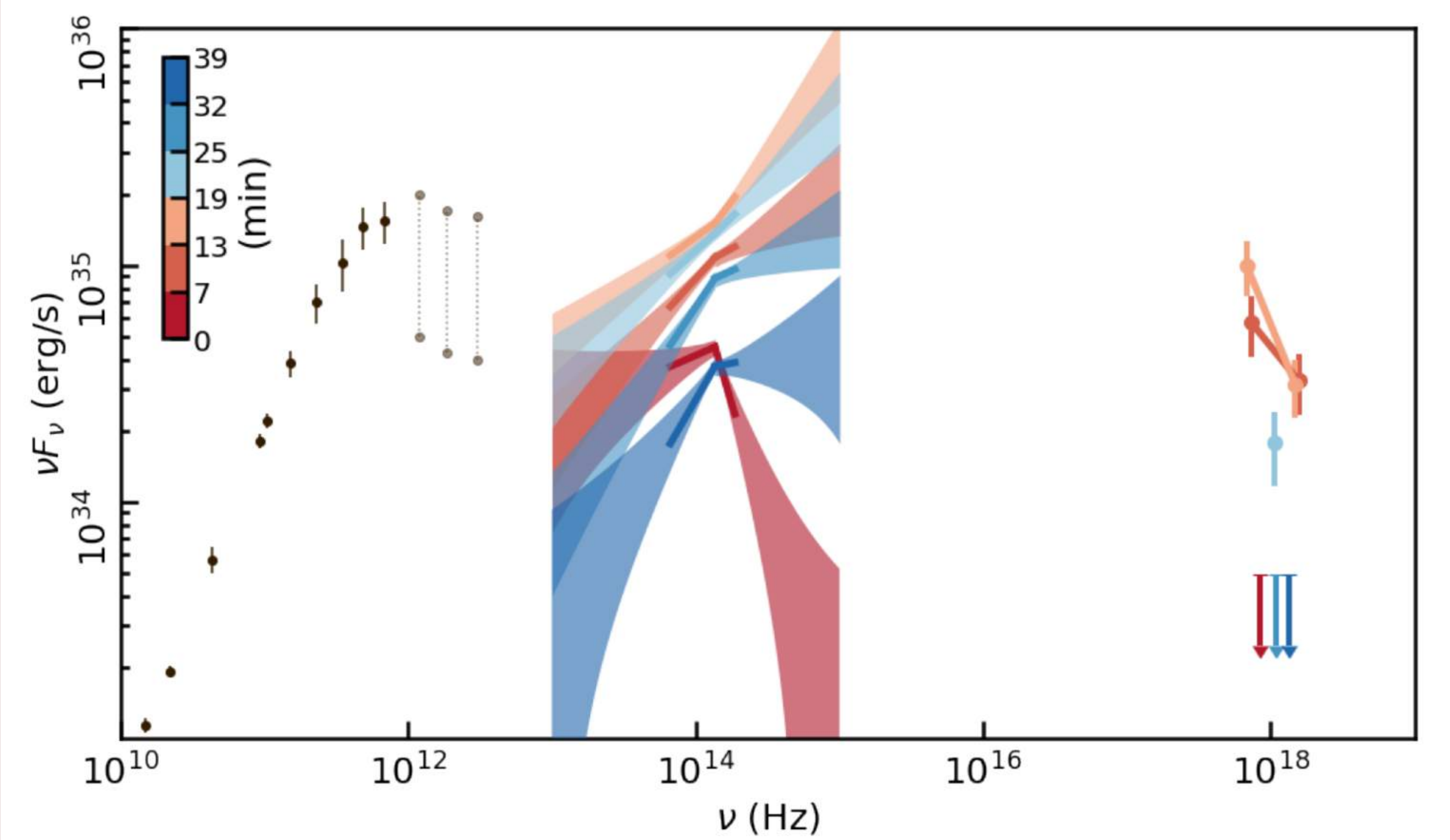

Sgr A* NIR/X-ray flare, *GRAVITY+SWIFT (2021)*

- RTI-mediated reconnection (?)
- dissipating magnetized "blob" in the disk (?)
- relatively small compactness $l_B \ll 1$, $\sigma \sim 1000$, $\gamma_{\rm rad} \gg \sigma$ (weak cooling)

orbiting post-flare "blob", *GRAVITY (2018)*

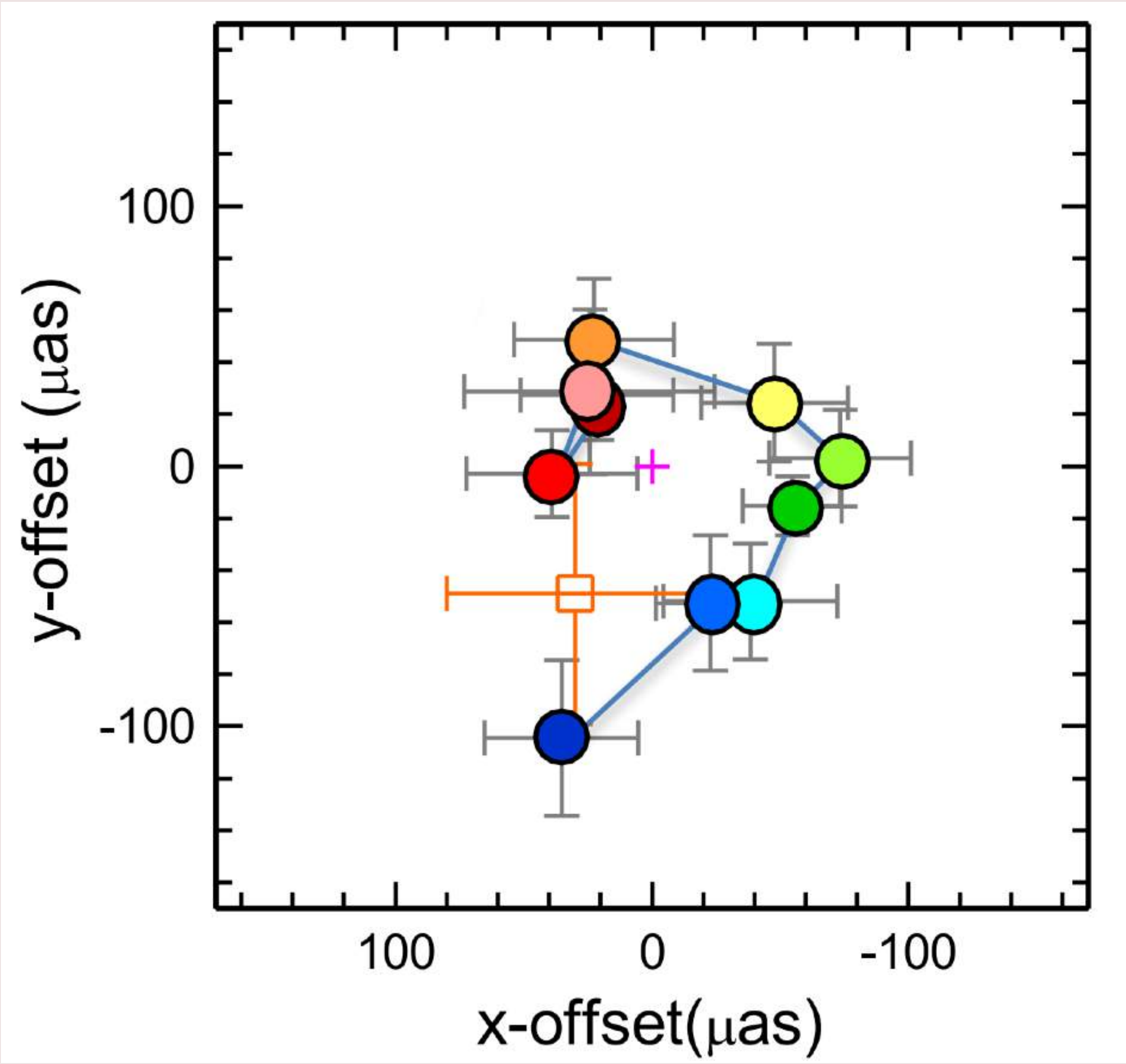

Thomson optical depth

$\gg 1$

~ 1

$\ll 1$

XRB coronae

AGN jets

Sgr A* acc. flow

1 $1\ldots10$ 10^3 10^6 $\geq 10^8$

magnetization (σ)

see *Philippov+ (2014-2018), Chen+ (2014), Cerutti+ (2016), HH+ (2019, 2023)*

Astrophysical relevance

γ-ray emission efficiency, *Fermi (2013)*

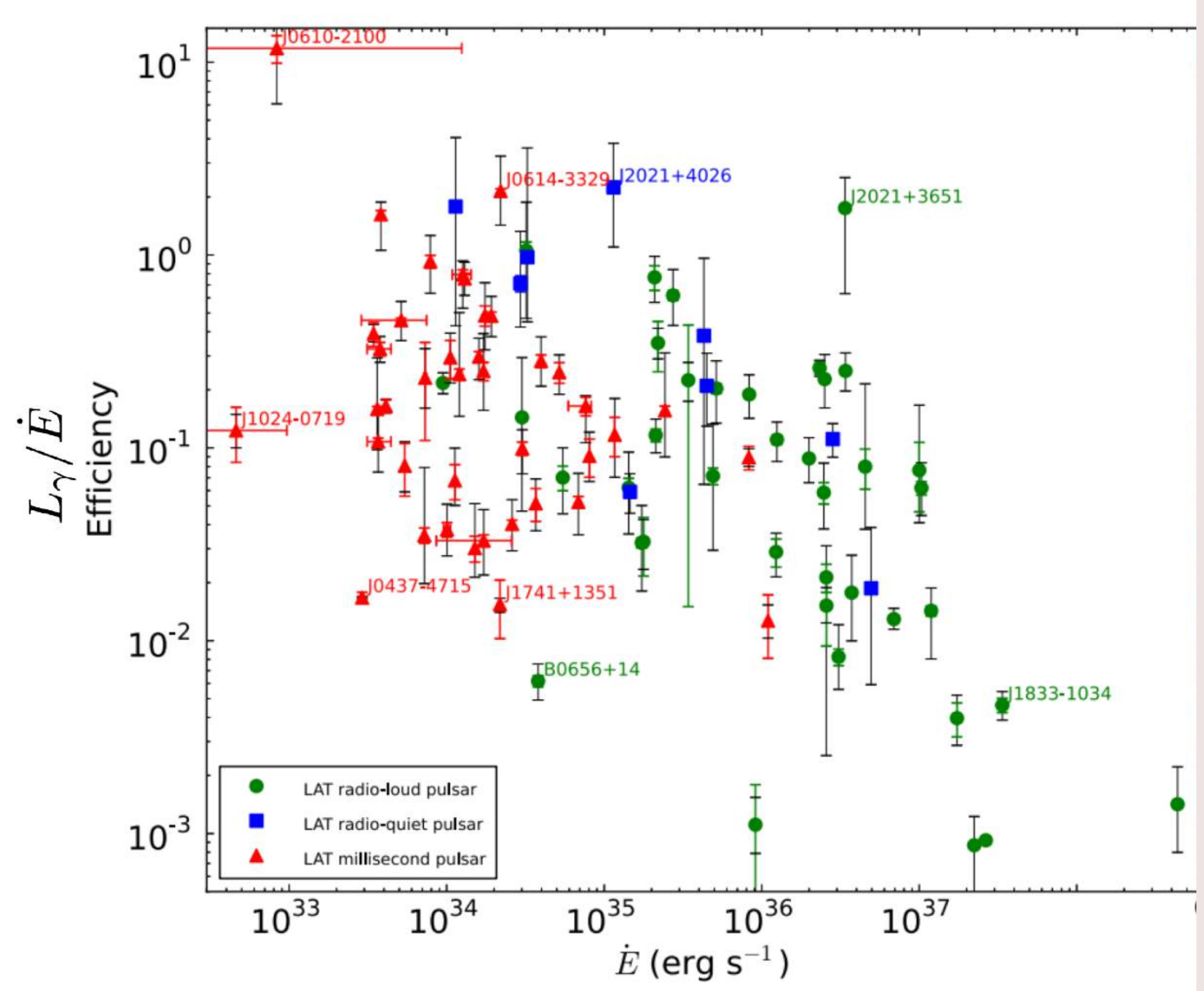

- pair-supply dominated by $\gamma\gamma \to e^{\pm}$, even though $\tau_{\gamma\gamma} \ll 1$
- $\sigma \sim 10^6$, $\gamma_{\rm rad} \leq \sigma$ (strong synchrotron cooling)
- Crab peaks around $\lesssim$ MeV, Vela peaks around GeV
- TeV emission observed

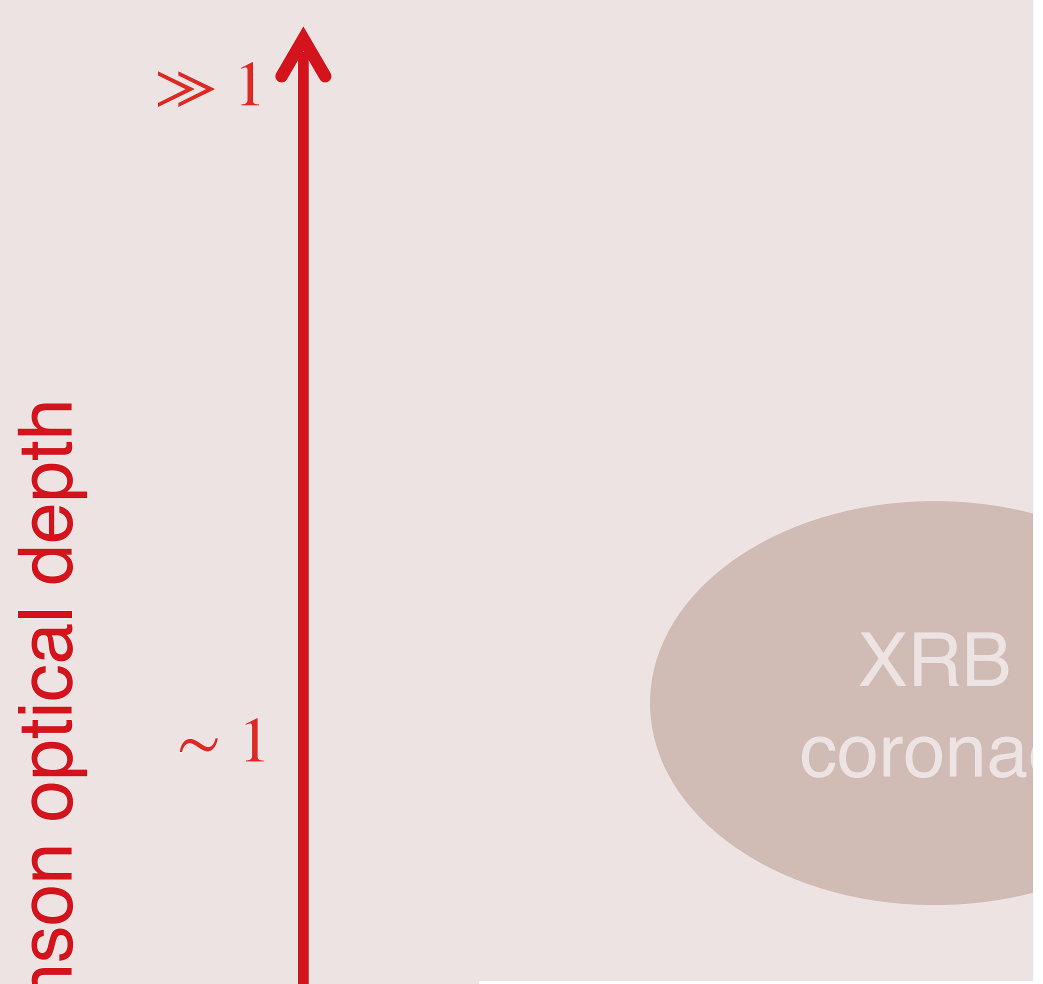

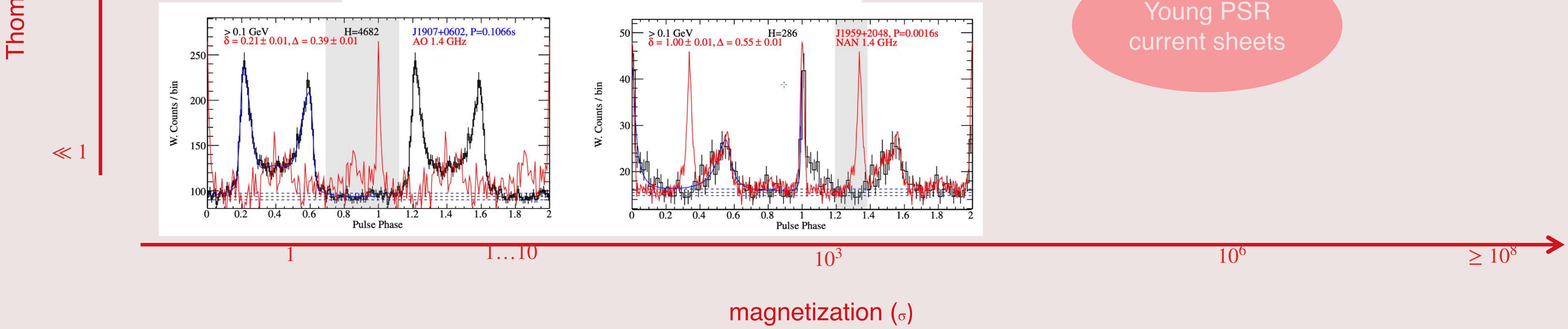

see *Ripperda+ (2022), Hakobyan+ (2023);*
also gap discharge models: *Levinson+ (2011, 2018), Chen+ (2018, 2020), Crinquand+ (2020)*

Astrophysical relevance

- high-luminosity TeV (+X-ray) flares
- $\sigma \geq 10^7$, $\gamma_{\rm rad} \leq \sigma$, peaks around 16 MeV
- jet base content is dominated by $e^{\pm}$-production
- periodicity is controlled by flux build-up/“eruption”

H.E.S.S. + MAGIC + Veritas: Abramowski+ (2012)

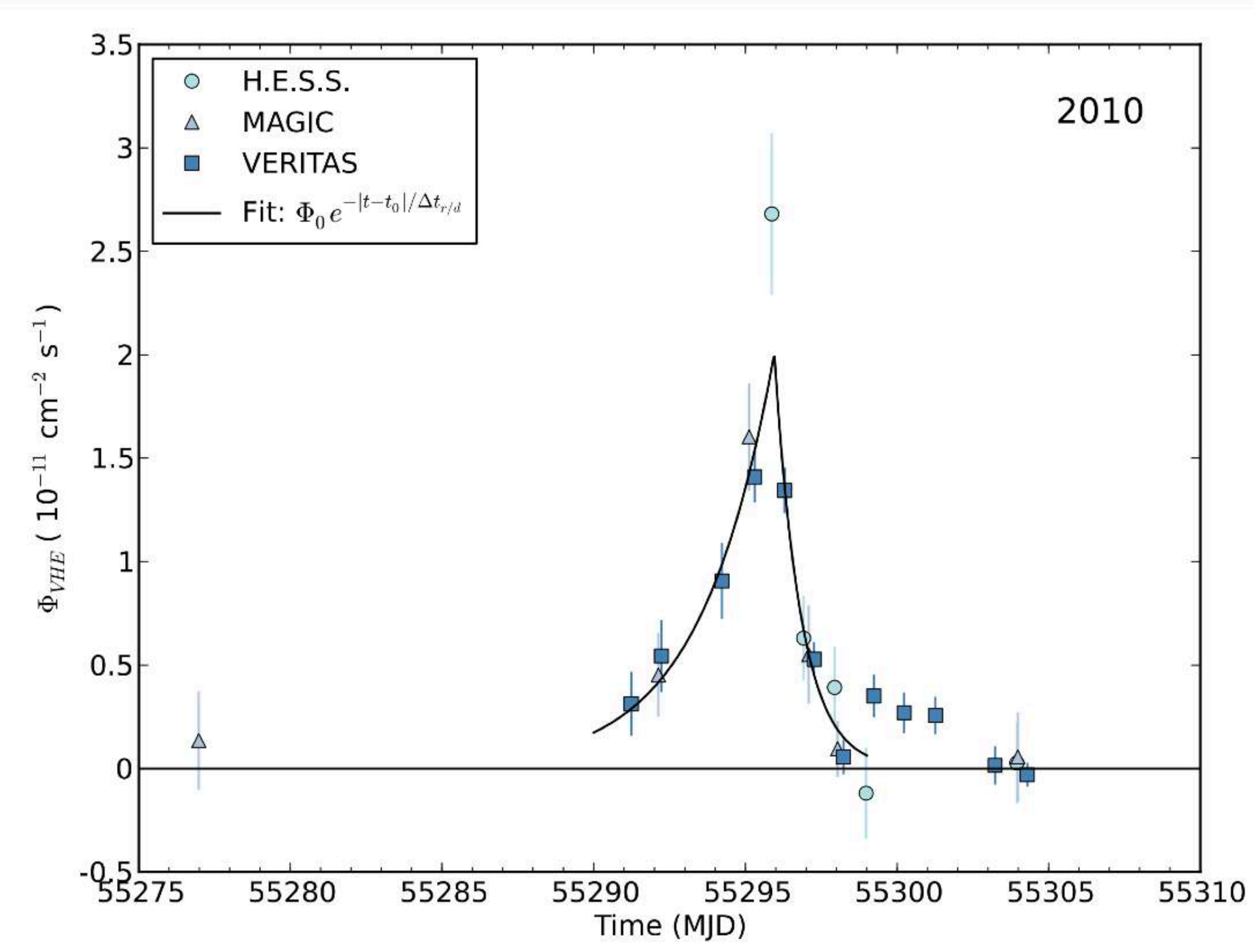

new data coming soon!

Algaba+ (2021)

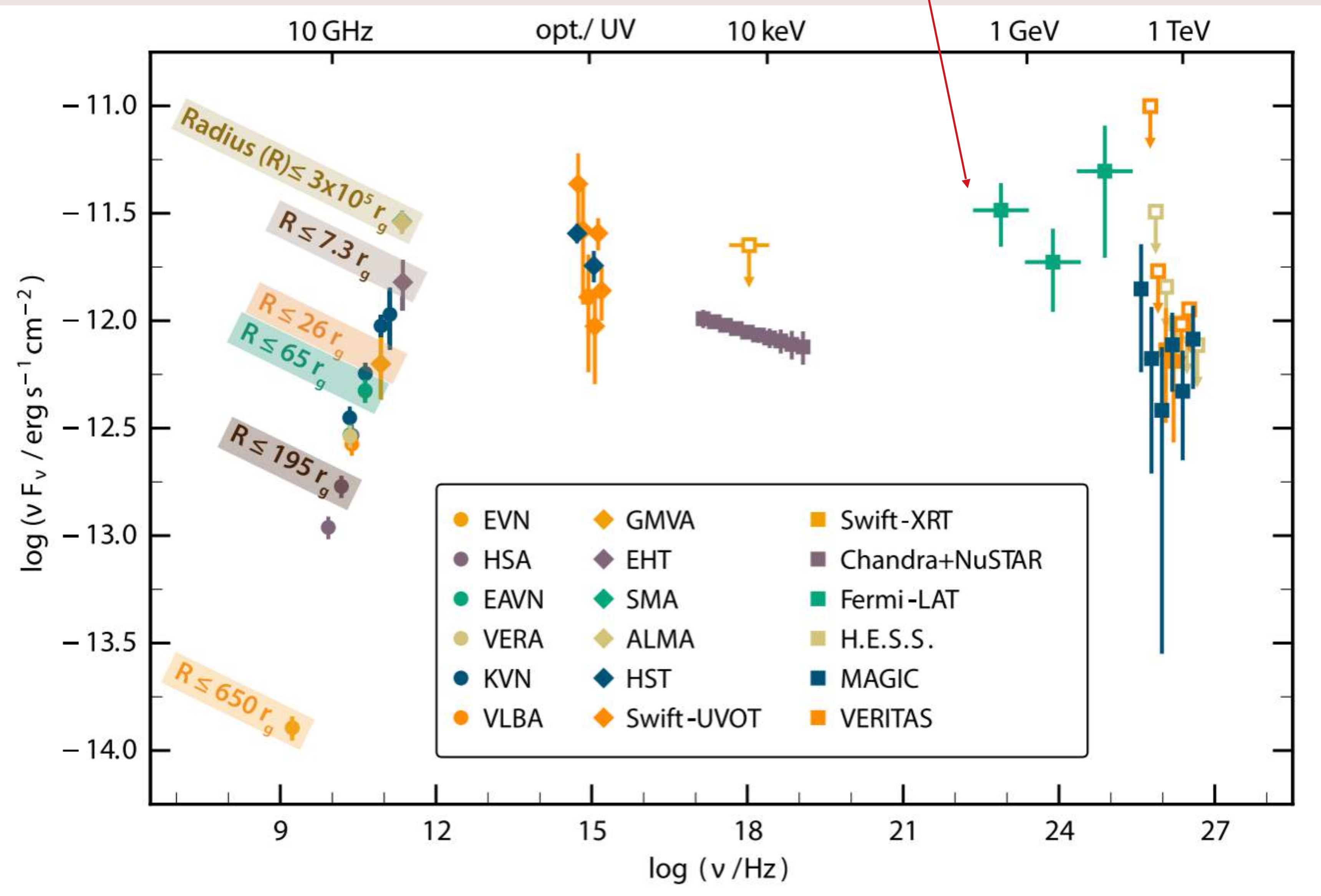

Thomson optical depth: $\ll 1$, ~ 1, $\gg 1$

Sgr A* acc. flow

Young PSR current sheets

M87* jet base

1 $1\ldots10$ 10^3 10^6 $\geq 10^8$

magnetization (σ)

see *Thompson (2008, 2020), Beloborodov (2013, 2021), Yuan+ (2020, 2022), Mahlmann+ (2022, 2023)*

Astrophysical relevance

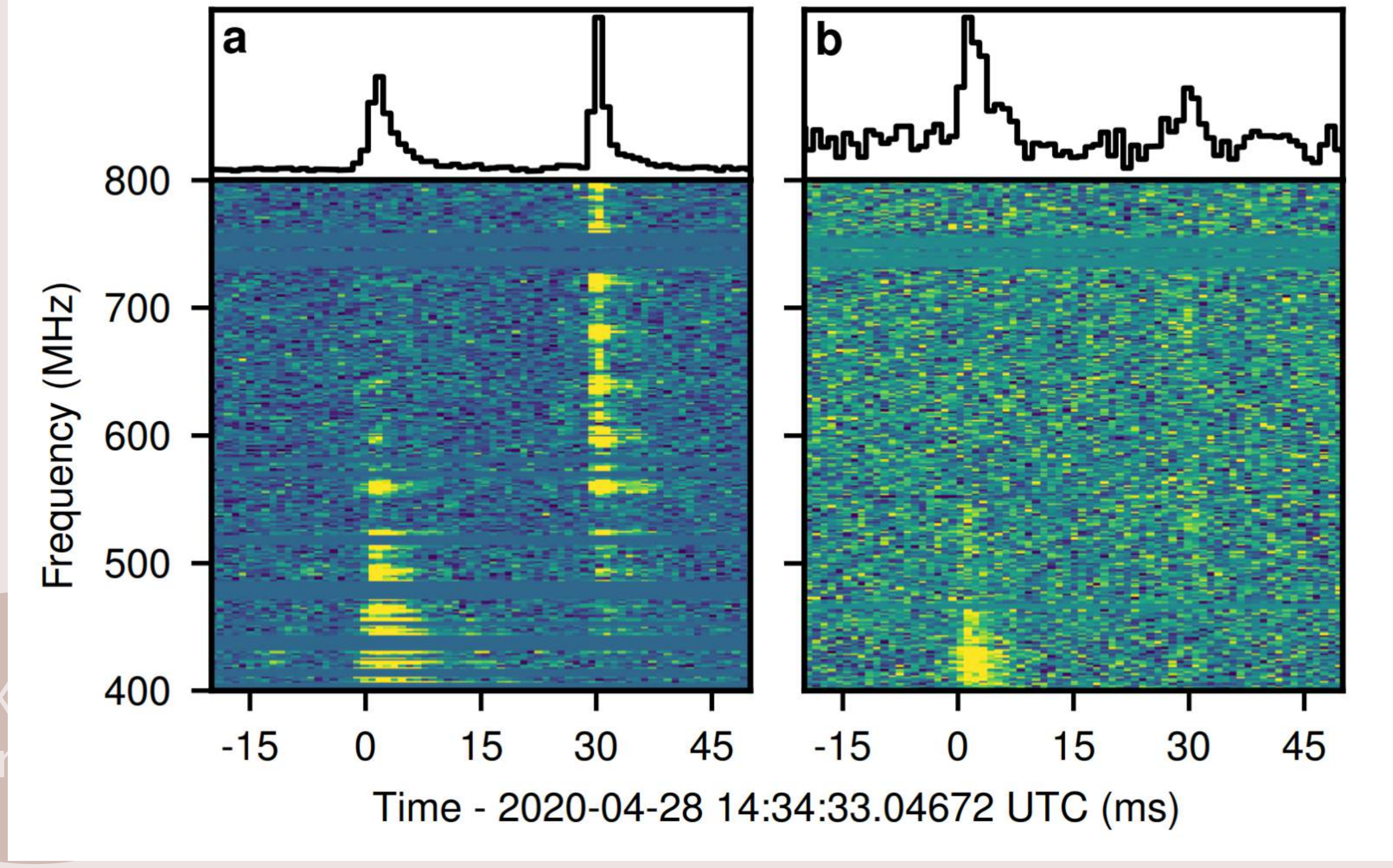

First FRB associated with a magnetar, *CHIME/FRB (2020)*

Magnetar flares

Reconnection near magnetar surface

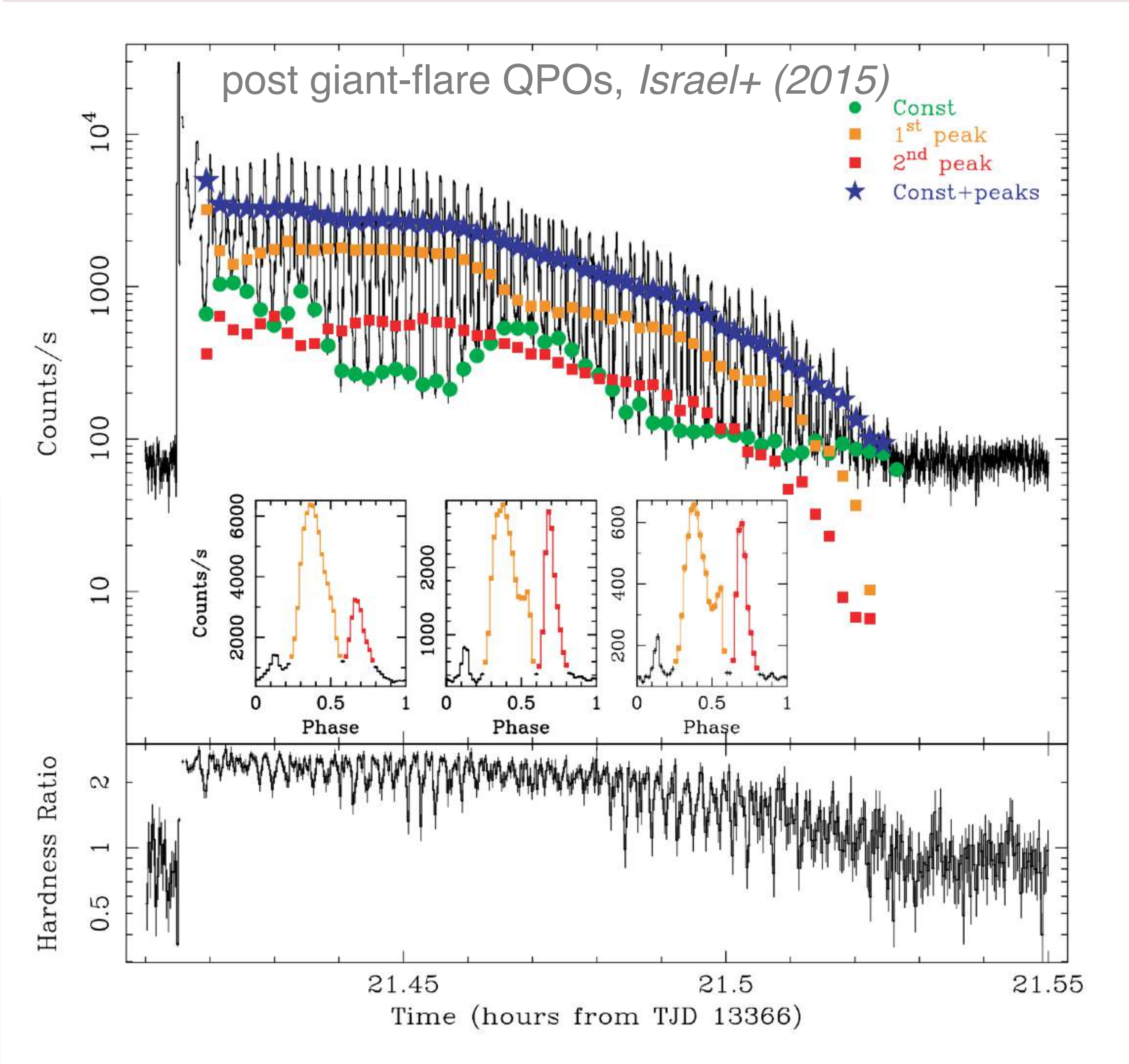

post giant-flare QPOs, *Israel+ (2015)*

AGN jets

Thomson optical depth: $\gg 1$, ~ 1, $\ll 1$

magnetization (σ): 1, $1\ldots10$, 10^3, 10^6, $\geq 10^8$

Astrophysical relevance

- We have now reached a point where we can simulate radiative/QED effects in reconnection (and not only) *ab-initio* (Tristan v2, Zeltron, OSIRIS)

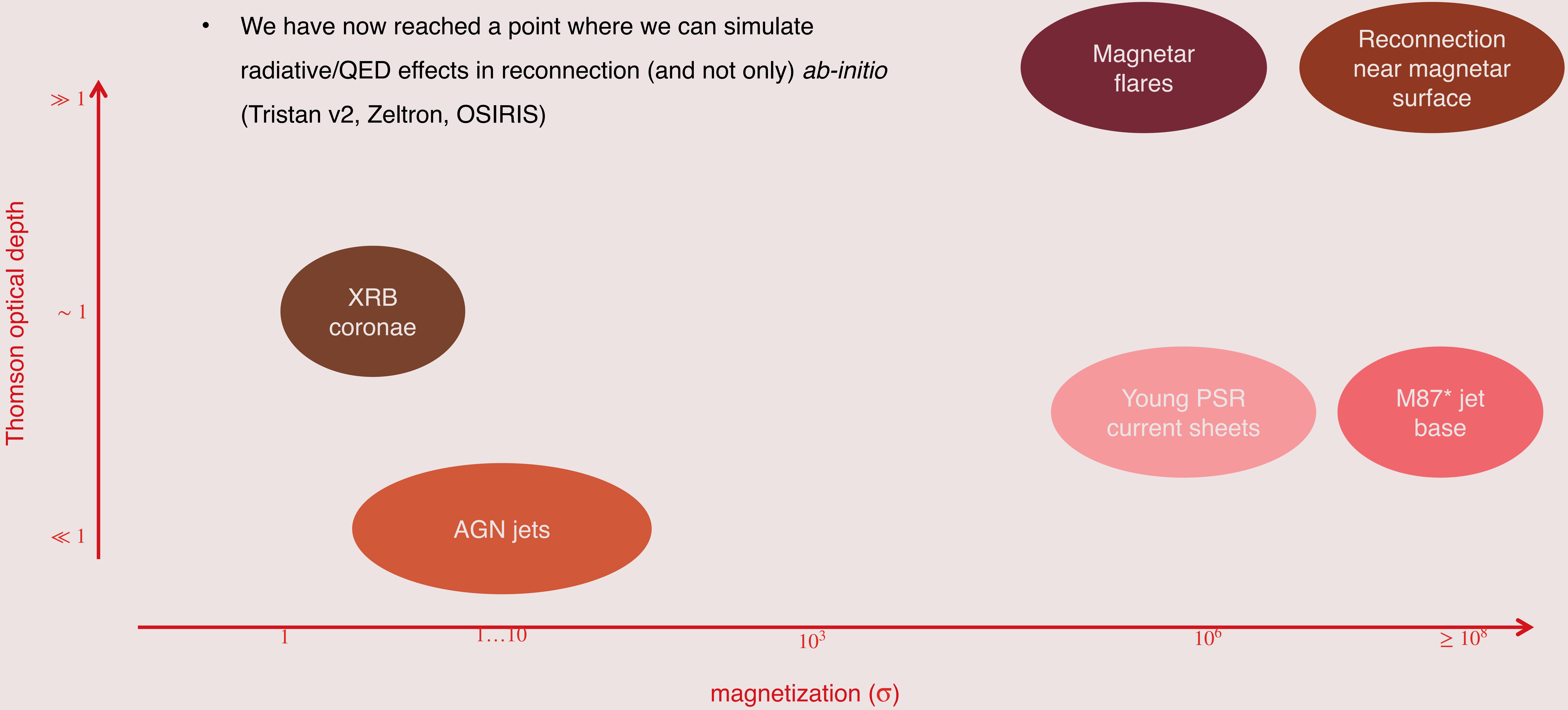

What is a pulsar?

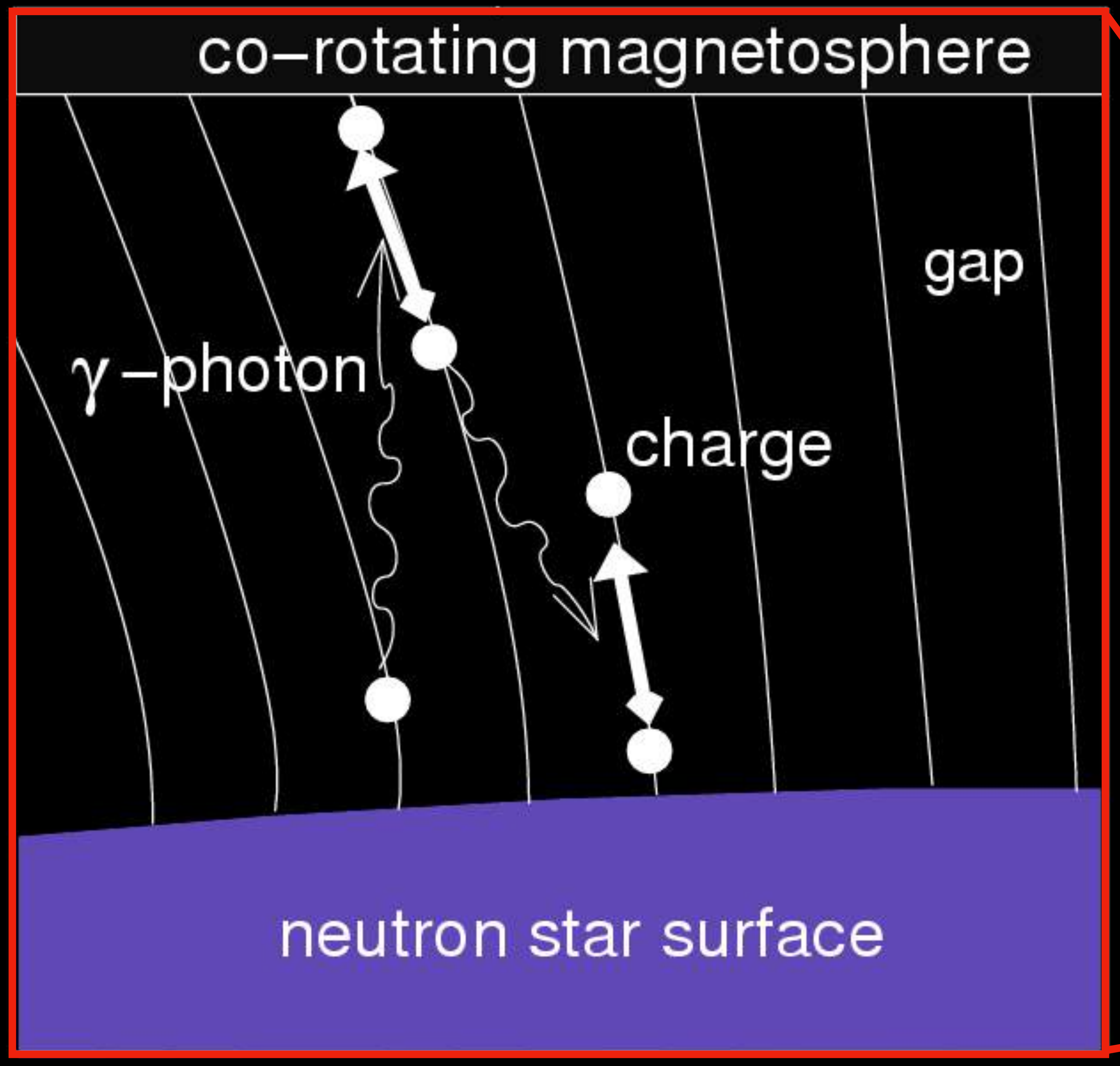

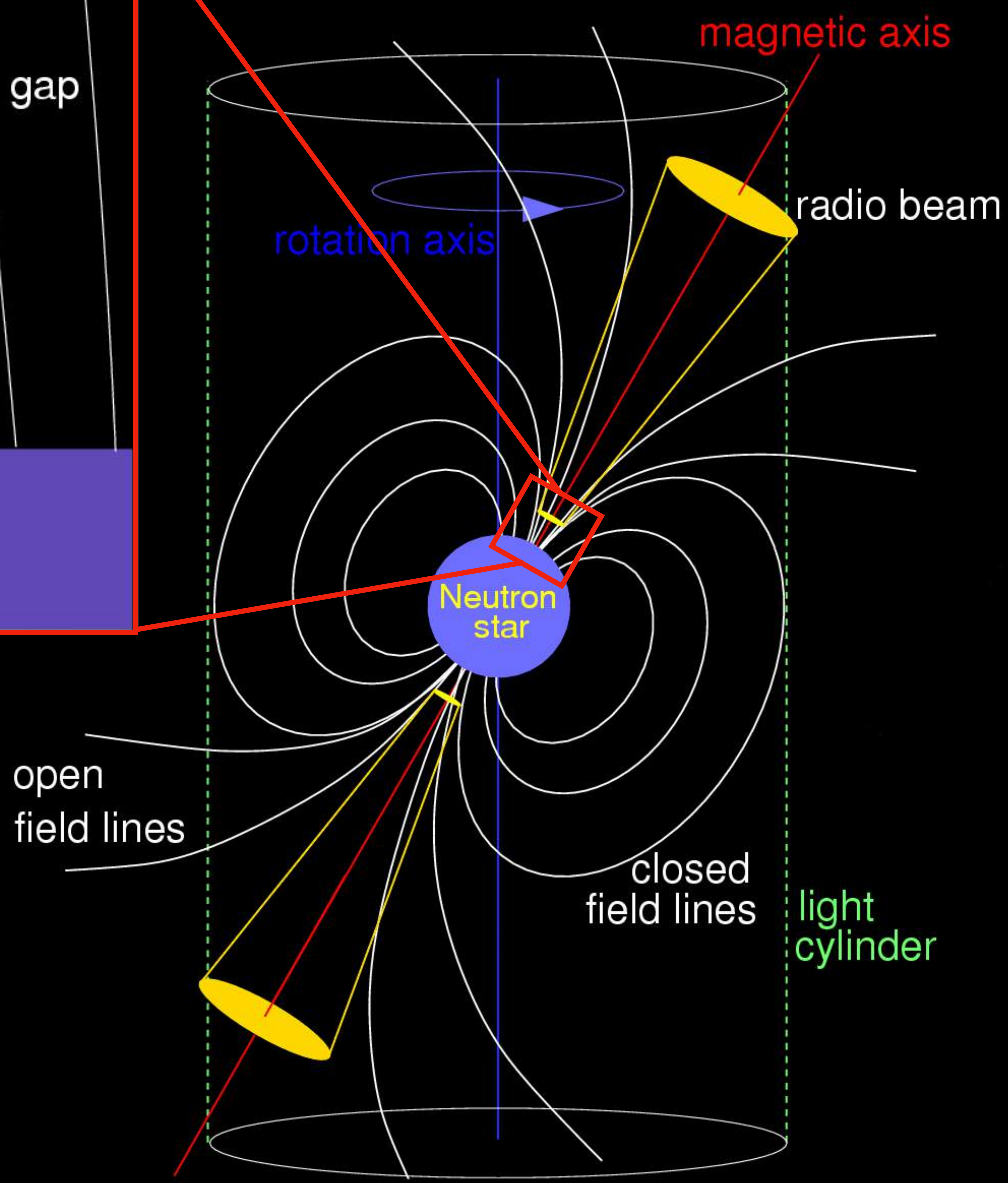

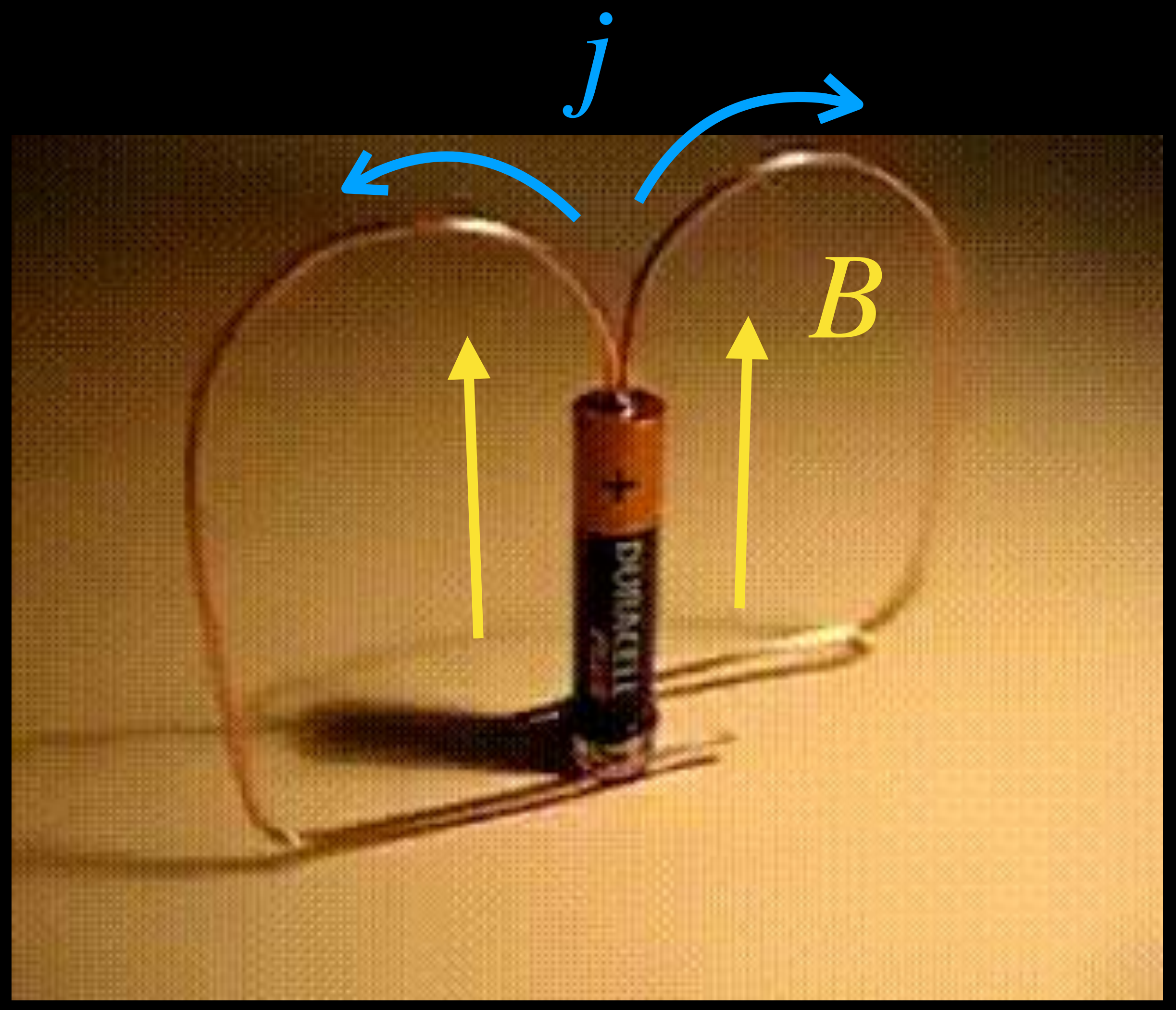

Unipolar induction

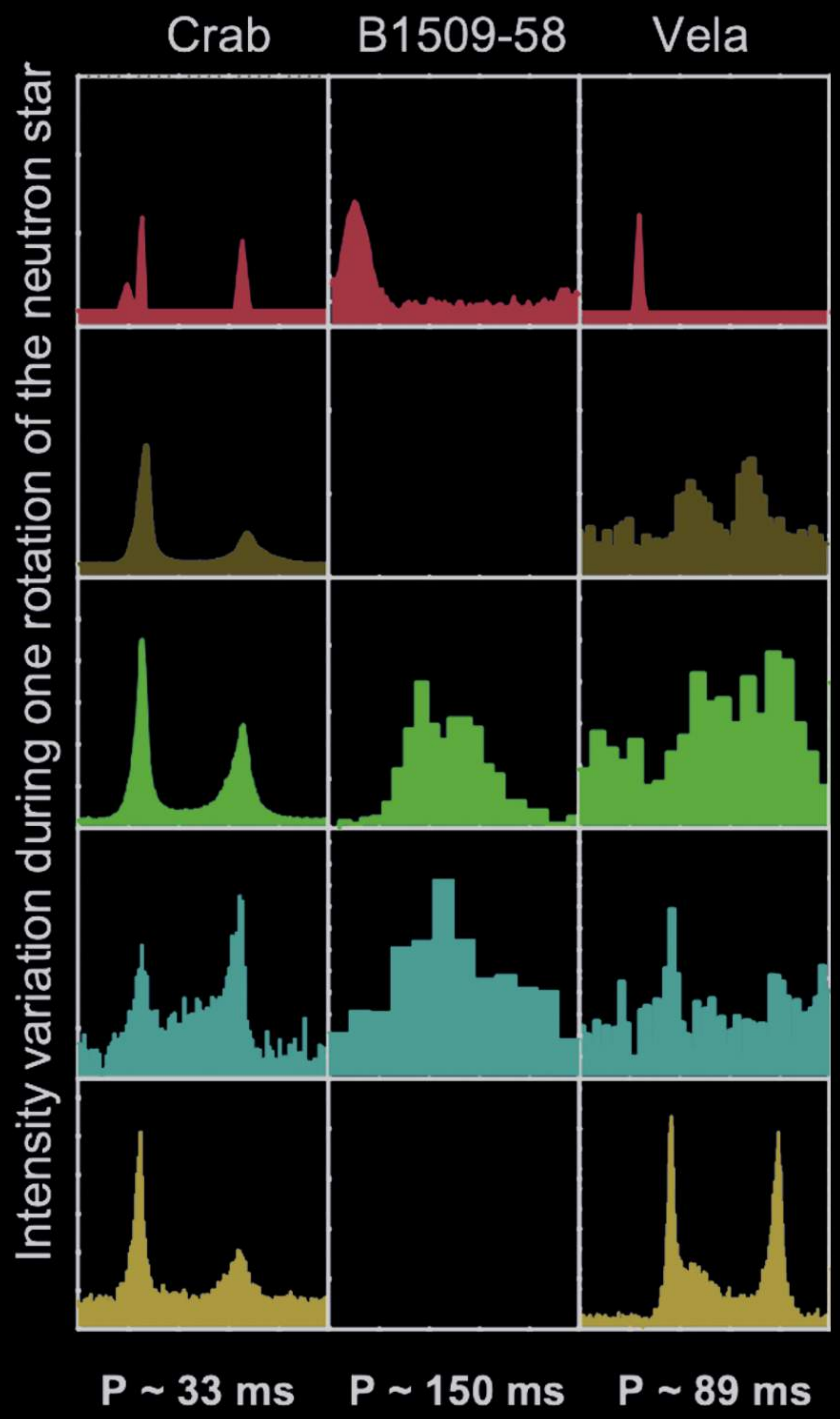

- corotation electric field: $\boldsymbol{E} + \dfrac{\boldsymbol{\Omega} \times \boldsymbol{r}}{c} \times \boldsymbol{B} = 0$;
- poynting flux: $\boldsymbol{E} \times \boldsymbol{B}$;
- electromagnetic energy losses
    - $B \sim 10^{12}$ G, $B^2/4\pi \gg \rho c^2$

Radiation:

- Electric field in the gap accelerates particles , which emit high-energy curvature photons.
- Synchrotron and resonant inverse-Compton photons are emitted by secondary pairs.

Pair production:

- Pairs are produced by all these photons.
  $\chi_a = \dfrac{1}{2} \dfrac{\epsilon_\gamma}{m_e c^2} \dfrac{B}{B_q} \sin\psi \sim \dfrac{1}{10}$ when $\tau(\chi_a) = 1$.
- Photon splitting, $\gamma -> \gamma + \gamma$, is only important in magnetars. The only pair source for $B \geq 4B_Q$ is the resonant scattering, which is very efficient for $\gamma \sim 10^3$.

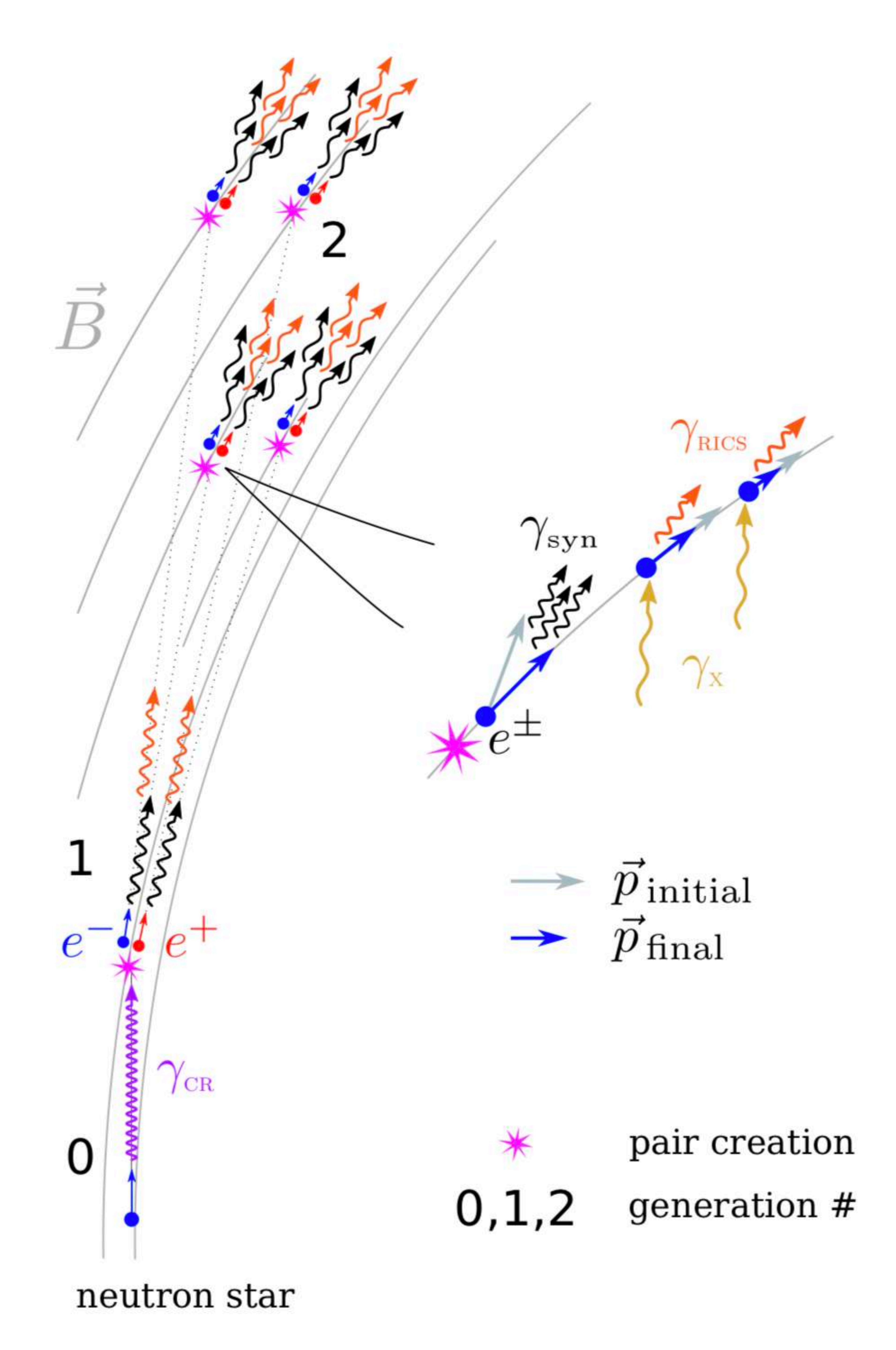

Timokhin, Harding (2015, 2019)

Theoretical cartoon: GJ model

- corotation electric field: $\boldsymbol{E} + \dfrac{\boldsymbol{\Omega} \times \boldsymbol{r}}{c} \times \boldsymbol{B} = 0$;
- sweepback of $\boldsymbol{B}$-field due to poloidal current;
- poynting flux: $\boldsymbol{E} \times \boldsymbol{B}$;
- electromagnetic energy losses.

$$\sigma = B^2/(4\pi\rho c^2) \gg 1$$

$$\rho_{\rm GJ} = -\frac{\boldsymbol{\Omega} \cdot \boldsymbol{B}}{2\pi c}$$

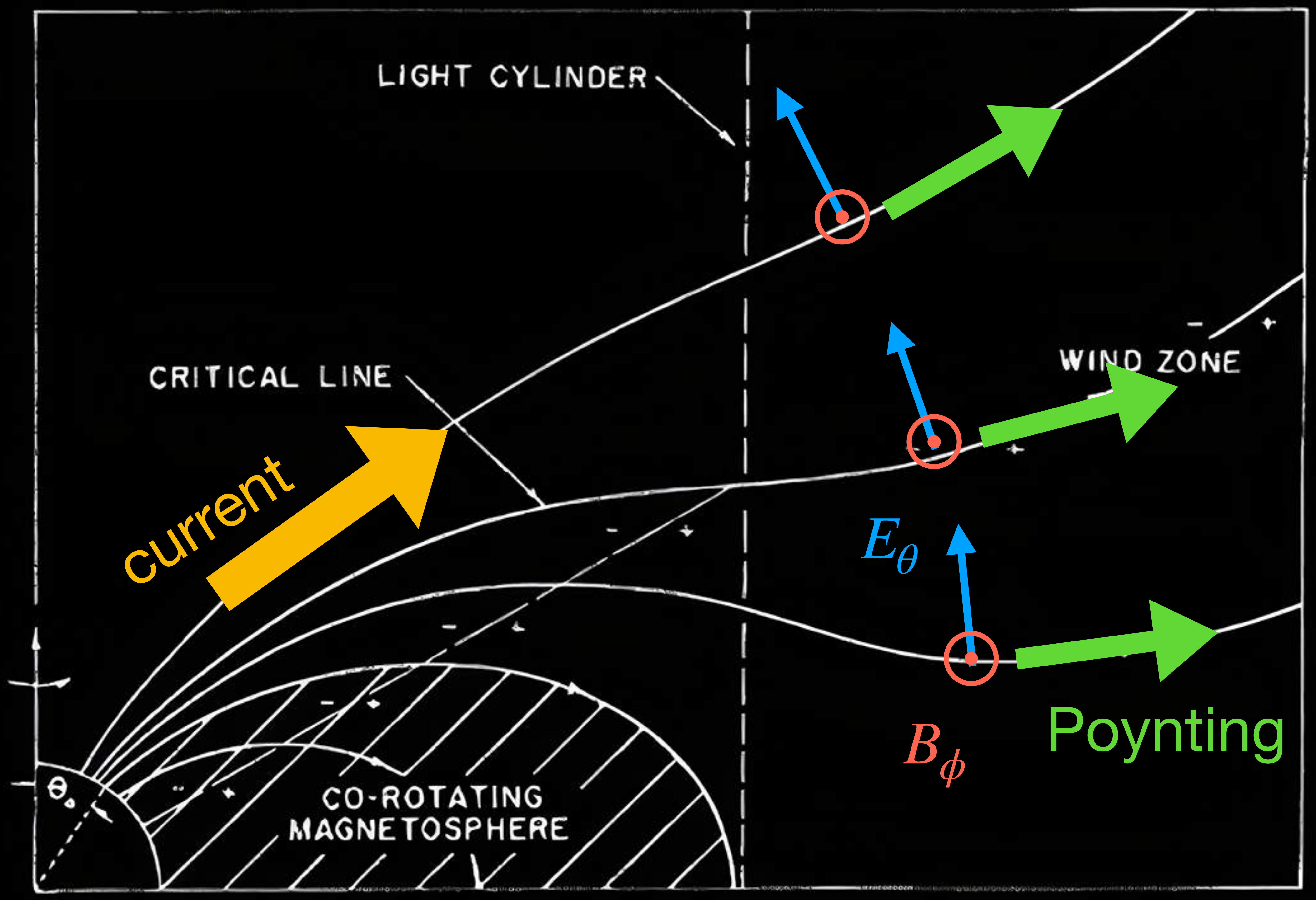

Goldreich & Julian (1969)

Standard pulsar

Force-free paradigm:

$$4\pi\rho_c = \nabla\cdot\boldsymbol{E}$$

$$\rho_c \boldsymbol{E} + \boldsymbol{j}\times\boldsymbol{B} = \frac{\mathrm{d}\rho_m \boldsymbol{u}}{\mathrm{d}t} + \text{pressure},\ \boldsymbol{E}\cdot\boldsymbol{B} = 0 \quad\Rightarrow\quad \boldsymbol{j} = \frac{c}{4\pi}\nabla\cdot\boldsymbol{E}\frac{\boldsymbol{E}\times\boldsymbol{B}}{B^2} + \frac{c}{4\pi}\frac{(\boldsymbol{B}\cdot\nabla\times\boldsymbol{B} - \boldsymbol{E}\cdot\nabla\times\boldsymbol{E})\,\boldsymbol{B}}{B^2}$$

$$+$$

$$\frac{1}{c}\frac{\partial \boldsymbol{E}}{\partial t} = \nabla\times\boldsymbol{B} - \frac{4\pi}{c}\boldsymbol{j}, \qquad \frac{1}{c}\frac{\partial \boldsymbol{B}}{\partial t} = -\nabla\times\boldsymbol{E}$$

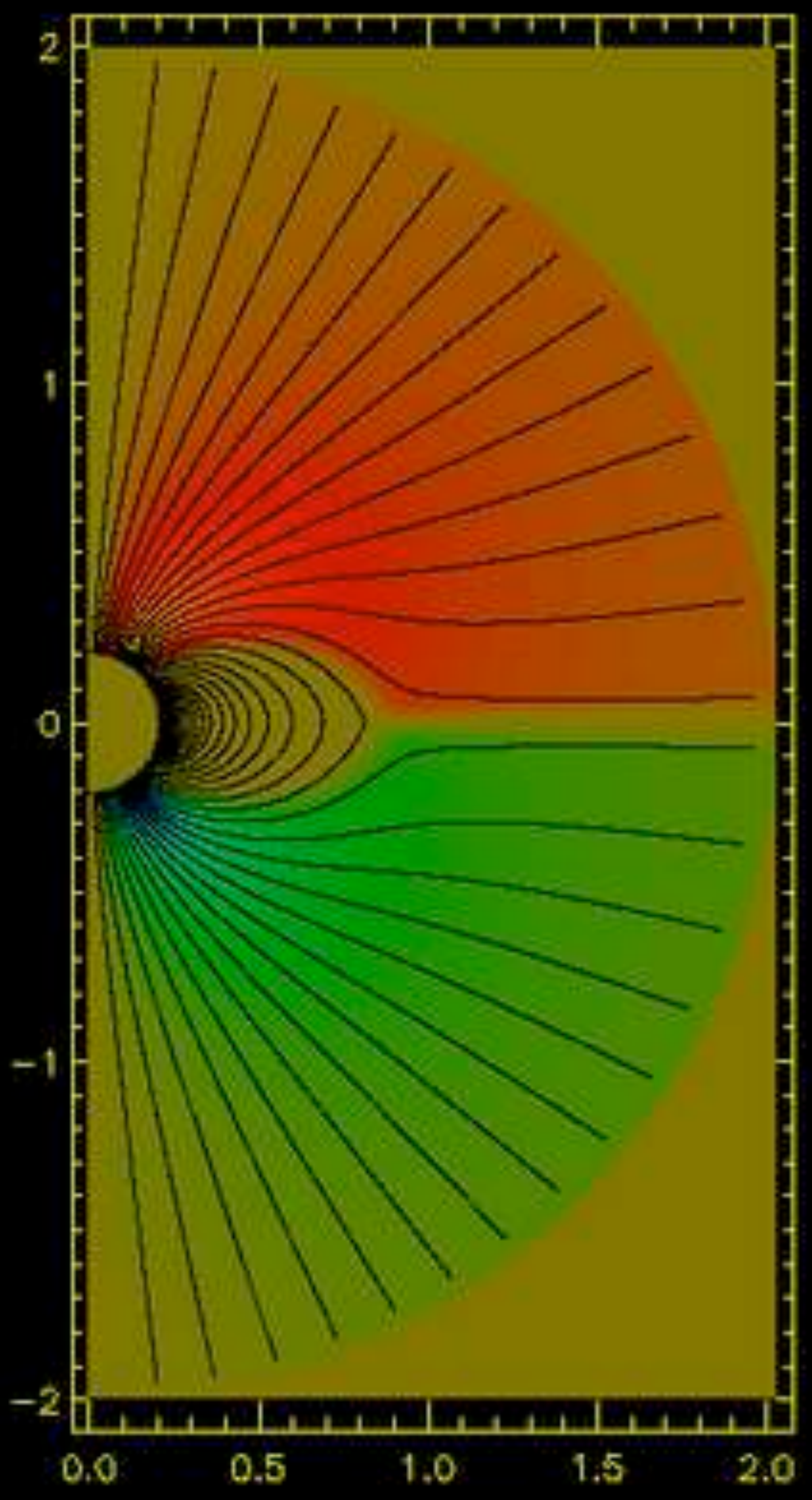

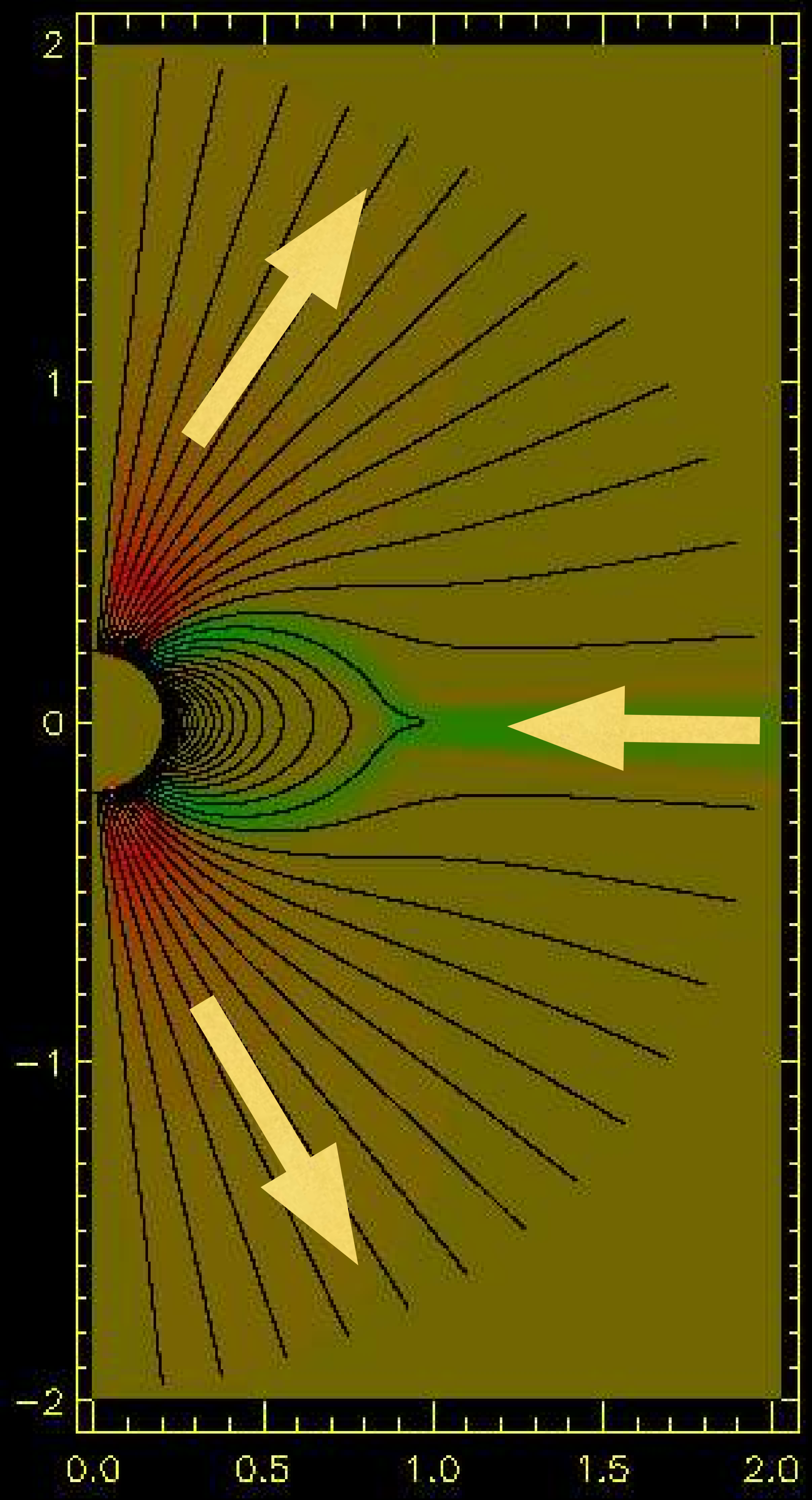

- Y-point;
- closed/open field lines;
- current sheet;
- field lines are asymptotically radial;
- predicts the spindown law:

$$L_{\mathrm{psr}} = k_1\frac{\mu^2\Omega^4}{c^3}\left(1 + k_2\sin^2\alpha\right)$$

Contopoulos+ (1999), Spitkovsky (2006), Kalapotharakos (2009), Petri (2012), Tchekhovskoy+ (2014) (MHD)

Plasma Physics on a computer: (GR)(R)PIC

$$\frac{\mathrm{d}x^i}{\mathrm{d}t} = \frac{\alpha}{m\Gamma}p^i - \beta^i$$

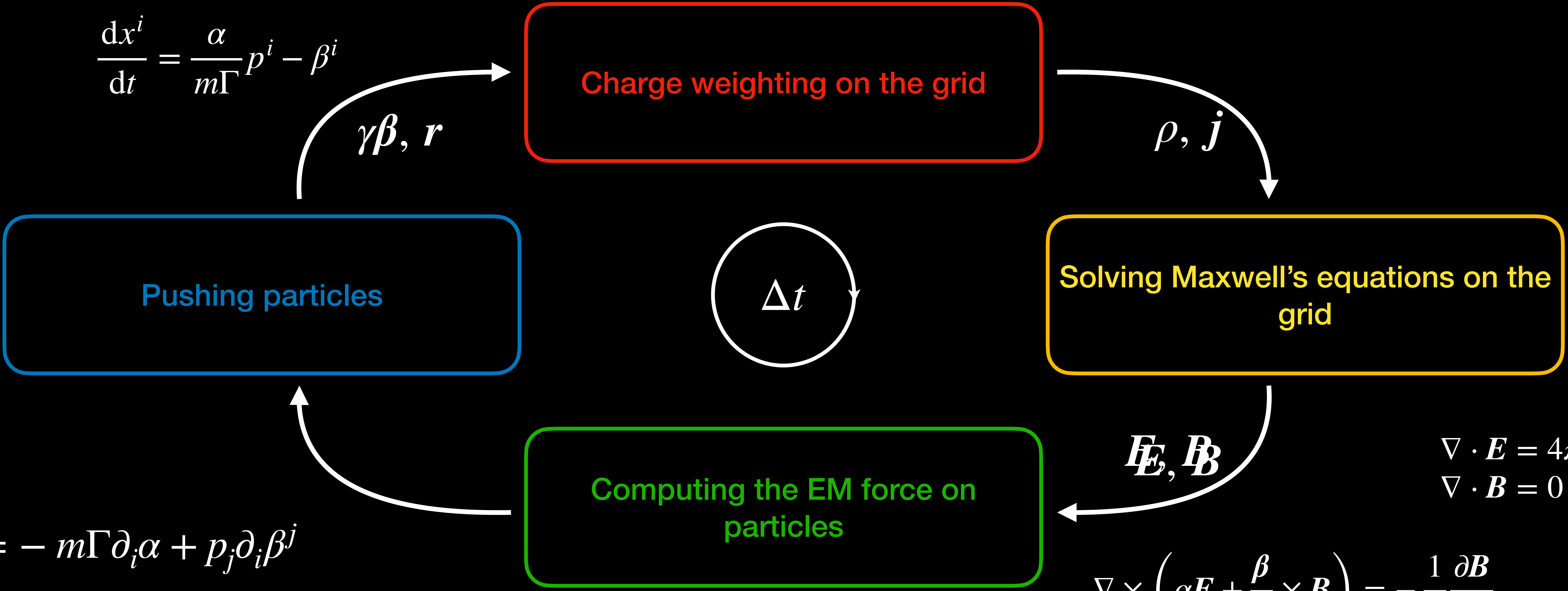

$$\nabla \cdot \boldsymbol{E} = 4\pi\rho$$
$$\nabla \cdot \boldsymbol{B} = 0$$

$$\frac{\mathrm{d}p_i}{\mathrm{d}t} = -m\Gamma\partial_i\alpha + p_j\partial_i\beta^j - \frac{\alpha}{2\Gamma m}\partial_i\left(\gamma^{lm}\right)p_l p_m + q\left\{\alpha D_i + \epsilon_{ijk}(v^j + \beta^j)B^k\right\}$$

$$\nabla \times \left(\alpha \boldsymbol{E} + \frac{\boldsymbol{\beta}}{c} \times \boldsymbol{B}\right) = -\frac{1}{c}\frac{\partial \boldsymbol{B}}{\partial t}$$

$$\nabla \times \left(\alpha \boldsymbol{B} - \frac{\boldsymbol{\beta}}{c} \times \boldsymbol{E}\right) = \frac{1}{c}\frac{\partial \boldsymbol{E}}{\partial t} + \alpha\boldsymbol{j} - \rho\boldsymbol{\beta}$$

(R) = radiation reaction force, photon emission, multiple pair production mechanisms

3D aligned rotator

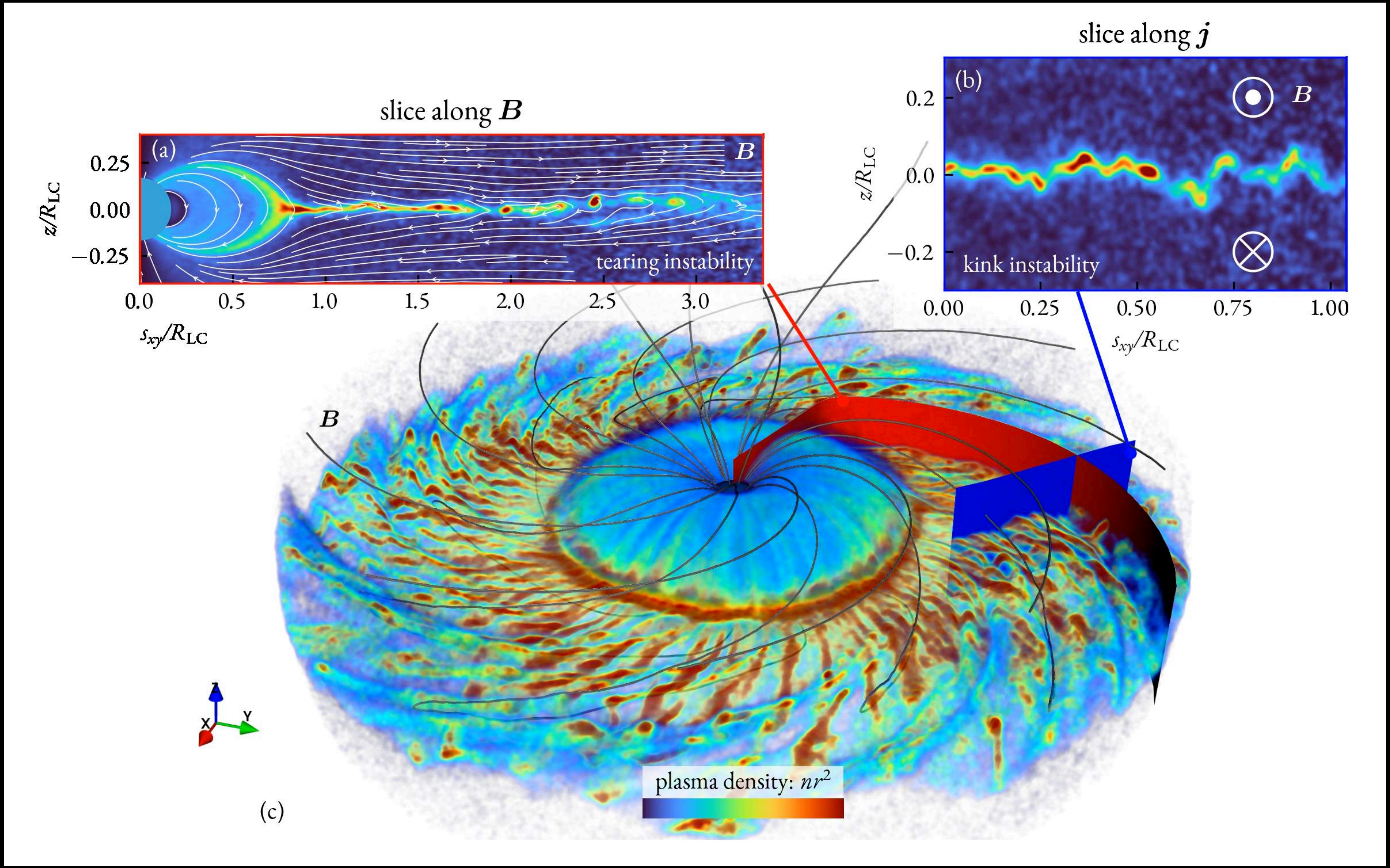

- Non-stationary discharge powers coherent radio emission
- Relativistic magnetic reconnection in the current sheet powers high-energy emission
- Current sheet is unstable to plasmoid (tearing) and drift-kink instabilities

Hakobyan et. al., 2023, ApJ

(GR) Oblique rotator with pair production

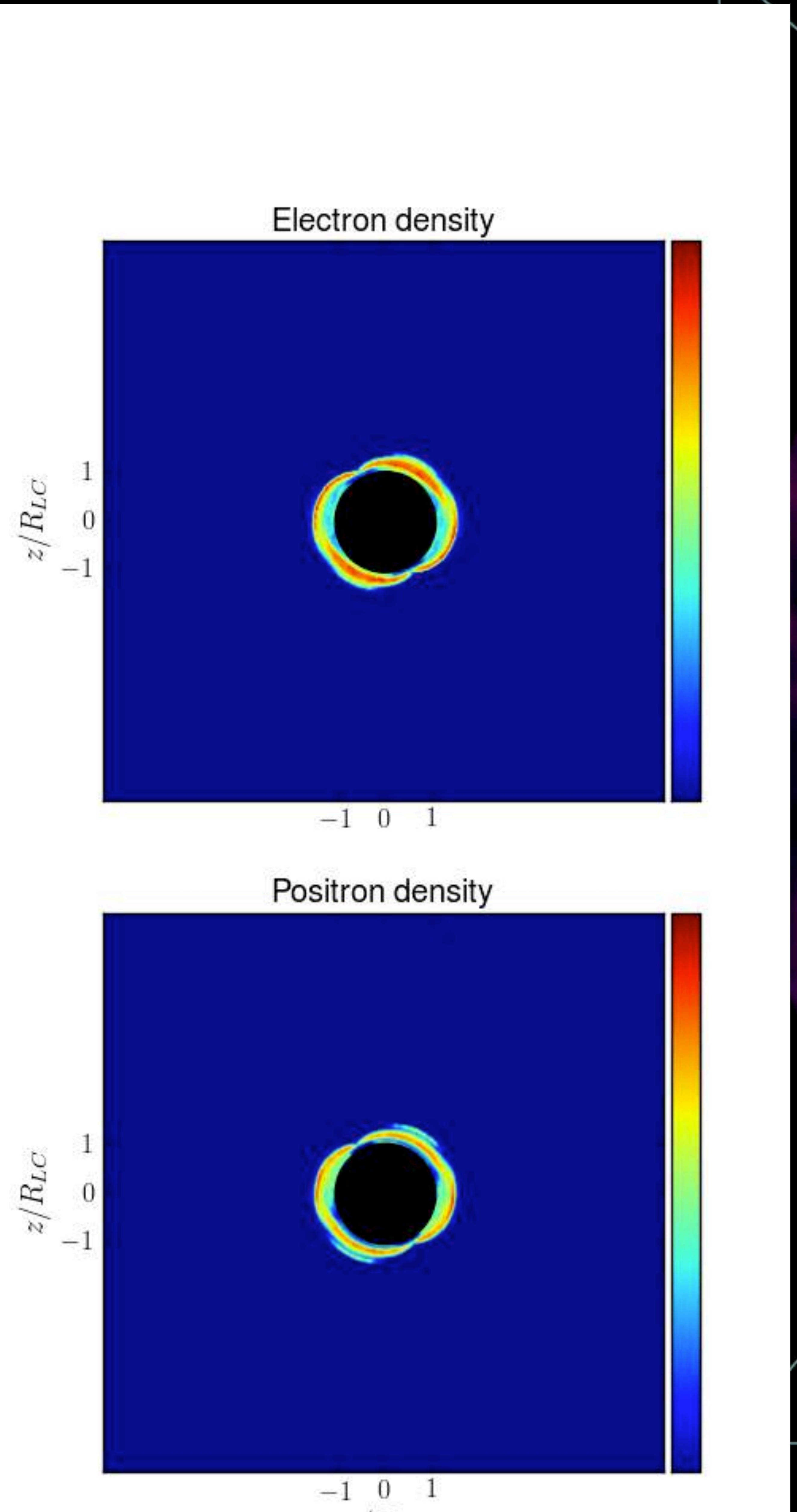

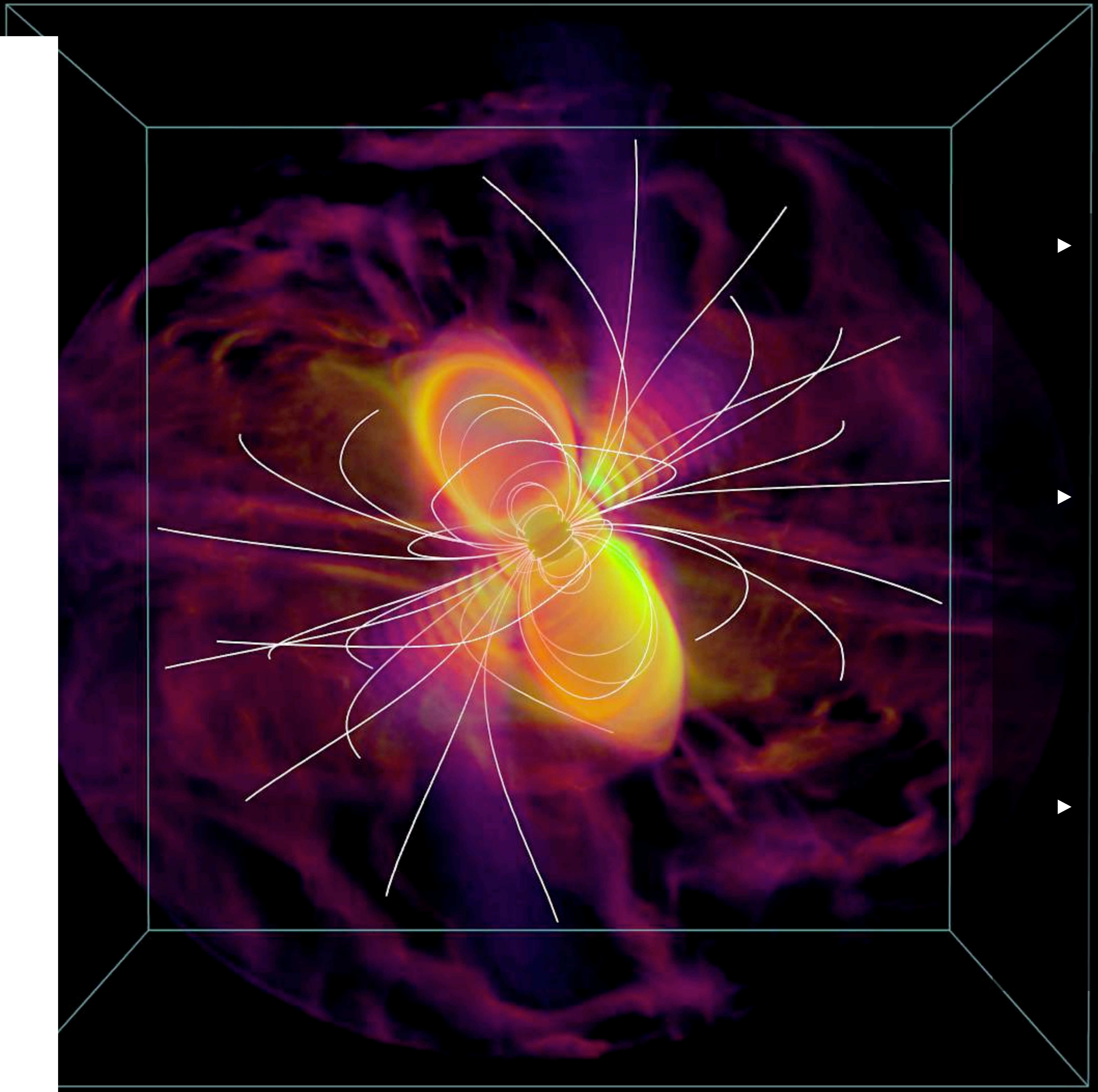

Philippov, Spitkovsky (2018)

- Non-stationary discharge powers coherent radio emission
- Relativistic magnetic reconnection in the current sheet powers high-energy emission
- Current sheet is unstable to plasmoid (tearing) and drift-kink instabilities

Gamma-ray modeling

Simulations prefer current sheet as a particle accelerator. Particles radiate synchrotron emission.

Observe caustic emission.

Predict gamma-ray efficiencies 1-20% depending on the inclination angle and pair production efficiency in the sheet. Higher inclinations are less dissipative.

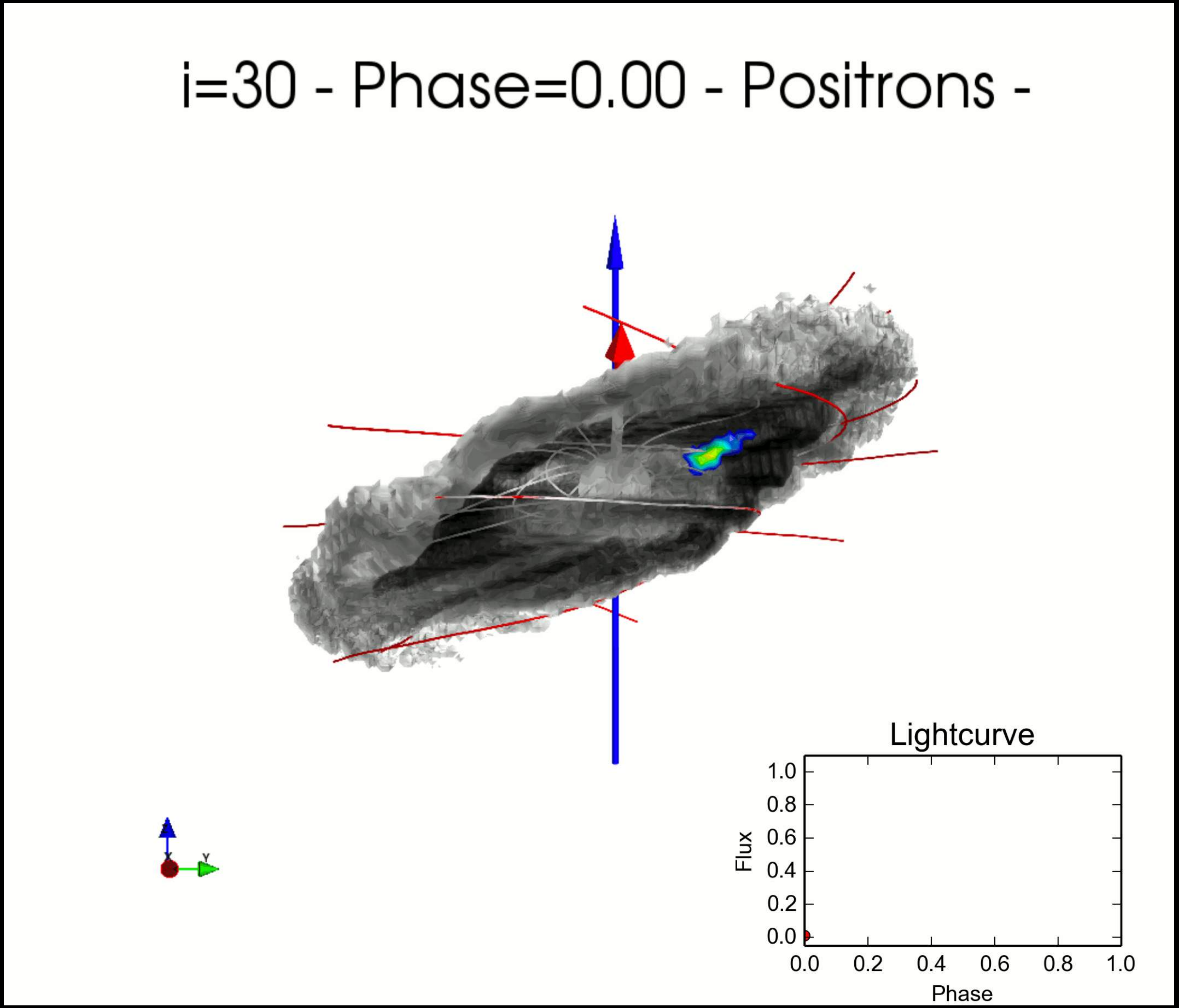

Cerutti, Philippov, Spitkovsky (2016); Philippov, Spitkovsky (2018)

Polar radio emission

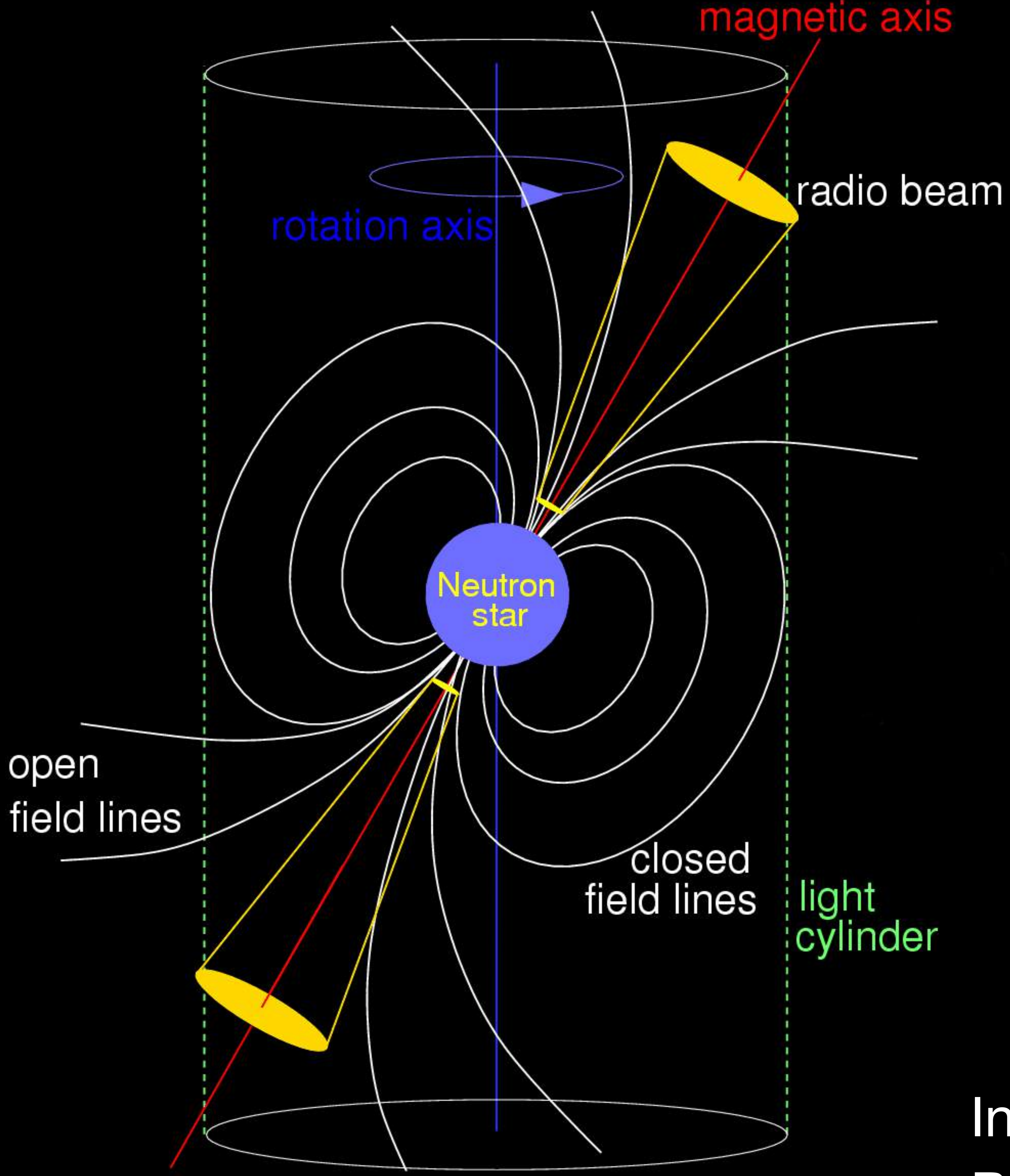

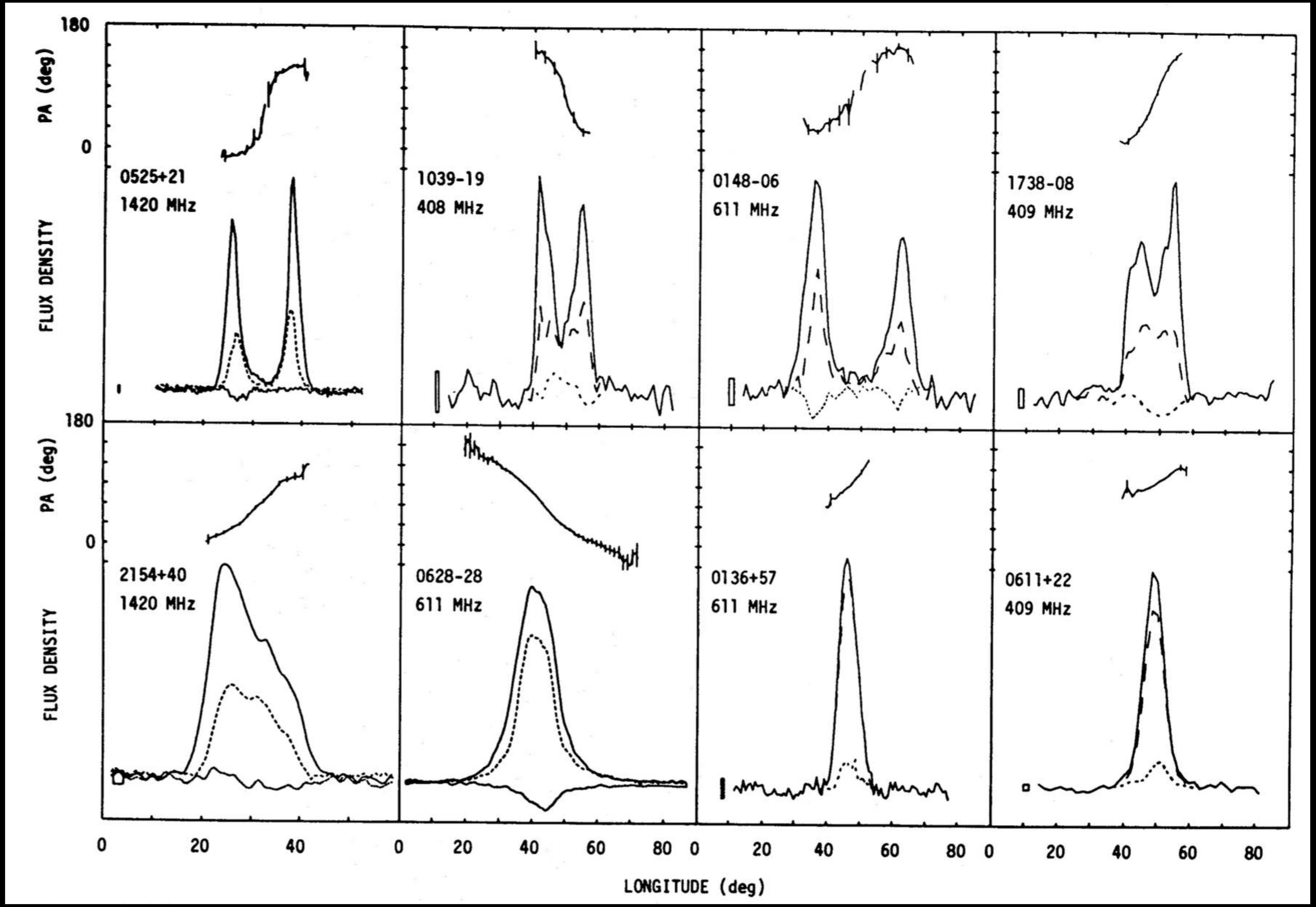

Lyne, Manchester (1988)

In most cases we see one short pulse per period.

Beam width is related to the polar cap size.

Local simulation of 2D discharge

Philippov, Timokhin, Spitkovsky (2020) PRL

Spectrum of 1D discharge

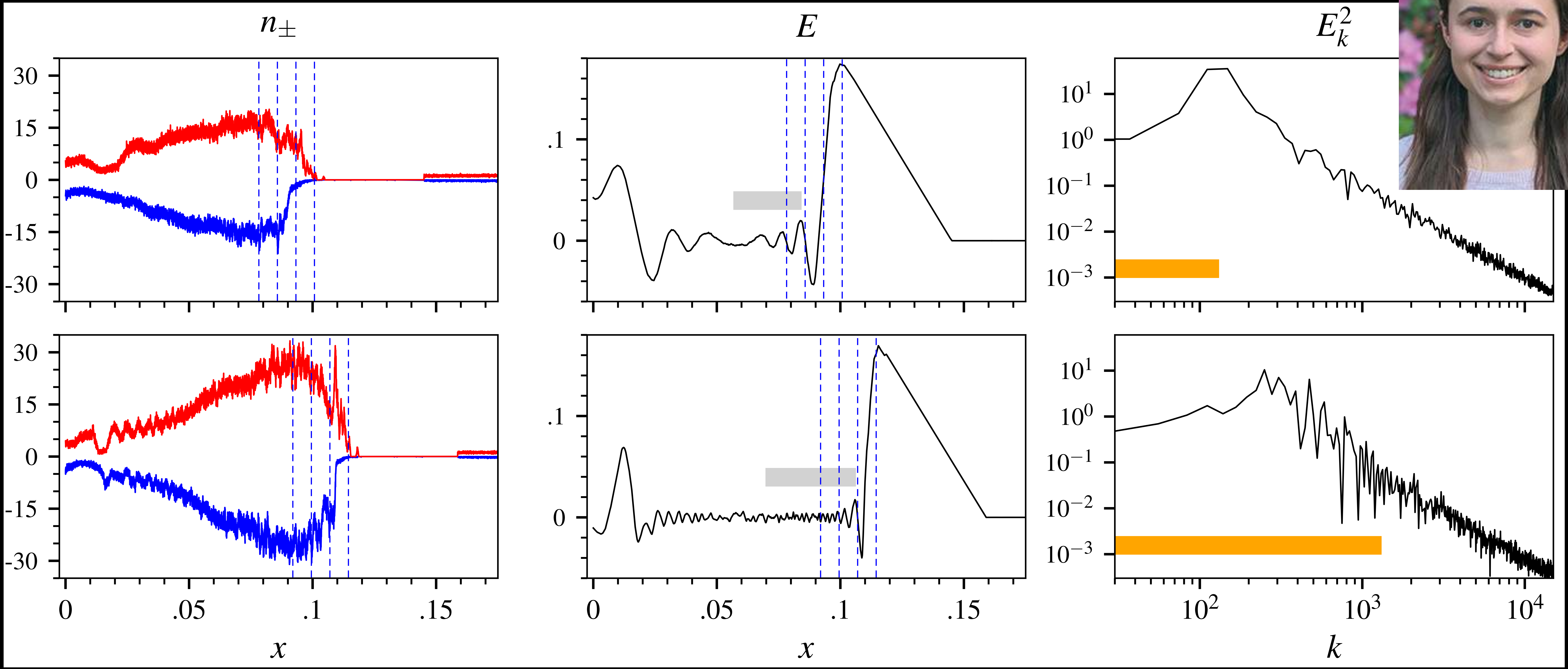

Clearly a broad-band mechanism. Power cascades to a maximum plasma frequency in the cloud.

Philippov, Timokhin, Spitkovsky (2020) PRL
Tolman, Philippov, Timokhin (2022) ApJL

$$\nu \simeq \sqrt{4\pi e^2 \kappa n_{\rm GJ}/\langle\gamma^3\rangle m_e^3}/2\pi = 26\sqrt{\kappa_5 B_{12}/r^3 P_{0.1}\gamma_{10}^3}\ \text{GHz}$$

Confirmation with different codes

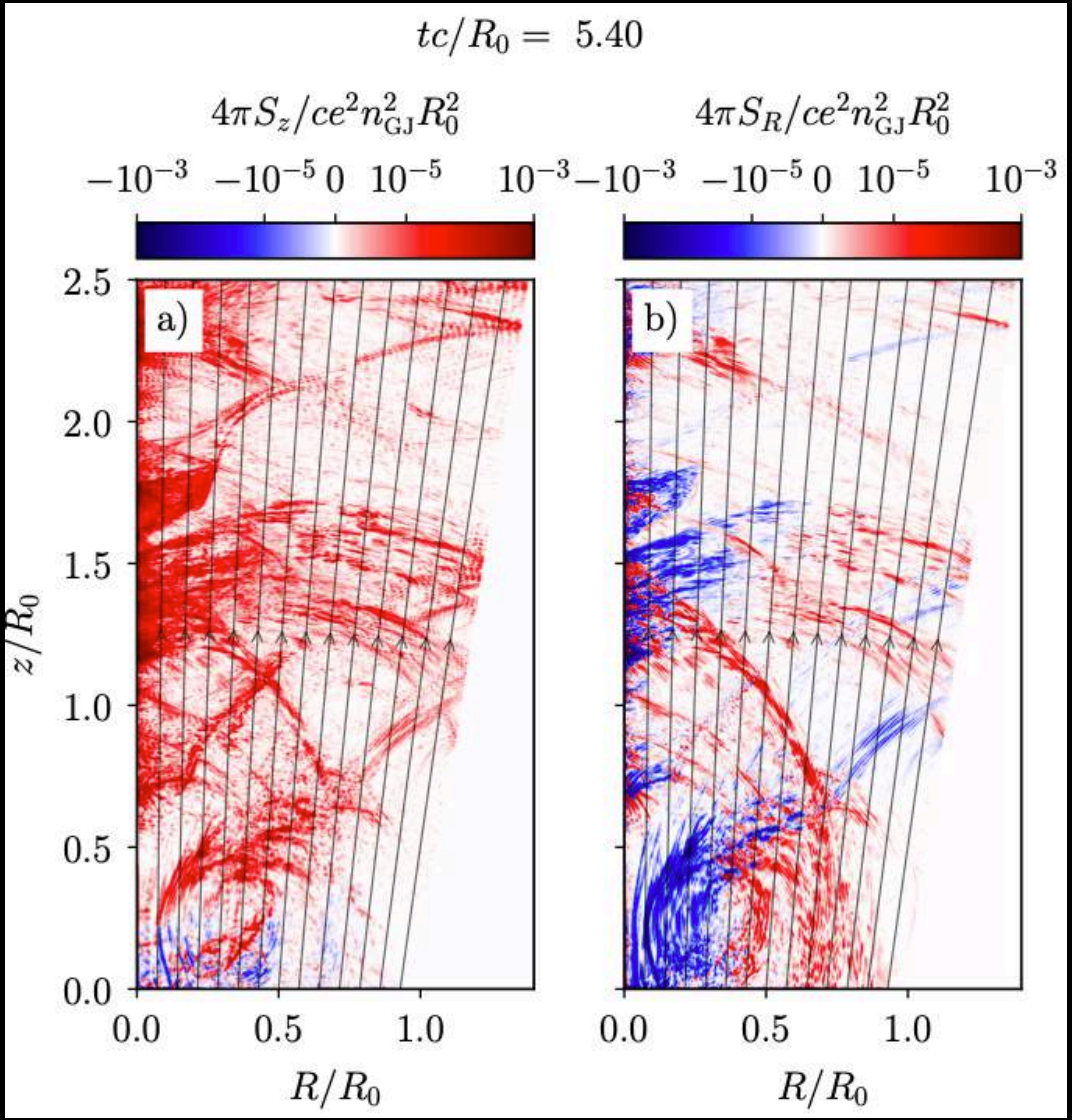

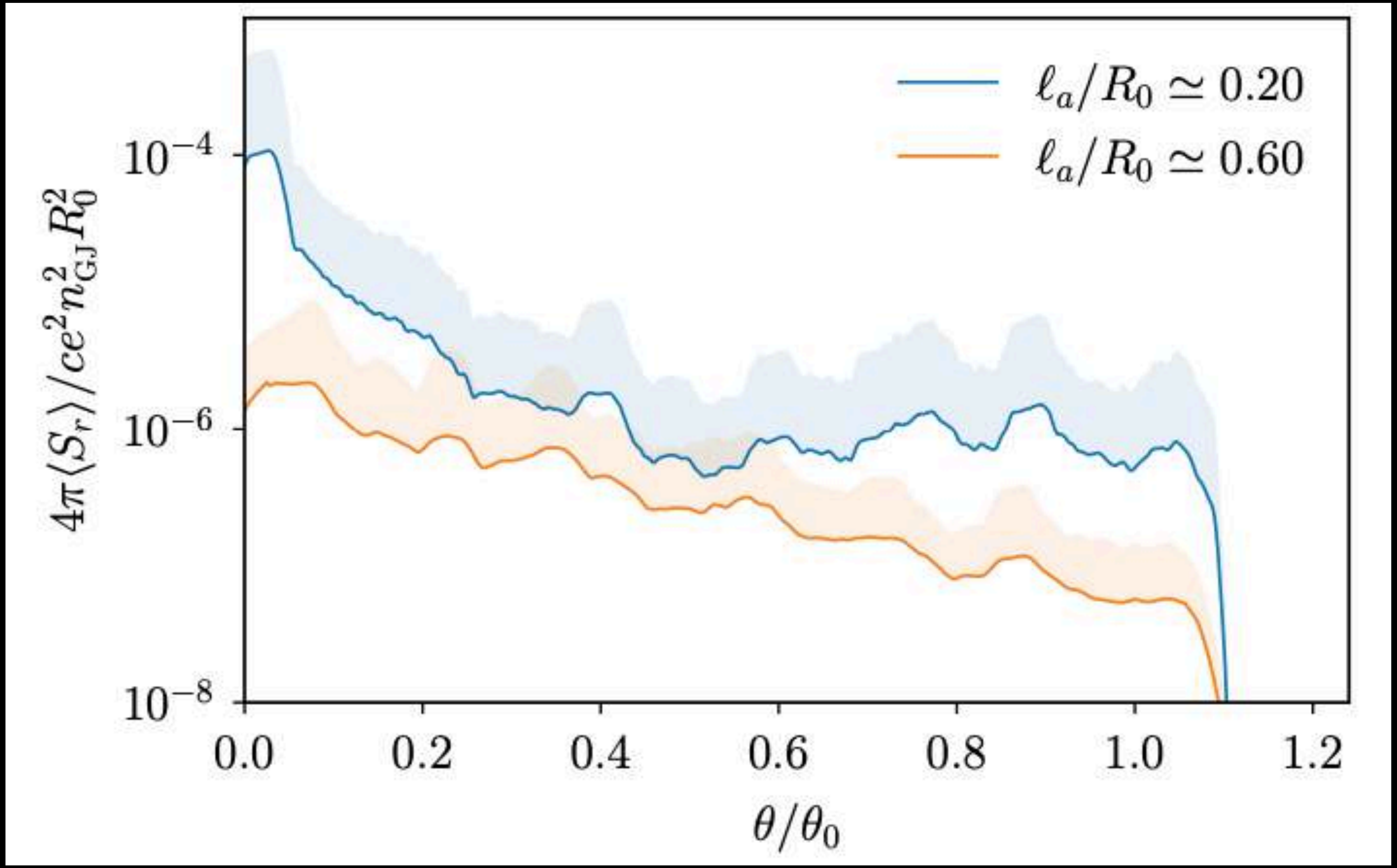

Confirms order-of-magnitude luminosity

Core-cone geometry of the emission beam

QED-PIC simulations with Osiris

Cruz et. al., (2021) ApJL

Magnetar bursts

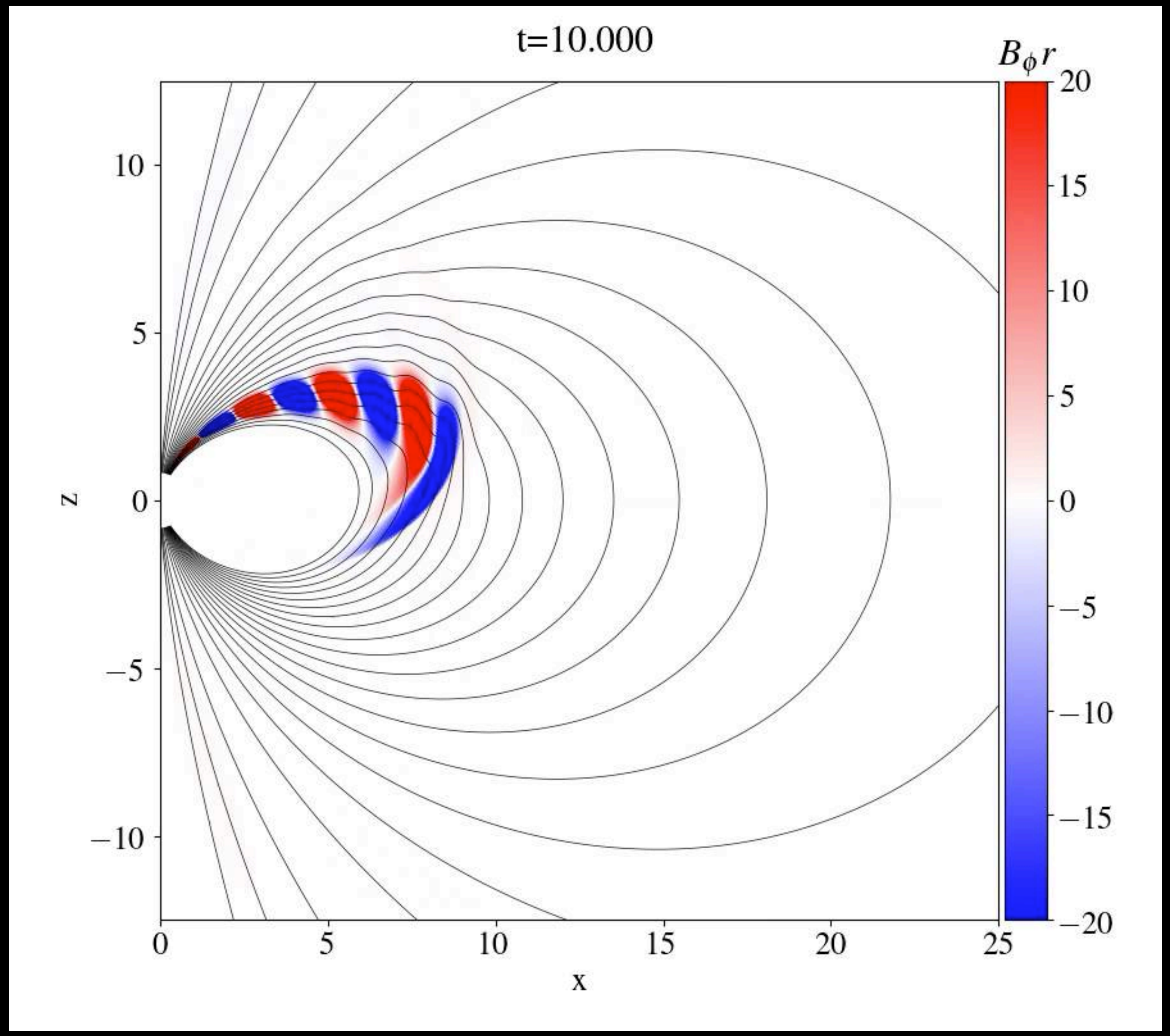

Potentially applicable to X-ray and FRB from galactic magnetar

X-rays come from reconnection, FRB either from plasmoid mergers or synchrotron maser when the bubble shocks

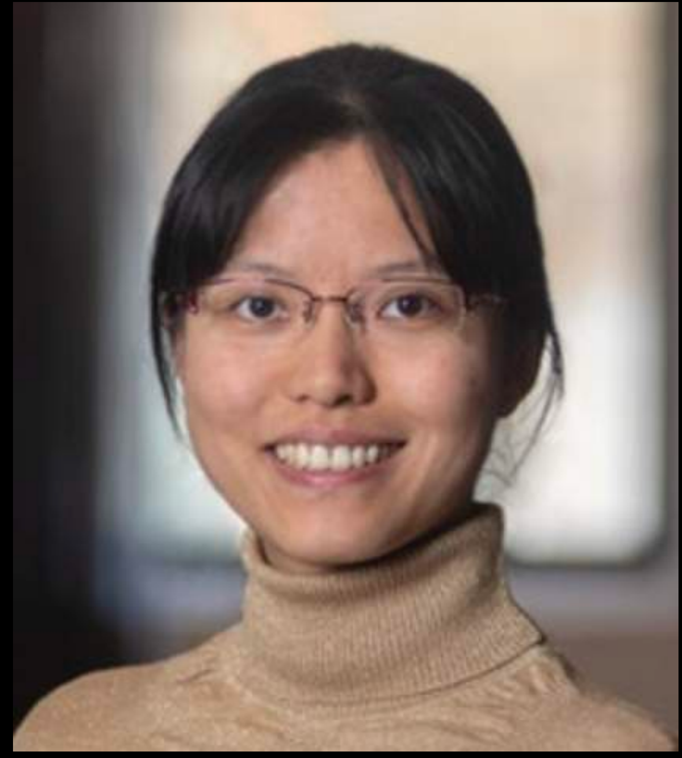

2D

Yuan et. al., 2020, ApJL

3D

Yuan et. al. (including Philippov), 2022, ApJ

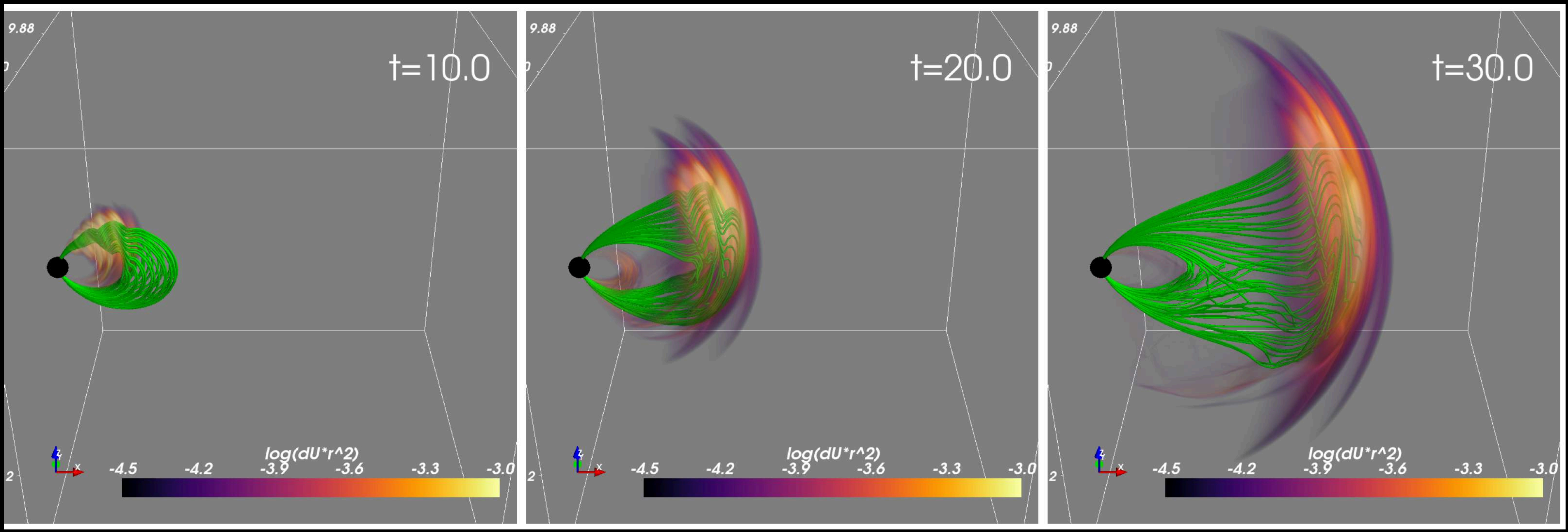

SgrA* and M87(*)

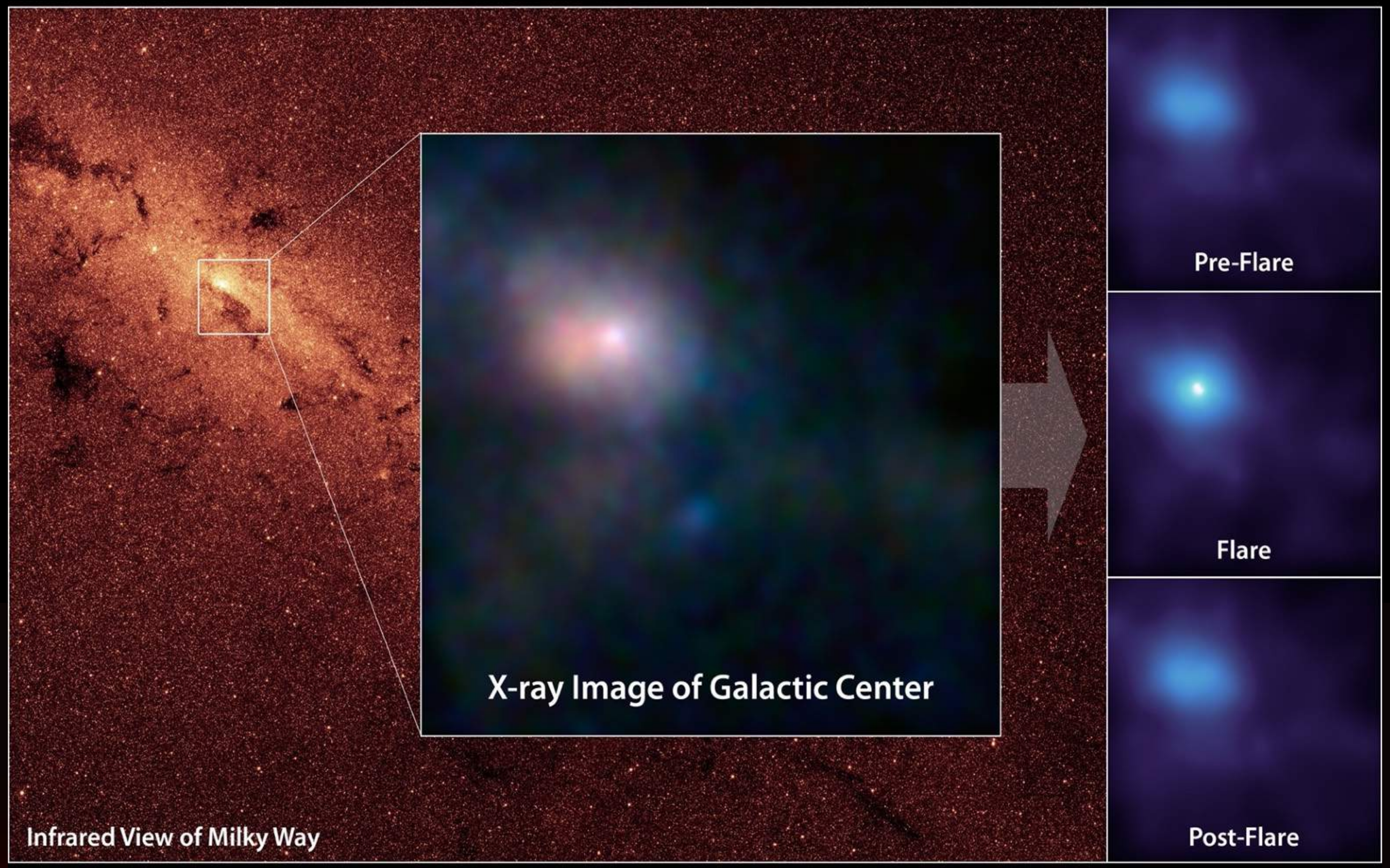

conditions imply macroscopically collisionless, but strongly magnetized plasma

large-scale jet is observed for M87

Multi-wavelength flares (NIR/X-ray for SgrA*, TeV for M87)

$$B \sim 10\text{G}$$
$$n_e \sim 3 \cdot 10^4 \text{cm}^{-3}$$
$$T_e \sim 1\text{MeV}$$

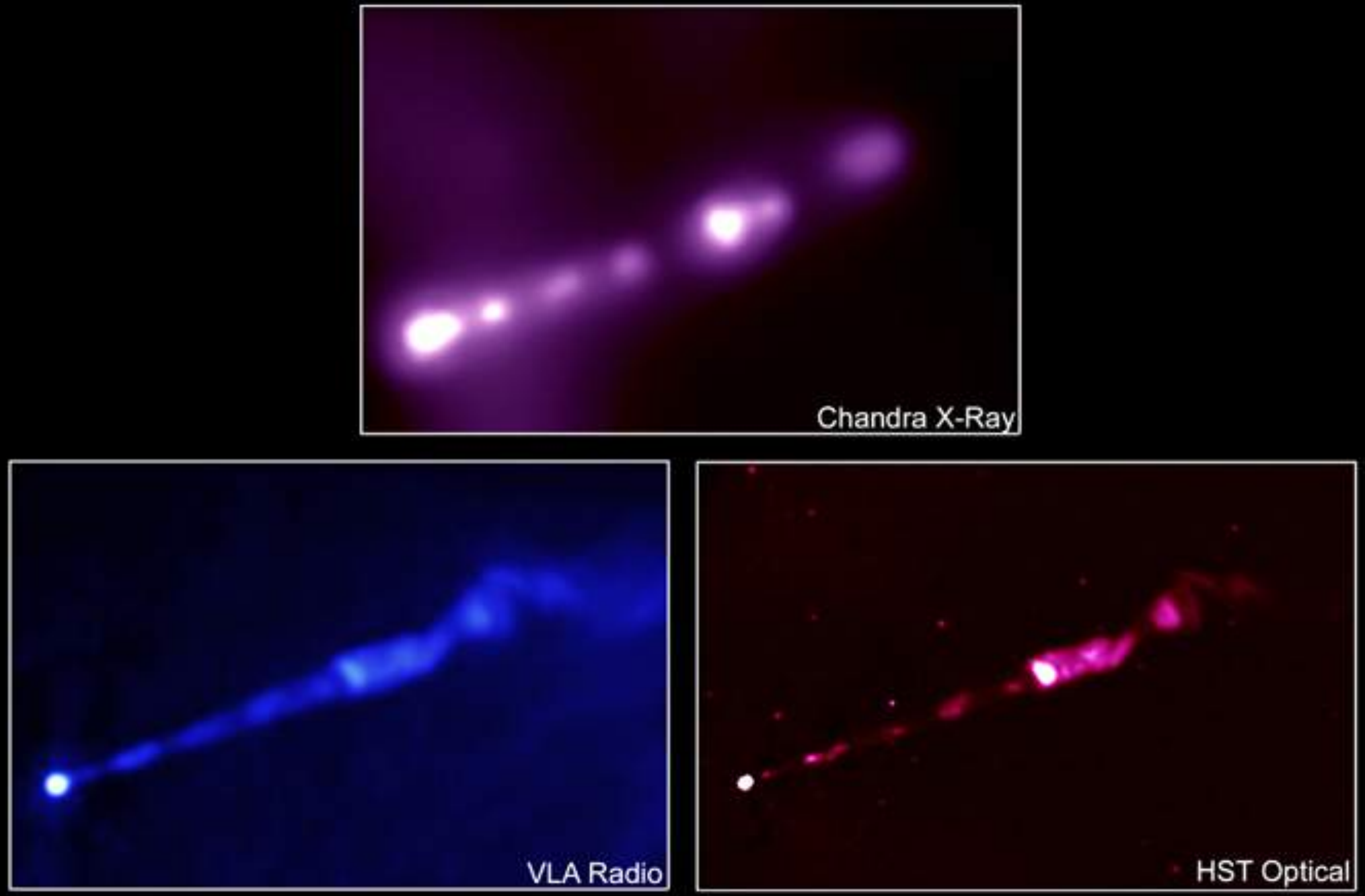

SgrA* and M87(*)

Multi-wavelength flares (NIR/X-ray for SgrA*, TeV for M87)

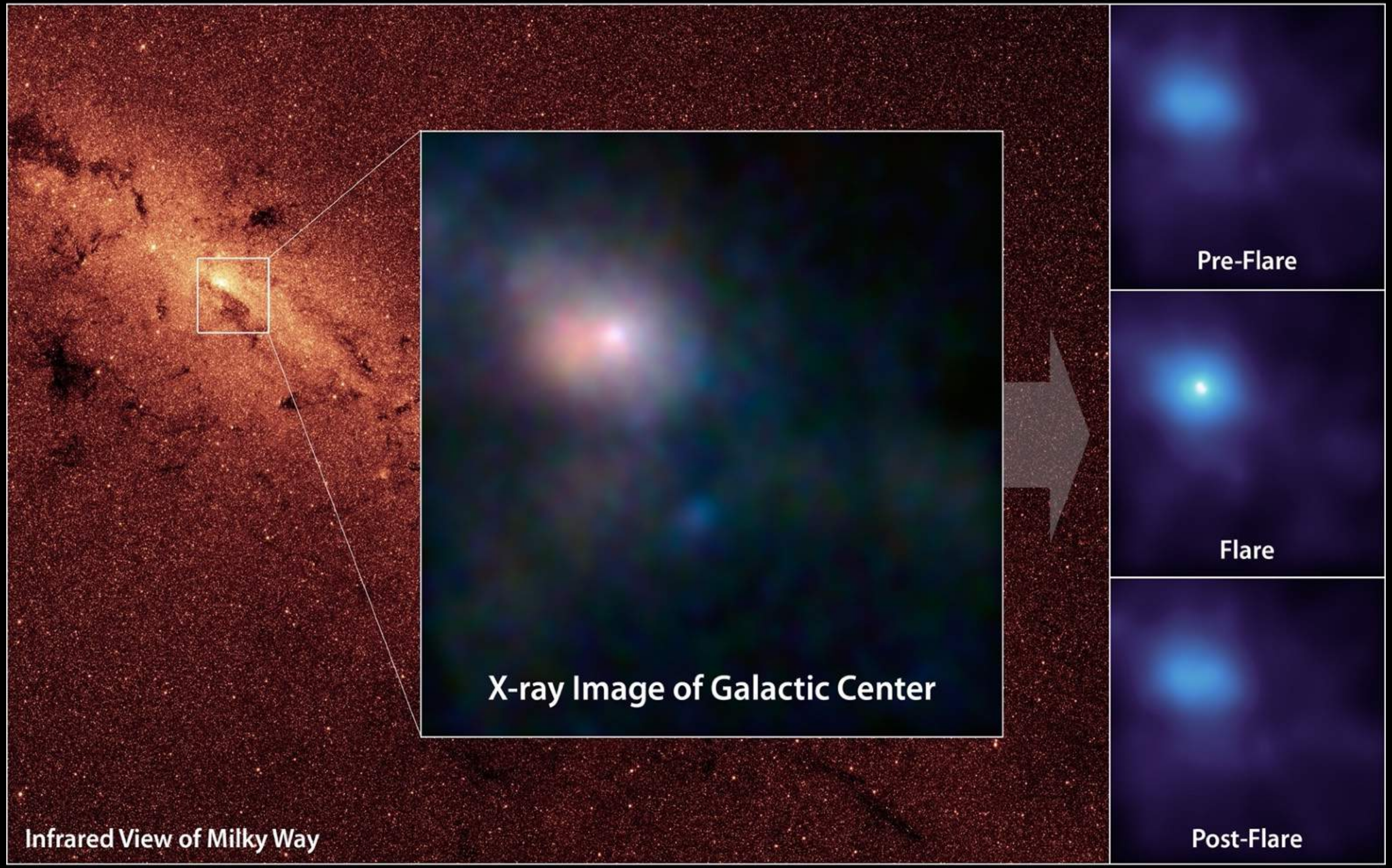

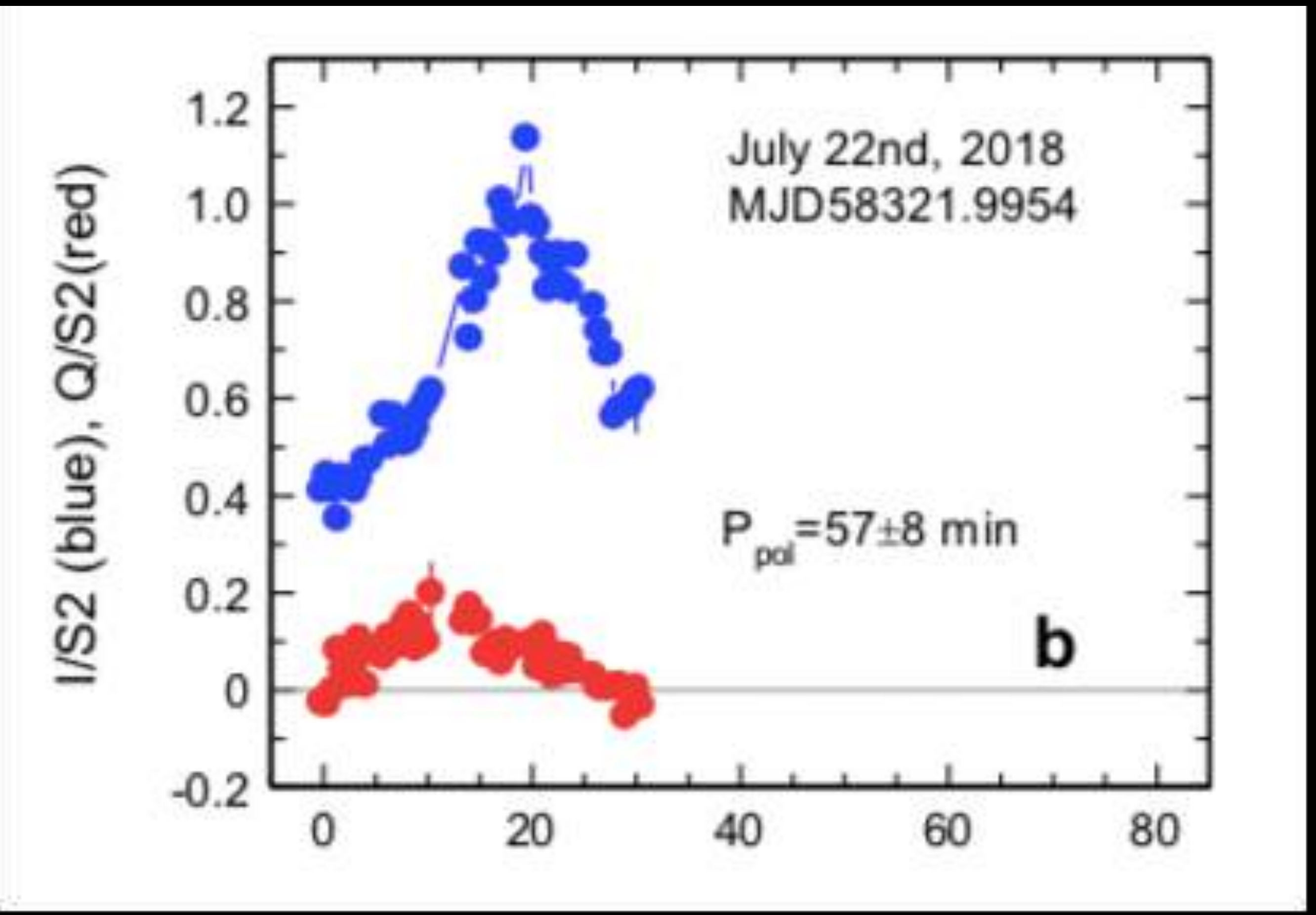

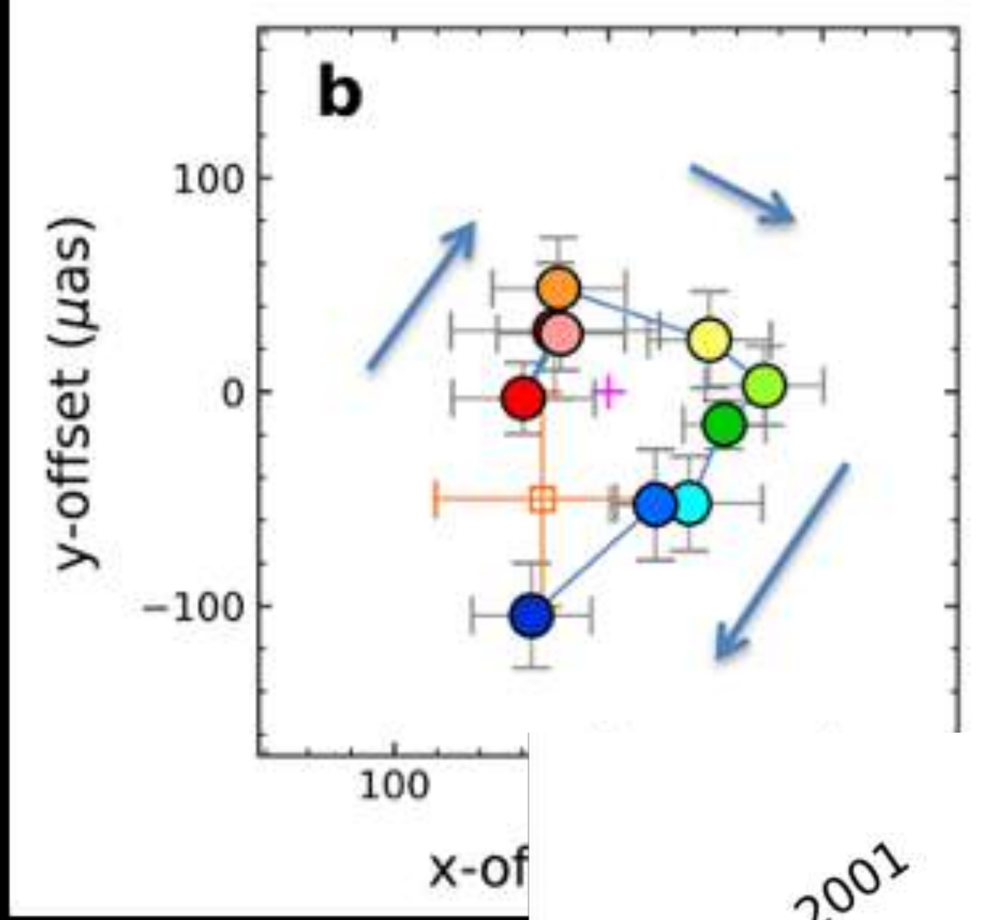

GRAVITY collaboration, A&A (2018)

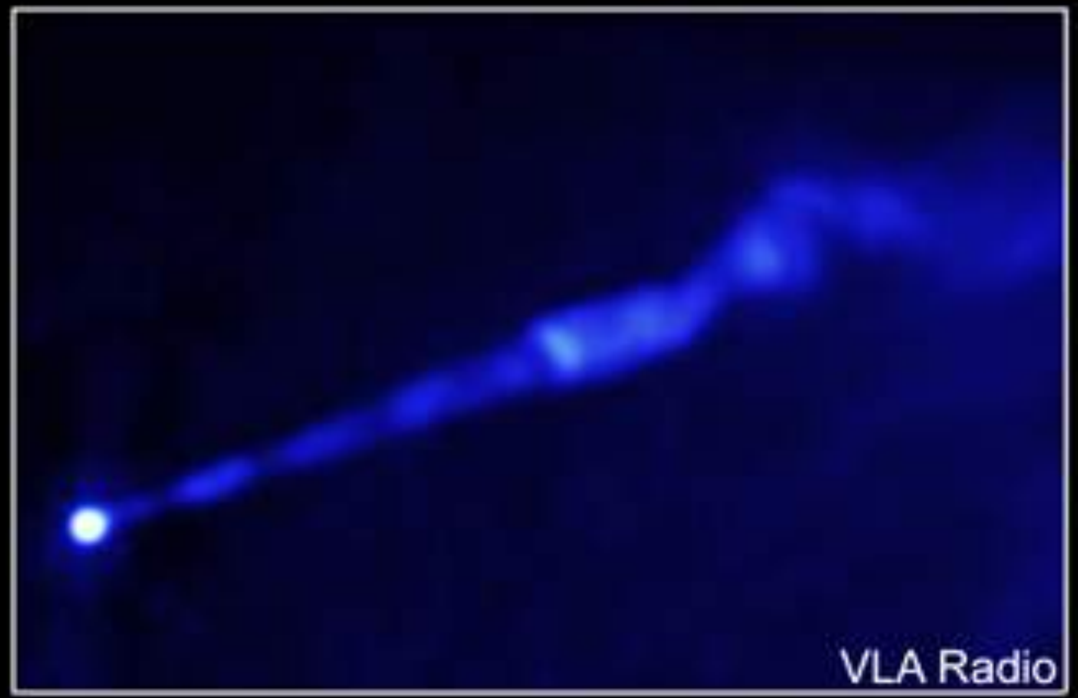

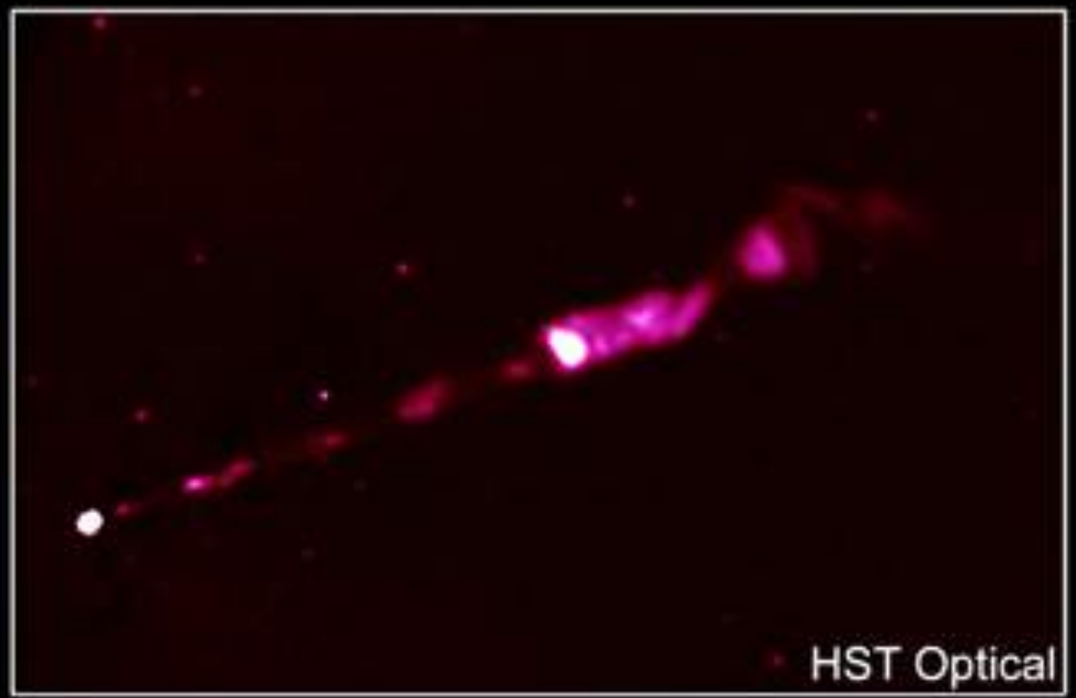

Abramowski et. al., ApJ (2012)

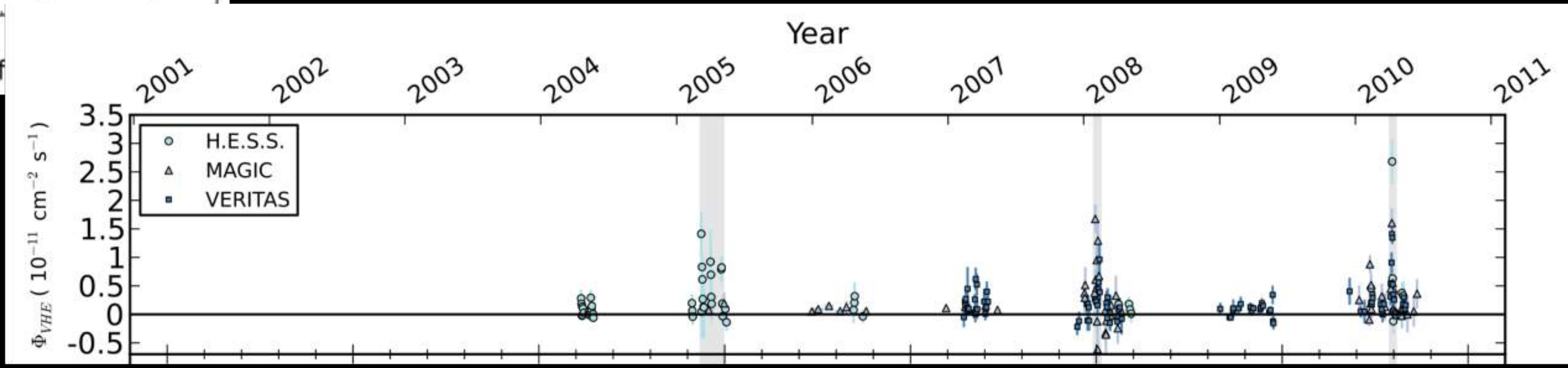

Theoretical cartoon: Plasmas around black holes

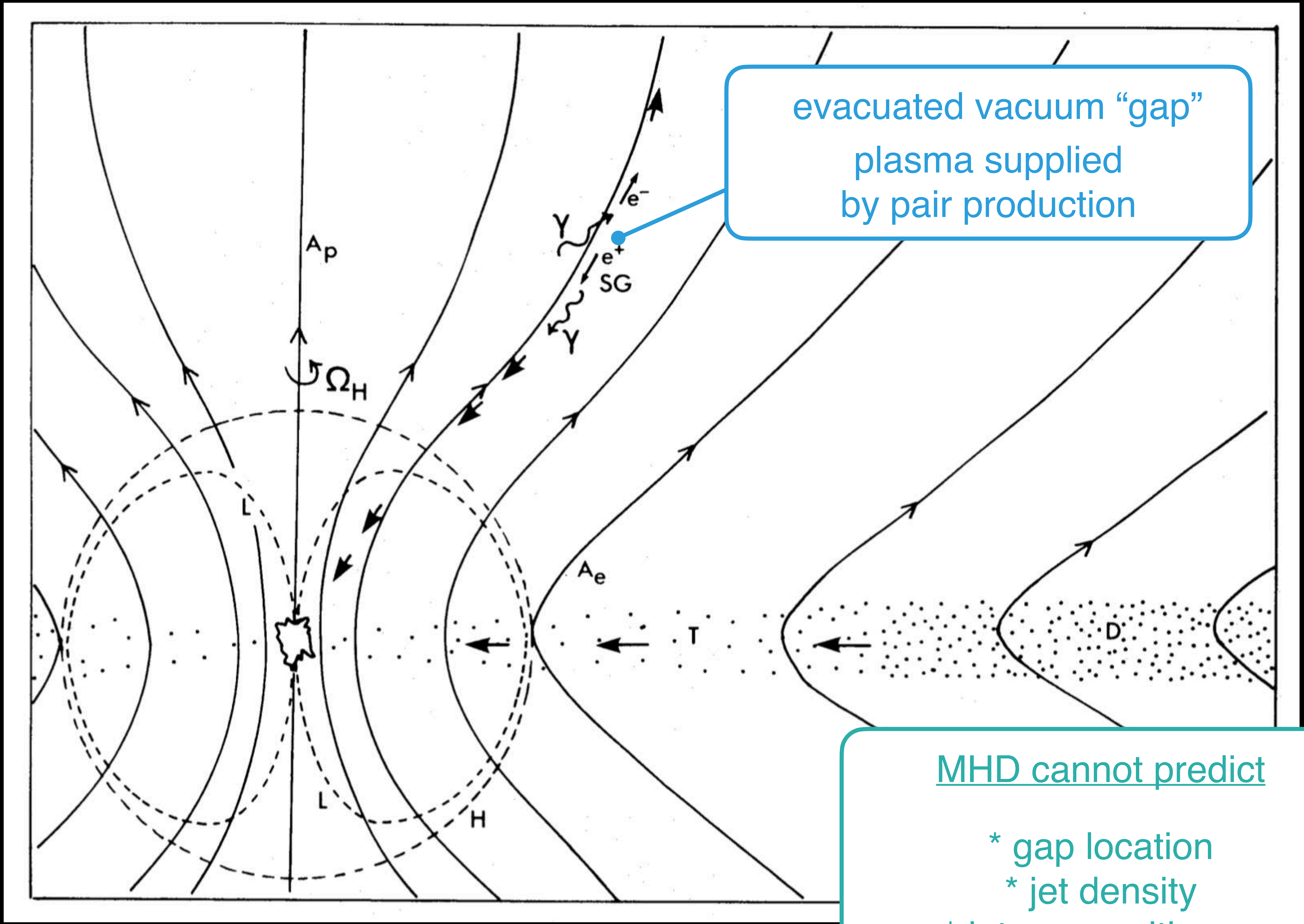

evacuated vacuum “gap”
plasma supplied
by pair production

Blandford, Znajek, 1977

State-of-the-art MHD (fluid) model

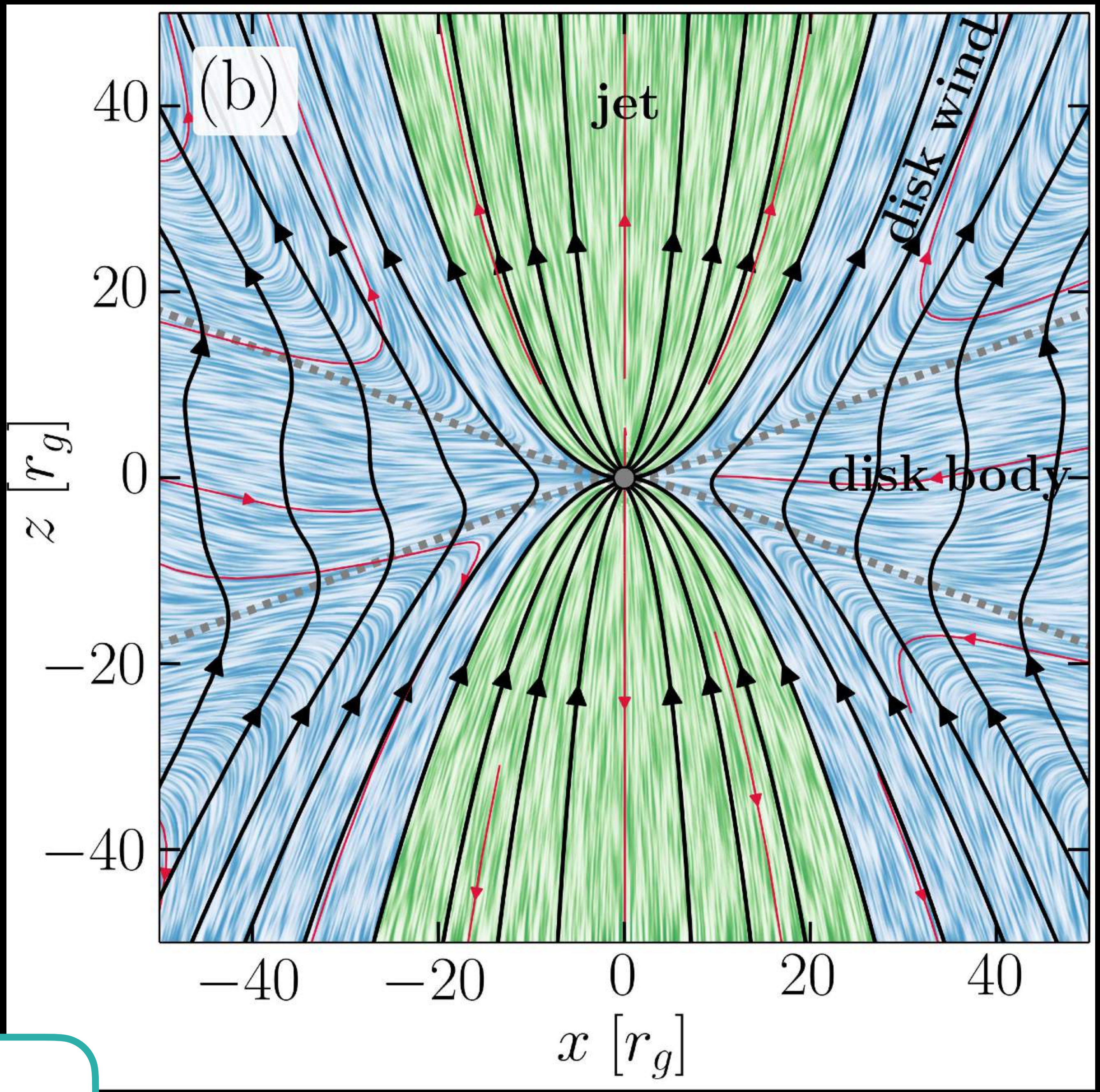

Tchekhovskoy, 2015

<u>MHD cannot predict</u>

* gap location
* jet density
* jet composition ...

First GR kinetic simulation of jet launching

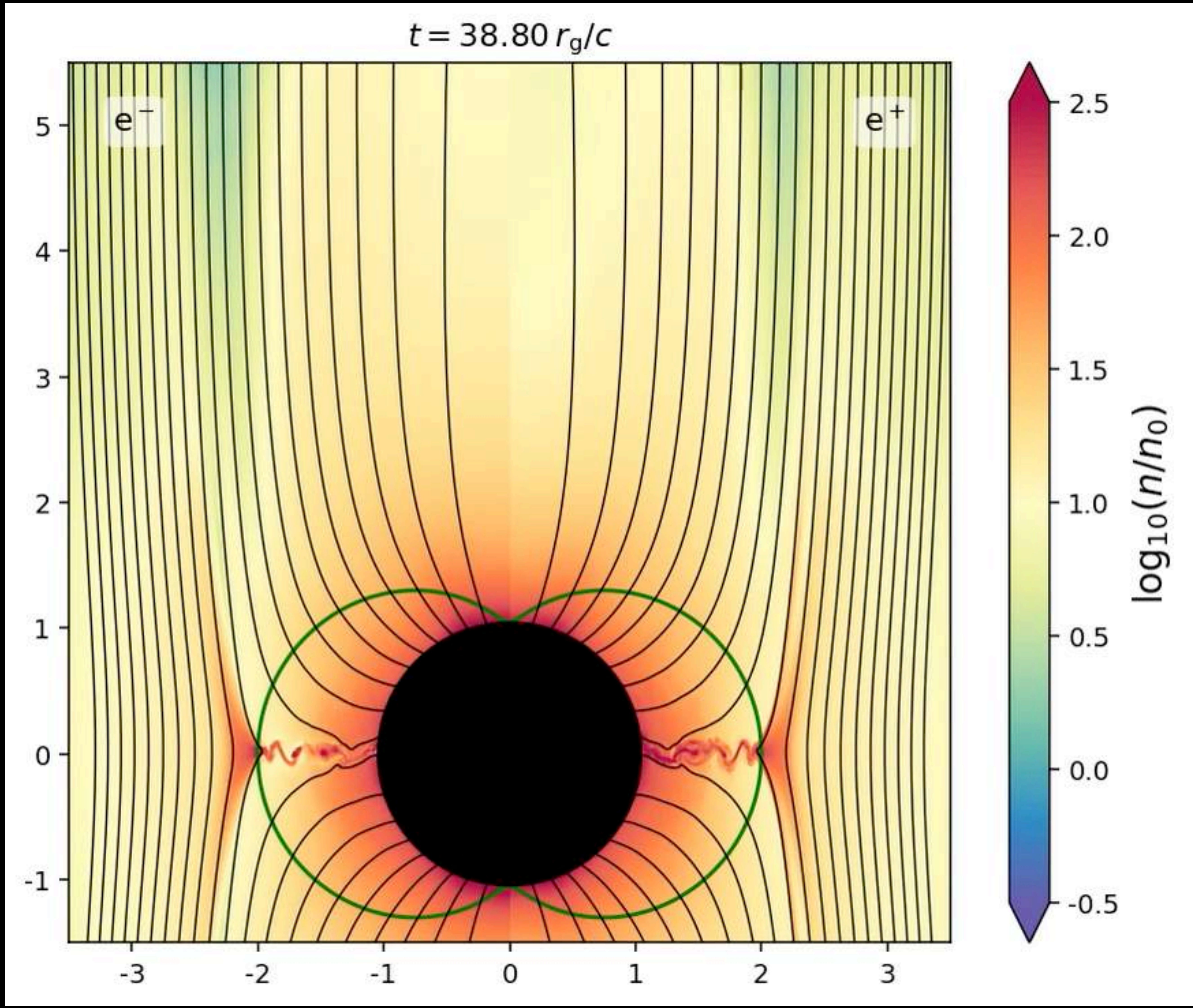

Parfrey, Philippov, Cerutti, cover of PRL, 2019

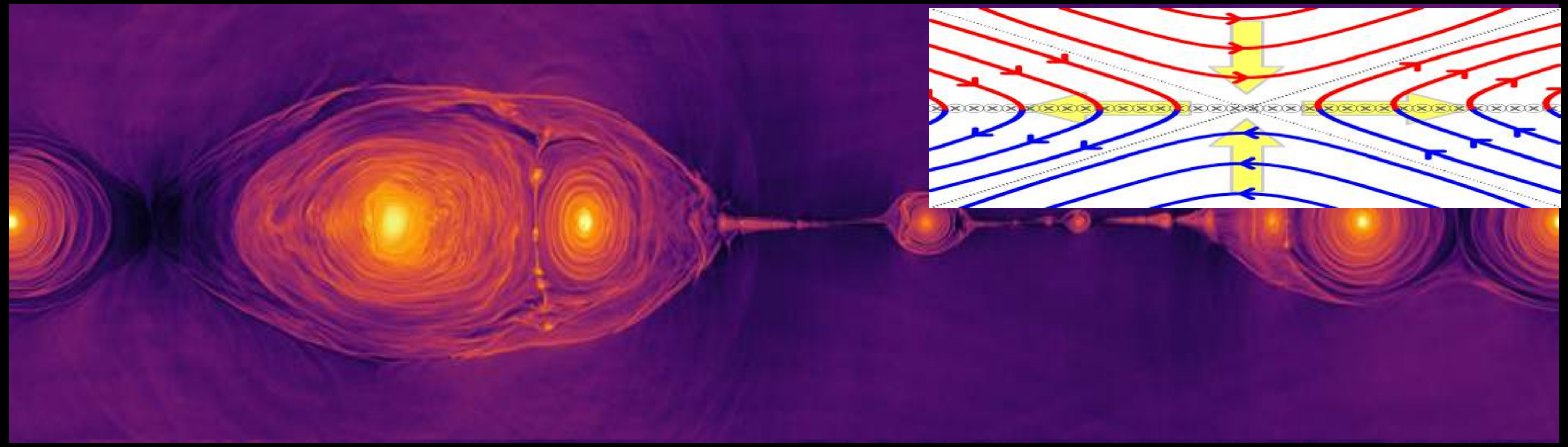

e^- *e^+*

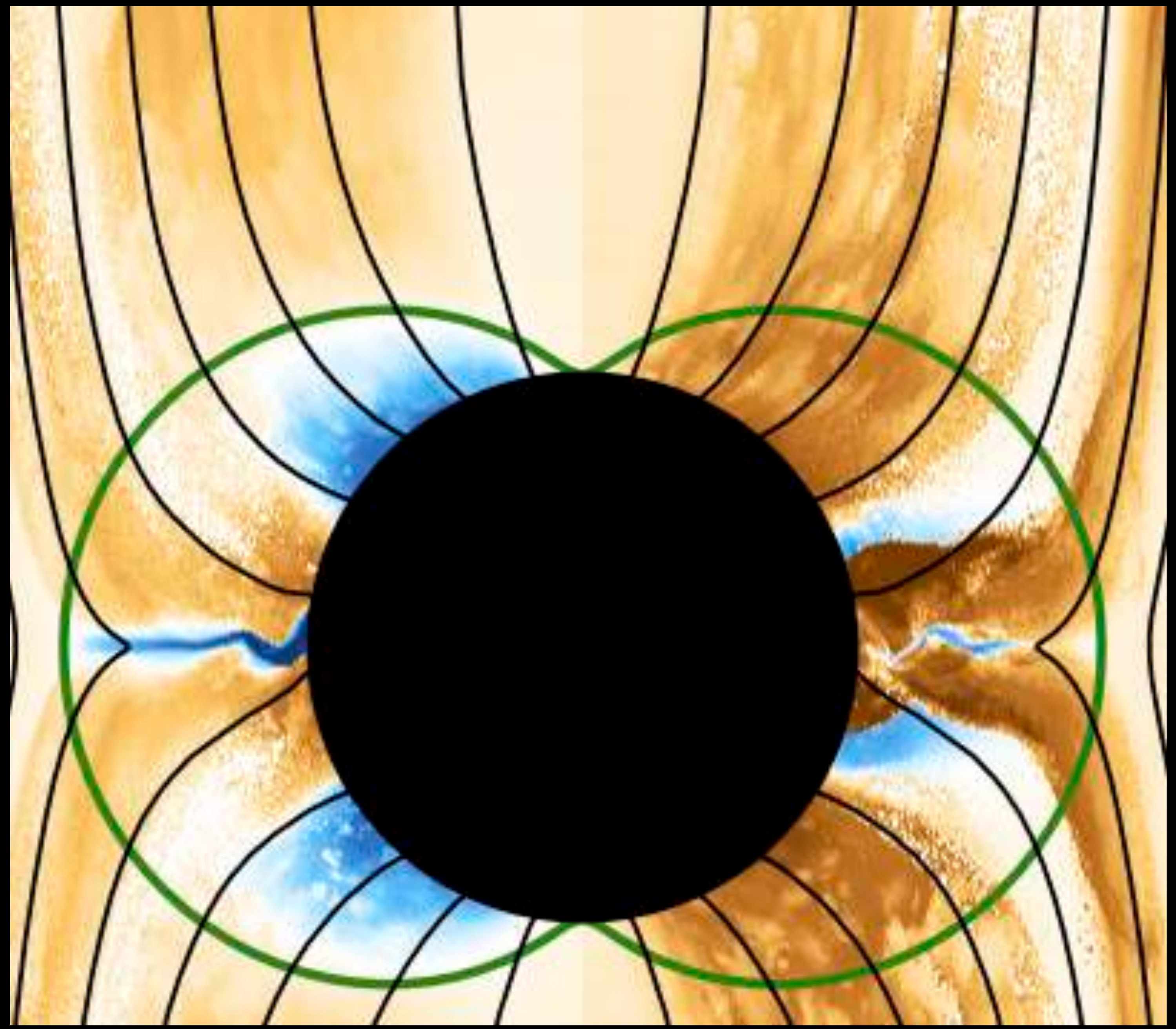

Penrose-like process of
energy extraction in the current sheet

analytics by Comisso, Asenjo, PRD, 2021

Anti-matter production: QED lightning near the EH

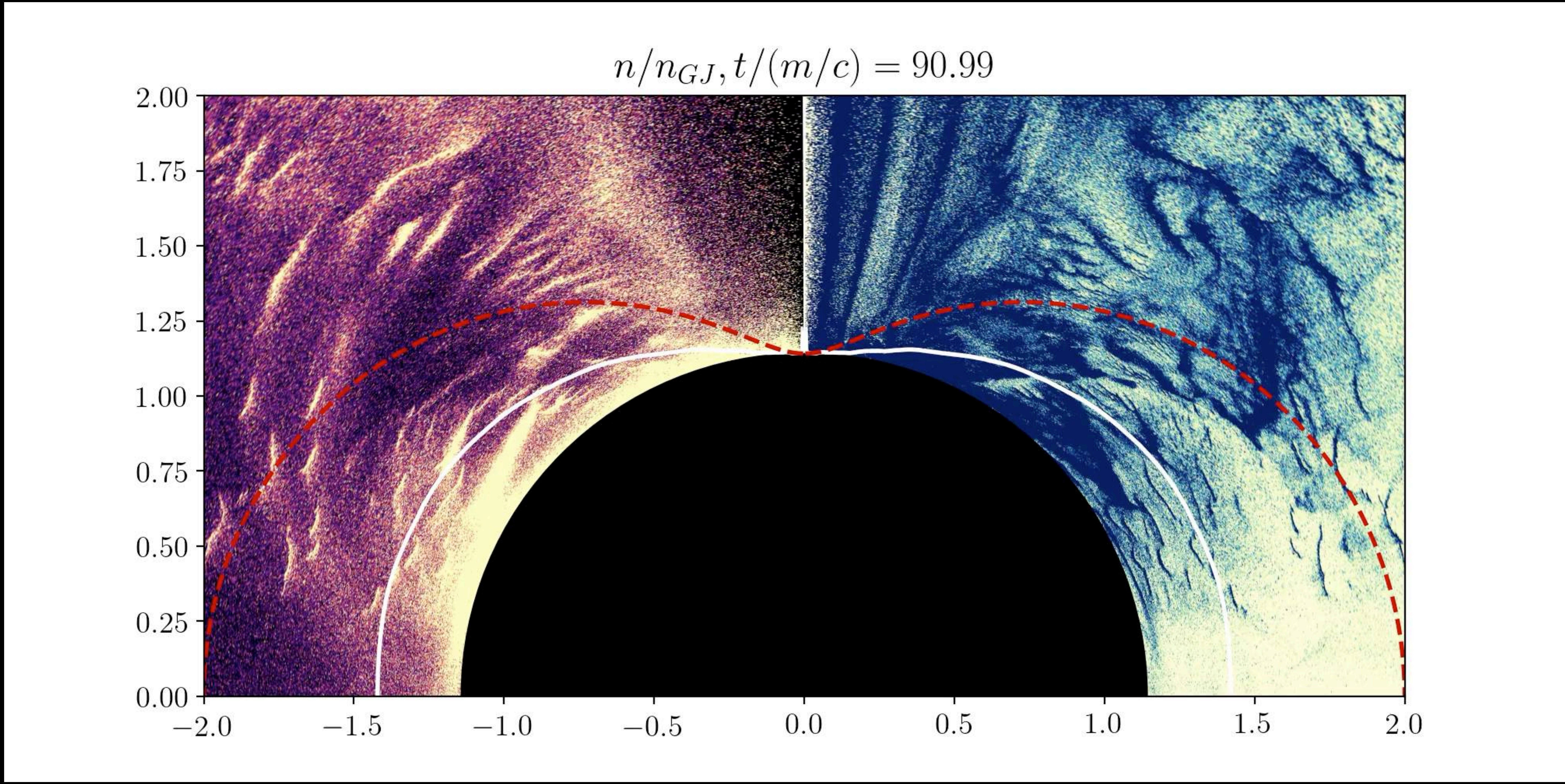

Solves the problem of plasma creation in jets. Intrinsic discharge intermittency is probably not sufficient to explain large TeV flares from M87.

Three-dimensional GR PIC simulations are still challenging….

Crinquand, Cerutti, Philippov, et. al., PRL, 2020

Large Flares: Magnetic Reconnection near the EH

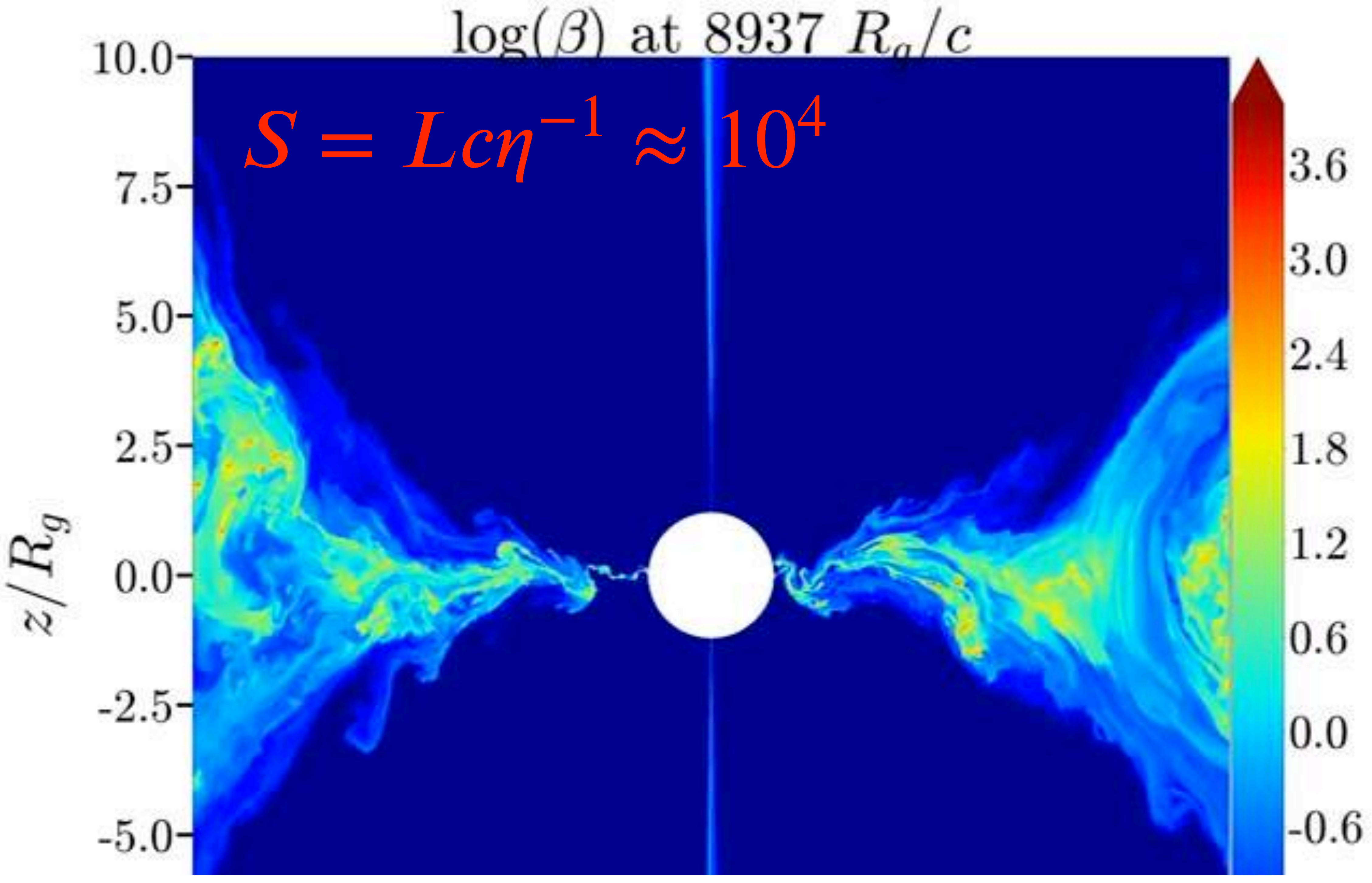

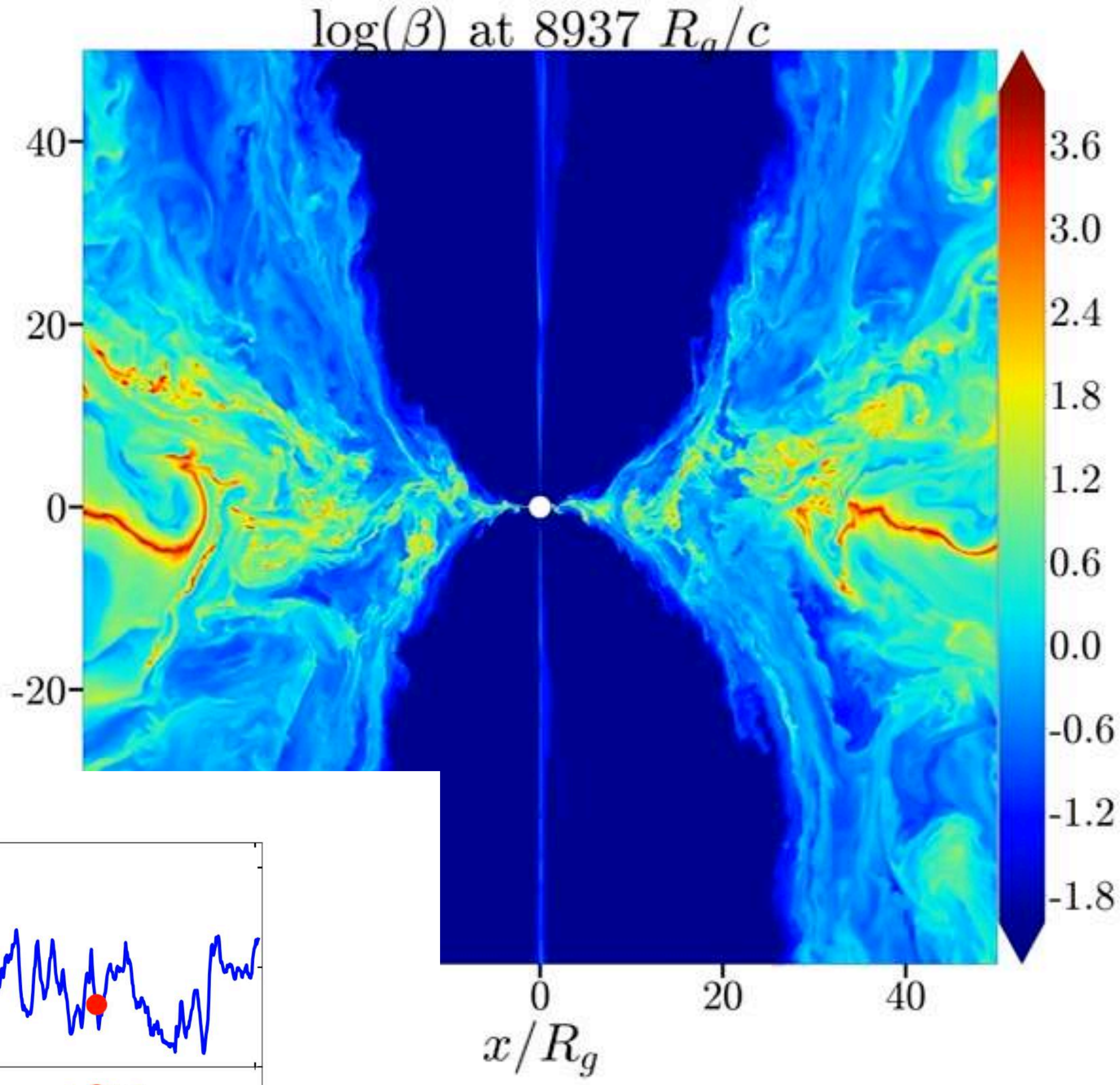

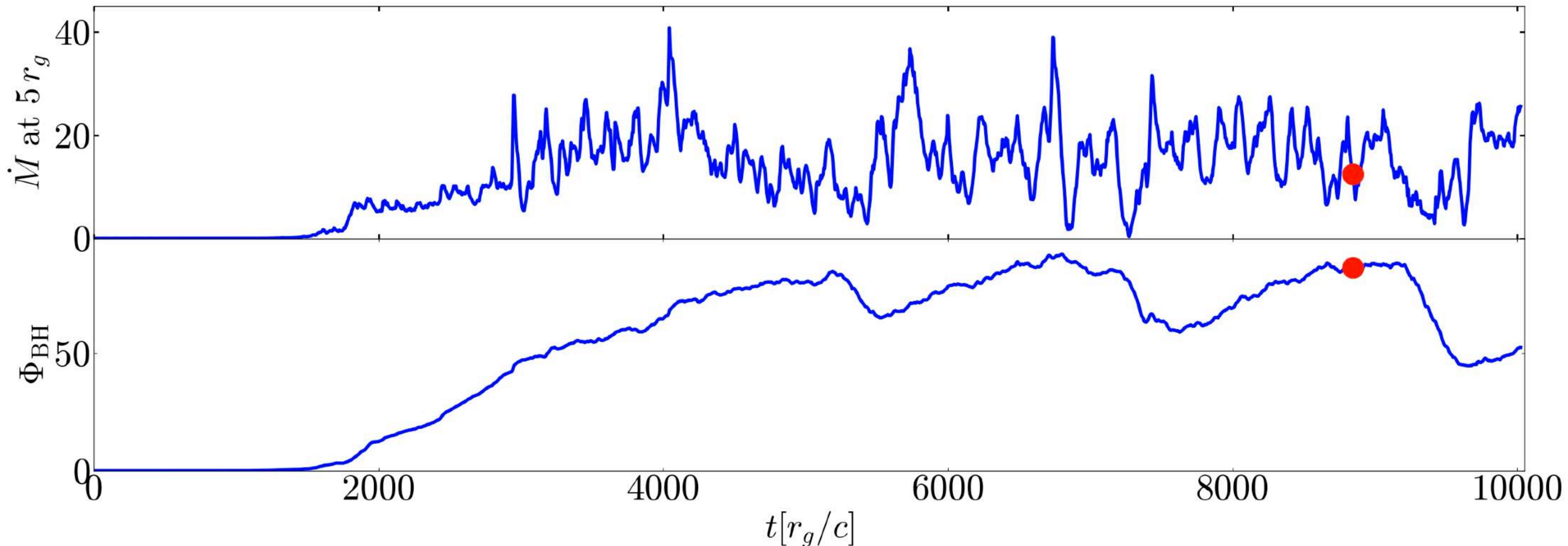

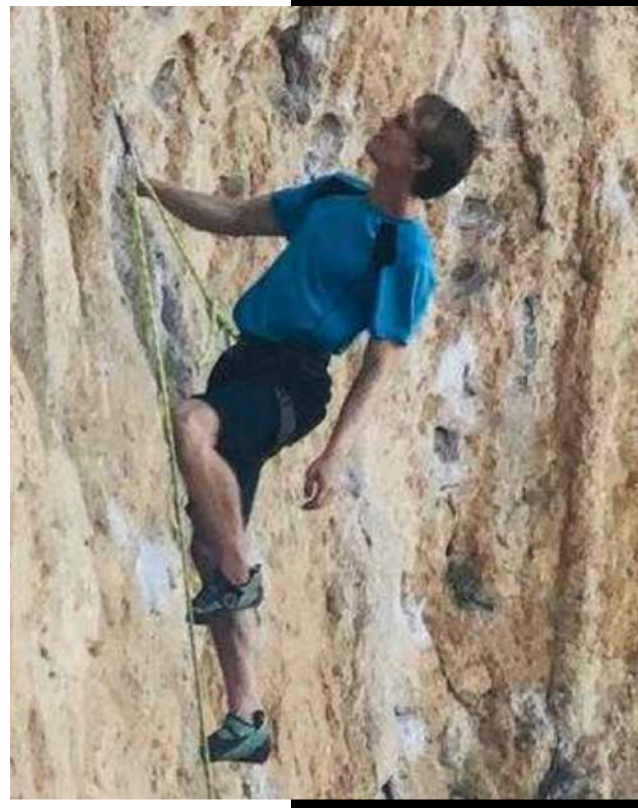

Ripperda, Liska, Chattarjee, et. al., 2022, ApJL

Toy model: “Balding” black hole

(First proposed by Lyutikov, 2011, PRD)

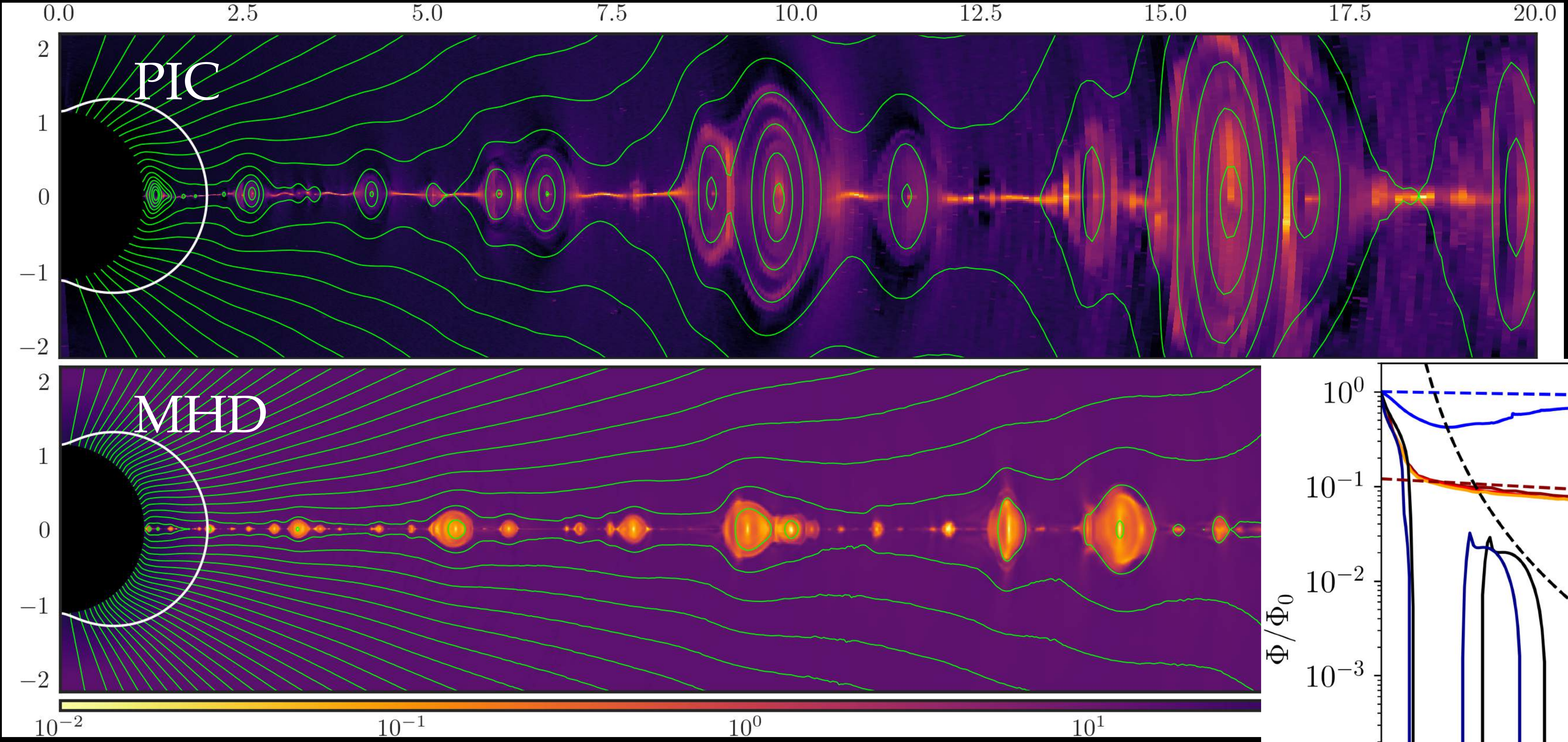

Bransgrove, Ripperda, Philippov, 2021, cover of PRL

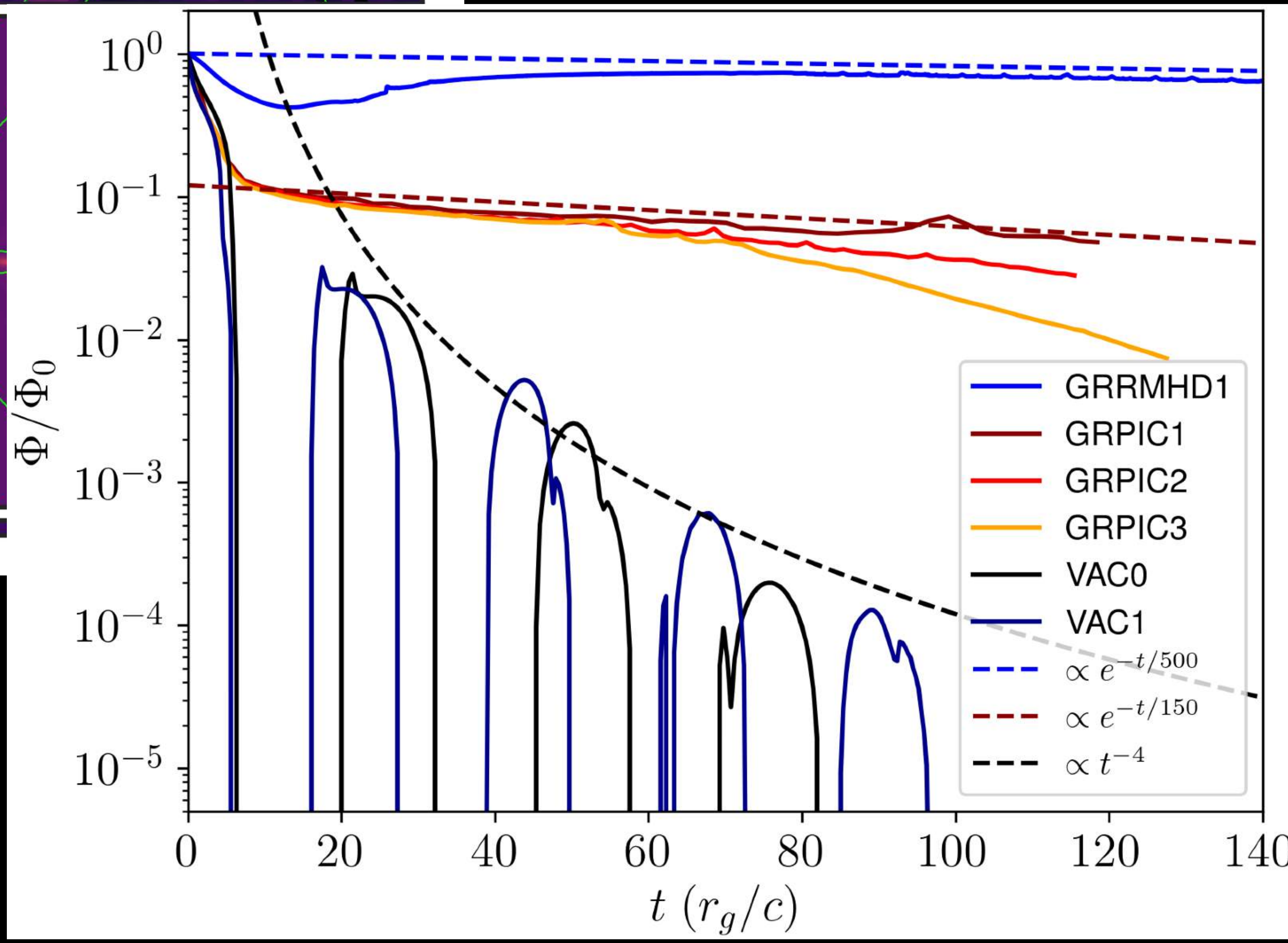

The time for magnetic flux to escape the event horizon is controlled by the plasma physics of magnetic reconnection

Regime of radiative reconnection

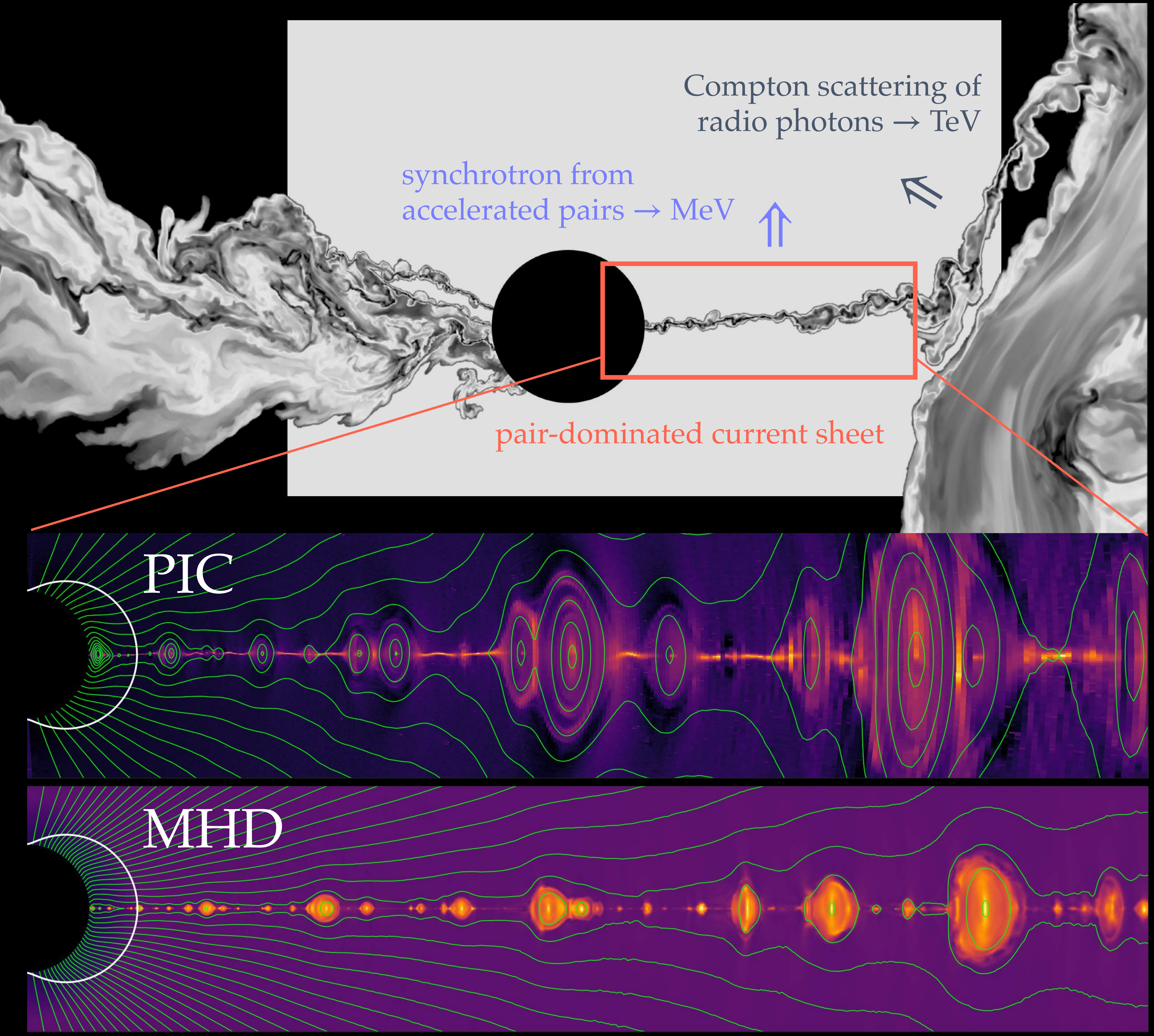

Ripperda et. al. (2022)
Bransgrove, Ripperda, Philippov (2021)

$B \sim 10^2$ G, $B^2/4\pi \gg \rho c^2$, $\sigma \sim 10^7$

Inverse Compton radiation:

- $t_{\rm acc} \ll t_{\rm IC} \ll L/c \;\; \Rightarrow$ moderate IC drag compared to acceleration, but important on dynamical timescales

Synchrotron cooling:

- $t_{\rm acc} \sim t_{\rm sync} \;\; \Rightarrow$ synchrotron cooling affects particle acceleration

Pair production:

- plasma density is dominated by $e^{\pm}$ pairs
- $\tau_{\gamma\gamma} \ll 1$, annihilation ($\gamma\gamma \leftrightarrow e^{\pm}$) is not important (but important in X-ray binaries)

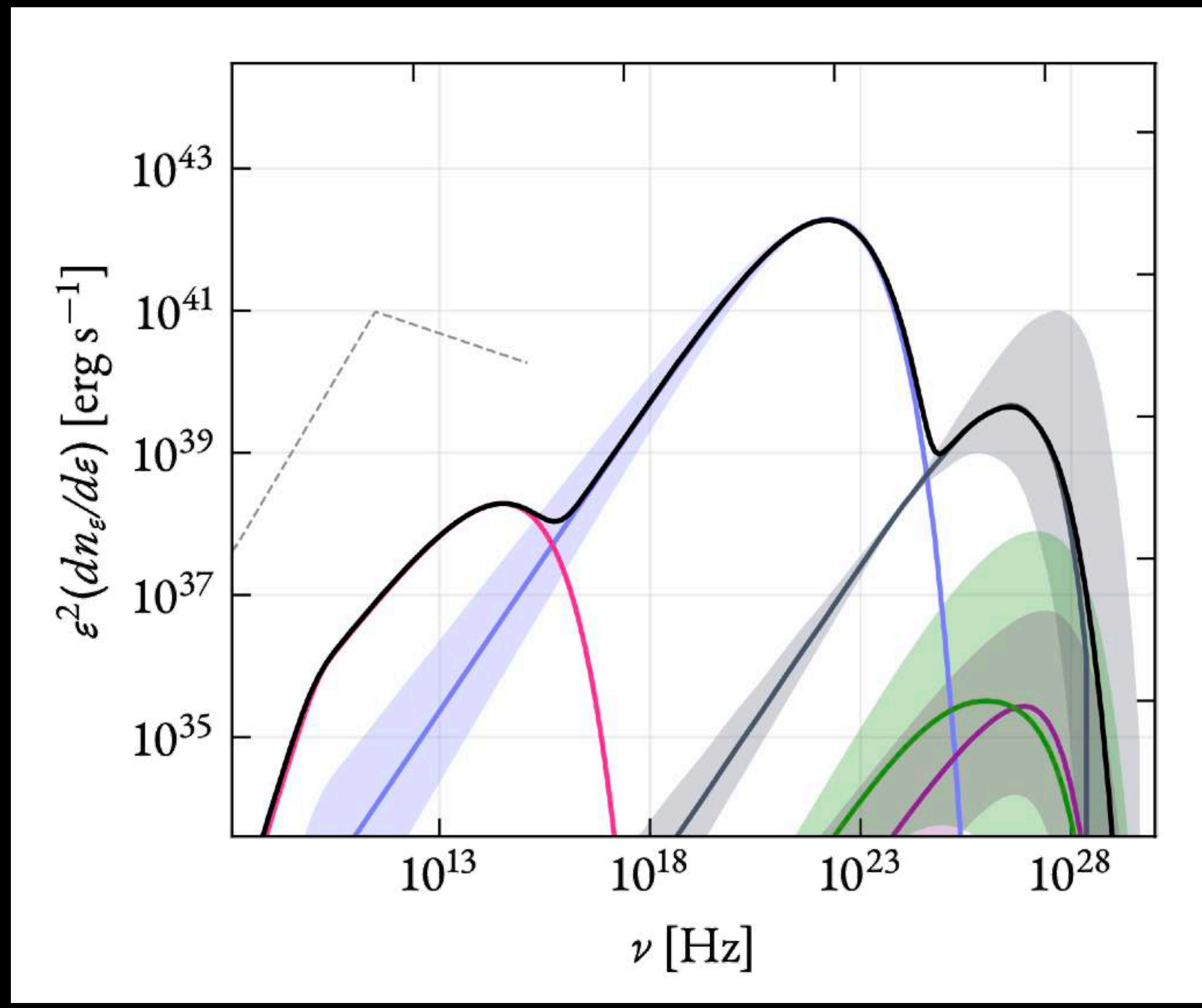

Hakobyan et. al., 2023, ApJL

Brightness dips in EHT imaging

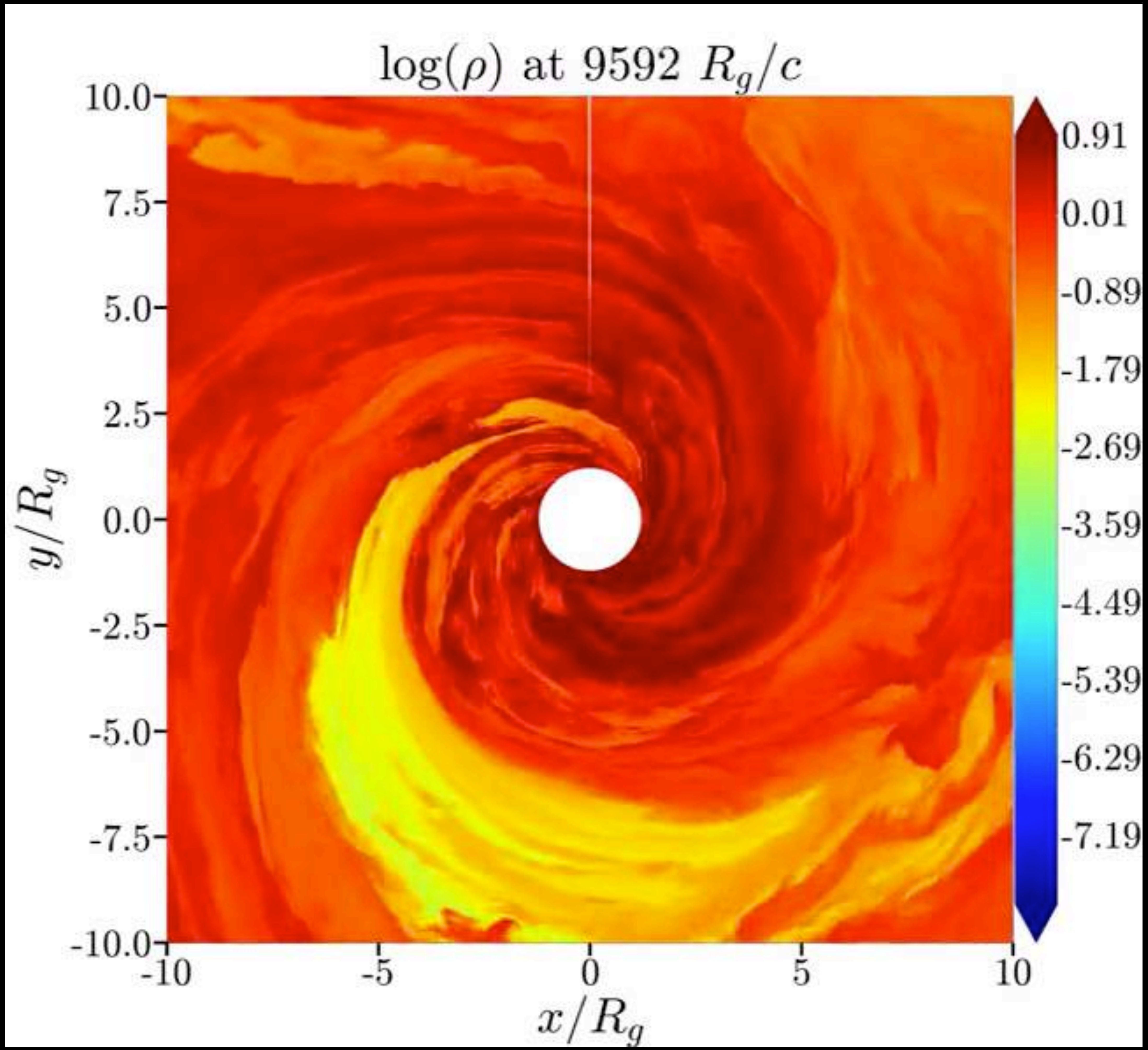

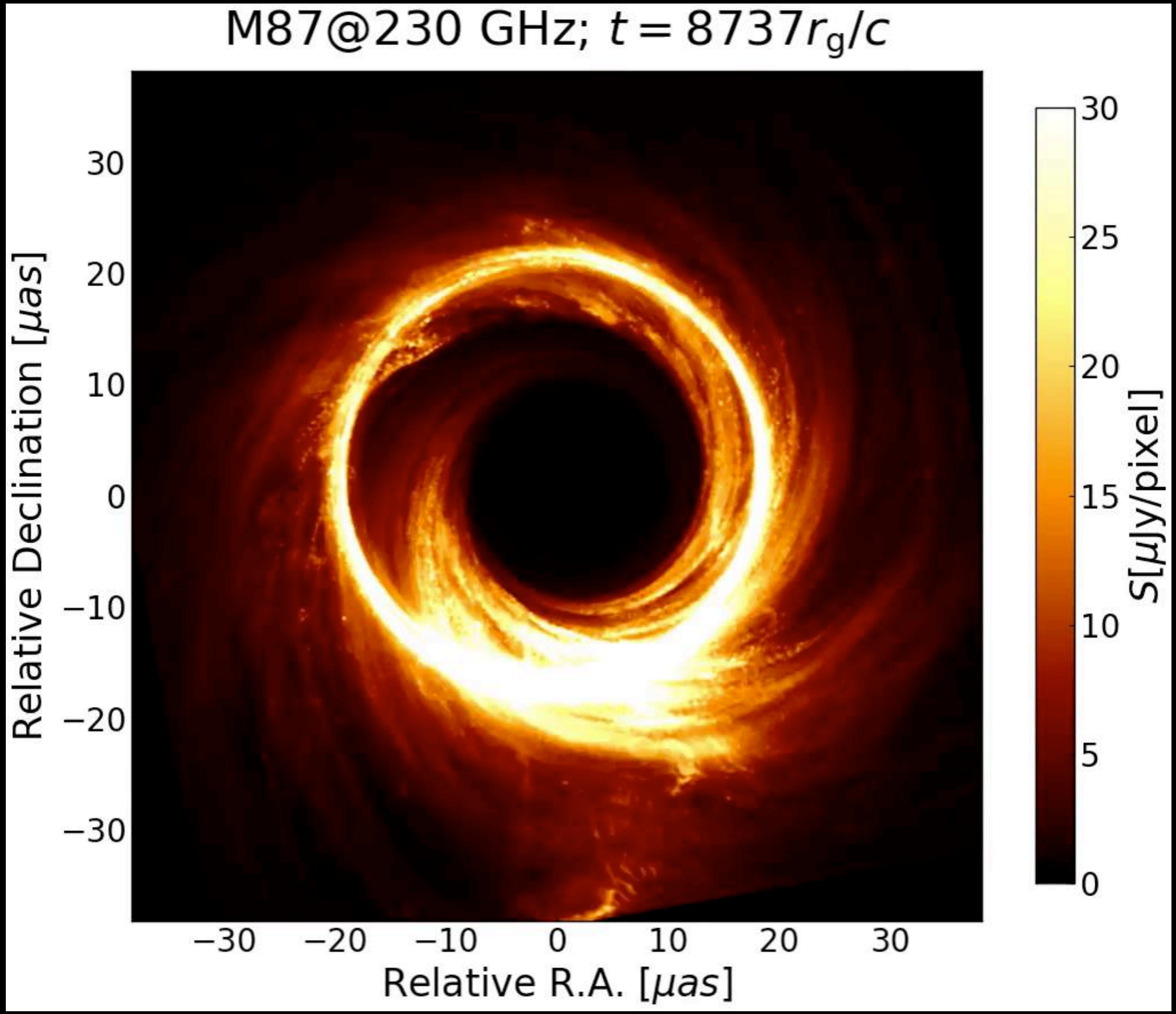

ngEHT can test this picture if observations can sample both the quiescence and flare; AND if observed signatures are different (prediction: dimming of the radio image).

He et. al., arXiv, 2023

Movie by Koushik Chatterjee